SANDIA REPORT
SAND2014-17667
Unclassified Unlimited Release
Printed September 2014

Radionuclide Inventory and Decay Heat Quantification Methodology for Severe Accident Simulations

Jeff Cardoni

Prepared by
Sandia National Laboratories
Albuquerque, New Mexico 87185 and Livermore, California 94550

Sandia National Laboratories is a multi-program laboratory managed and operated by Sandia Corporation, a wholly owned subsidiary of Lockheed Martin Corporation, for the U.S. Department of Energy's National Nuclear Security Administration under contract DE-AC04-94AL85000.

Sandia National Laboratories

Issued by Sandia National Laboratories, operated for the United States Department of Energy by Sandia Corporation.

Available to DOE and DOE contractors from
U.S. Department of Energy
Office of Scientific and Technical Information
P.O. Box 62
Oak Ridge, TN 37831

Telephone: (865) 576-8401
Facsimile: (865) 576-5728
E-Mail: reports@adonis.osti.gov
Online ordering: http://www.osti.gov/bridge

Available to the public from
U.S. Department of Commerce
National Technical Information Service
5285 Port Royal Rd.
Springfield, VA 22161

Telephone: (800) 553-6847
Facsimile: (703) 605-6900
E-Mail: orders@ntis.fedworld.gov
Online order: http://www.ntis.gov/help/ordermethods.asp?loc=7-4-0#online

SAND2014-17667
Unclassified-Unlimited Release
Printed September 2014

Radionuclide Inventory and Decay Heat Quantification Methodology for Severe Accident Simulations

Jeff Cardoni
Sandia National Laboratories
P.O. Box 5800
Albuquerque, New Mexico 87185-MS0748

Abstract

The MELCOR and MACCS computer codes require inputs for radionuclide inventory and decay heat in order to simulate severe accident phenomenology, source term, and consequences. Therefore, Sandia National Laboratories (SNL) has developed accurate and automated methods using SCALE6 in conjunction with automation scripts to directly generate MELCOR and MACCS input records for radionuclide inventories and decay heating. Consistent information between the two codes is essential for realistic modeling of severe nuclear accidents–it is the radionuclide inventory and decay power that are the principal safety problems of any severe accident that assumes successful reactor shutdown. SNL plans to conduct best-estimate calculations and uncertainty analyses using MELCOR and MACCS for several reactors, including units 1-3 of Fukushima Daiichi, which entail accurate and technically-scrutable information for the input models. The SNL methodology for generating radionuclide and decay power inputs directly from SCALE6 calculations is mostly presented in the context of supporting Fukushima modeling efforts. Furthermore, certain historical assumptions used by MELCOR and MACCS in the abstraction of radionuclide classes and their properties are reviewed, and these assumptions are compared to modern code predictions by SCALE6.

ACKNOWLEDGEMENTS

The author would like to acknowledge the U.S. Department of Energy's Office of Nuclear Energy and the U.S. Nuclear Regulatory Commission for providing the funding that supported the documentation of this work. The author would also like to thank Doug Osborn, J.D. Smith, Don Kalinich, and Jesse Phillips for providing helpful comments and reviews. Matt Denman is acknowledged for contributing to the uncertain parameter discussion in Section 4.4.

CONTENTS

FIGURES

TABLES

ACRONYMS

1F1	Fukushima Daiichi unit 1
1F2	Fukushima Daiichi unit 2
1F3	Fukushima Daiichi unit 3
ANS	American Nuclear Society
BSAF	Benchmark Study of the Accident at the Fukushima Daiichi
BWR	boiling water reactor
COR	MELCOR core package
CVH	MELCOR control volume hydrodynamics package
DCH	decay heat / MELCOR decay heat package
DOE	Department of Energy
ECCS	emergency core cooling system
LOCA	loss of coolant accident
LWR	light water reactor
MACCS	MELCOR Accident Consequence Code System
MCCI	molten corium-concrete interactions
MELCOR	SNL/NRC severe accident code (not an acronym)
MELMACCS	Interface code between MELCOR and MACCS
NRC	Nuclear Regulatory Commission
ORIGEN	Oak Ridge Isotope Generation Code
ORNL	Oak Ridge National Laboratory
PWR	pressurized water reactor
RN	MELCOR radionuclide package
RPV	reactor pressure vessel
SCALE	Standardized Computer Analyses for Licensing Evaluation
SOARCA	State of the Art Reactor Consequence Analysis
SBO	station blackout
SNL	Sandia National Laboratories
SFP	spent fuel pool
TEPCO	Tokyo Electric Power Company
UA	Uncertainty analysis

1 INTRODUCTION

The radionuclide inventory and decay power generated in the fuel are the principal safety problems of severe accidents that assume successful reactor shutdown. Large power reactors, such as pressurized water reactors (PWRs) and boiling water reactors (BWRs), operate at high power and burnup levels; hence the decay power generated by the radionuclides created in the fuel/core is sufficient to drive core uncovering in a matter of hours under severe accident conditions. The subsequent mismatch between decay heat generation and removal rates leads to increased fuel and cladding temperatures, eventually resulting in rapid steam-cladding oxidation reactions (creating even more heat), rapid radionuclide releases from the fuel, and core degradation. The radionuclides may then transport throughout the plant to the environment as vapors, aerosols, and in liquid pools, and are hence the primary cause of radiological safety concerns. PWRs and BWRs contain large quantities of medium and long-lived[1] fission products, actinides, activation products, and decay daughters in the fuel that can be released and transported to the environment following core overheating and plant damage.

Oxidation energy rates between zirconium and steam (or air) can exceed the decay power considerably, even by an order of magnitude, but only for relatively brief time periods. Overall energy production in the shutdown reactor is still dominated by decay power, and it is the decay power that drives increased fuel and cladding temperatures to the point of rapid oxidation with steam or air. Even after the onset of rapid Zircaloy oxidation, decay power can have first-order impacts on key severe accident signatures such as steam and non-condensable gas (H_2 and CO) generation, molten core-concrete interactions (MCCI), release fractions, and event timing (e.g. reactor pressure vessel (RPV) failure and containment overpressure) [1]-[9].

The decay power and inventory information for severe accident simulations are therefore some of the most basic and essential inputs for MELCOR and MACCS [10][11]. Modern neutronics codes can accurately and quickly calculate these quantities for use in MELCOR and MACCS models. SNL has chosen to develop a tool suite that uses ORIGEN-S and Automatic Rapid Processing (ARP) from the SCALE6.1.3 code package [12], along with automation scripts that implement fuel assembly-specific data from the plant to be modeled. The ARP module allows for burnup-dependent (i.e., problem-dependent) cross sections to be used in the ORIGEN-S calculations, and ARP data libraries can be supplied via the TRITON sequence in SCALE. The plant data provides ORIGEN-S/ARP inputs such as overall power level, operating time, local power peaking factors (axial and radial), fuel assembly type and enrichments, burnup distributions, and fuel shuffling schemes. Some of these quantities could in-principal be 'predicted' with a full-scale neutronic analysis; this entails much more detailed steady-state neutron transport, reactivity control, and burnup analyses that are typically outside the scope of generating inventories and decay power for severe accident simulations. Given the availability of sufficiently-detailed plant data, ORIGEN-S/ARP can be used to infer the radionuclide quantities associated with the reactor's operation history and core design, and then perform decay calculations following reactor shutdown to provide decay heat curves for MELCOR models.

[1] In the remainder of the report, the terms short-lived and long-lived are used in relation to severe accident time frames, which are 2 to 7 days for typical MELCOR simulations.

1.1 Overview of Reactor Analysis Methods for Severe Accident Models

Severe accident scenarios for light water reactors (LWRs) typically assume successful reactor shutdown. Otherwise, the severe accident code itself would require some dynamic neutronic capabilities such as point kinetics or transient nodal diffusion; still, neutron transport codes are required to calculate point kinetic parameters, reactivity feedback coefficients, collapsed and homogenized cross sections, and diffusion parameters (diffusion coefficient, discontinuity factors, etc.). MELCOR currently has a point kinetics model, but is not utilized often since most scenarios assume successful reactor shutdown. Therefore, most MELCOR models simply require radionuclide inventory and decay heat information from reactor analysis codes.

There are several codes and methods available that can perform the nuclear reactor calculations necessary to support severe accident models. These codes are best described as 'neutronics' analysis codes, a subset of which are burnup/depletion codes such as ORIGEN-S that describe the time-dependent behavior of nuclides during reactor operation. ORIGEN-S and similar codes (e.g. CINDER90 [13]) solve a system of differential equations that govern the time-dependent quantities of nuclides as a function of: The production rate due to fission, production due to neutron transmutation, production due to decay in-growth from parent nuclides, loss due to neutron absorption, and loss due to radioactive decay (Figure 1.1). Various methods exist to go about solving these equations, the details of which can be found in the SCALE6 and CINDER90 manuals [12][13]. A common assumption is that the cross sections and reaction rates are constant over a time step, which is necessary to reduce the problem to a system of linear and first-order differential equations [12]. In principle, there are functional relationships between atom densities (N), neutron flux (Φ), and one-group cross sections (σ) that would make the equations nonlinear and much more difficult to solve. The neutron flux is a spatial and energy-averaged quantity that is also assumed constant over a computational step, and predictor-corrector algorithms are therefore used that allow for constant power depletion (i.e. time-varying flux) in coupled transport-burnup simulations, which is more representative of the burnup behavior of reactor fuel.

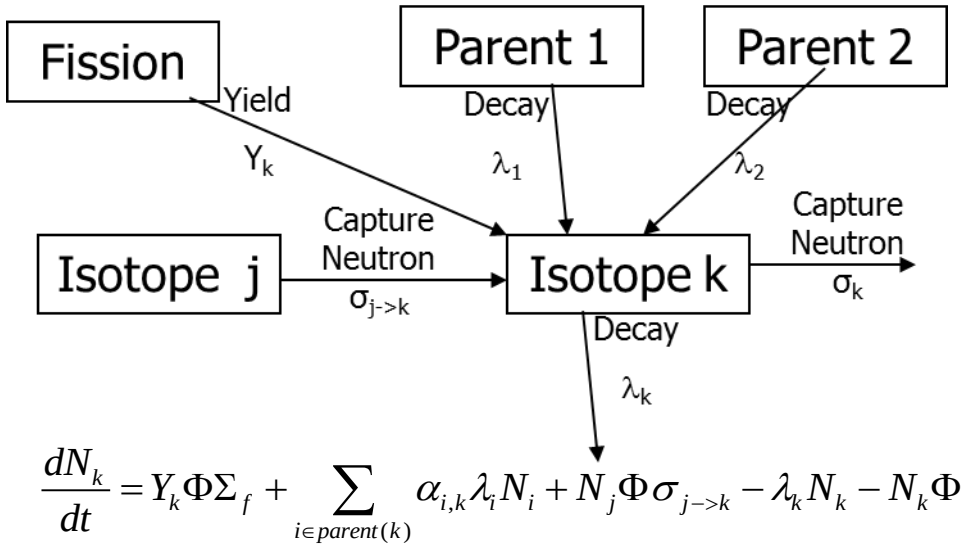

Figure 1.1. Time-dependent processes for buildup and decay of a specific nuclide [14][15].

A depletion code alone cannot accurately represent a reactor without some coupling and information from a neutron transport code. Codes like ORIGEN-S do not directly treat the spatial and spectral domain of the system; hence problem-dependent cross sections are required that reflect the spatial and spectral characteristics of the reactor, and these are calculated by neutron transport codes (e.g. NEWT, KENO, MCNP). Continuous energy or multigroup cross sections are collapsed to one-group values for ORIGEN-S by weighting the cross sections by the problem-dependent flux. The integrated burnup simulation then progresses in time by a cyclical process: starting from an initial neutron transport solution and a set of one-group cross sections, ORIGEN-S performs depletion and decay calculations for a specified time period, thereby calculating new number densities for each nuclide that are then used as input for the subsequent neutron transport calculation for next time step. For neutron transport with multigroup data, problem-dependent multigroup data must first be processed from point-wise data by resonance self-shielding calculations, such as the BONAMI and CENTRM modules in SCALE [12]. The cyclical coupling of neutron transport and depletion/decay calculations forms the foundation of reactor analysis methods that provide time-dependent predictions of core reactivities, flux distributions, and power distributions.

Generally, reactor burnup calculations with neutron transport are rather time-consuming: model setup, code execution, and post-processing can rival the resources required to create and execute severe accident models, which would tend to inhibit regular use of neutronics codes to support severe accident analyses. The CPU resources and user-time required for reactor analysis are naturally very dependent on the fidelity of the codes (e.g. diffusion, discrete ordinates, Monte Carlo) and resolution/size of the reactor model (i.e. full 3D with many axial levels, quarter-core 3D, 2D planar core, or 2D infinite lattice models). Depletion analyses of 2D lattice models can be accomplished on desktops and workstations with reasonable CPU times, while Monte Carlo burnup studies for millions of regions of a core require supercomputing resources.

Fortunately however, standalone ORIGEN-S calculations are indeed possible to support severe accident analyses. Severe accident codes like MELCOR use lumped inventory and decay heat information, and do not require the rigorous details that are necessary for core design or design-basis safety analysis (i.e. for reactivity control and local power distribution). Moreover, nuclide inventories for MACCS are most concerned with fission products that are important for consequence effects, such as Sr-90, I-131, Te-132, and Cs-137. Concentrations for these nuclides are strongly affected by fission yields, the overall power/burnup level of the core, and of course the one-group fission cross sections that can be calculated by neutron transport codes. Fission yields are nearly problem-independent with respect to neutron spectrum, since LWR spectrums tend to be very similar, but overall yields can vary more due to increased fission reactions with other actinides (e.g. Pu-239) as reactor burnup increases.

Of course several important fission products also accumulate due to decay in-growth during reactor operation from other fission/activation products and their daughters. For instance, I-137 ($t_{1/2}$ ~24.5 s) and Xe-137 ($t_{1/2}$ ~3.82 min) are high-yield fission products of thermal U-235 fission, and both contribute to the buildup of Cs-137; I-137 beta decays to Xe-137, which beta decays to Cs-137. After shutdown, continued buildup of Cs-137 due to decay in-growth is insignificant for severe accidents, owing to the much shorter half-lives (and hence smaller inventories) of its parent nuclides. According to ORIGEN-S/ARP calculations presented in

Section 4 of this report, Fukushima unit 3 contained 0.018 g of I-137 and 0.34 g of Xe-137 at shutdown, which are both trivial compared to the 74.1 kg of Cs-137 present at shutdown. Excellent overviews and depictions of the decay chains for all pertinent fission products for severe accidents can be found in Reference [16].

Several actinides that are important for health effects, such as Pu-238 and Pu-241, are formed in actinide burnup/decay chains (Figure 1.2) following irradiation of uranium. Compared to key fission products, several actinides like Pu-238 and Pu-241 can be relatively challenging to predict well even with highly mechanistic codes [17]. Assuming data libraries are available that adequately represent the involved cross sections (i.e. parasitic absorptions relative to fission), these nuclides can be calculated by standalone ORIGEN-S models with reasonable accuracy for gross core inventories. Pu-241 (10-15% of LWR plutonium) is formed mainly by successive Pu-239 n-gamma reactions, where Pu-239 is from n-gamma reaction of U-238 to U-239, which beta decays to Np-239, which then beta decays to Pu-239. U-239 and Np-239 are also very important for decay heating. The accurate prediction of Pu-241 production using ORIGEN-S depends on the effective Pu-240 absorption cross section, which varies considerably with burnup (see Figure D1.3.3 in the SCALE6 manual [12]). Thus, burnup-dependent cross sections are required for a faithful calculation of Pu-241 production. Pu-241 is also produced to a lesser degree by n-2n reactions with Pu-242 and alpha decay of Cm-245, as shown in Figure 1.2.

The production of Pu-238 in LWRs is more complicated and can be relatively challenging to predict at higher burnups, even with high-fidelity methods [17]. Pu-238 (1-2% of LWR plutonium) is a daughter product of Cm-242 alpha decay; Cm-242 is formed by Pu-241 undergoing beta decay to Am-241, which can then absorb a neutron to become Am-242, which subsequently undergoes beta decay to Cm-242. Pu-238 is also a beta-decay product of Np-238 that comes from n-gamma reactions with Np-237; Np-237 is the beta daughter of U-237, and Np-237 arises in rather significant quantities in Fukushima unit 3 (see Figure 6.7 in Section 6.2) from neutron absorptions with U-235 and U-236. The burnup and decay chains of important actinides for LWRs are depicted in Figure 1.2. It depicts the details involved with the production of key actinides for consequence analysis with MACCS, such as Pu-238 and Pu-241.

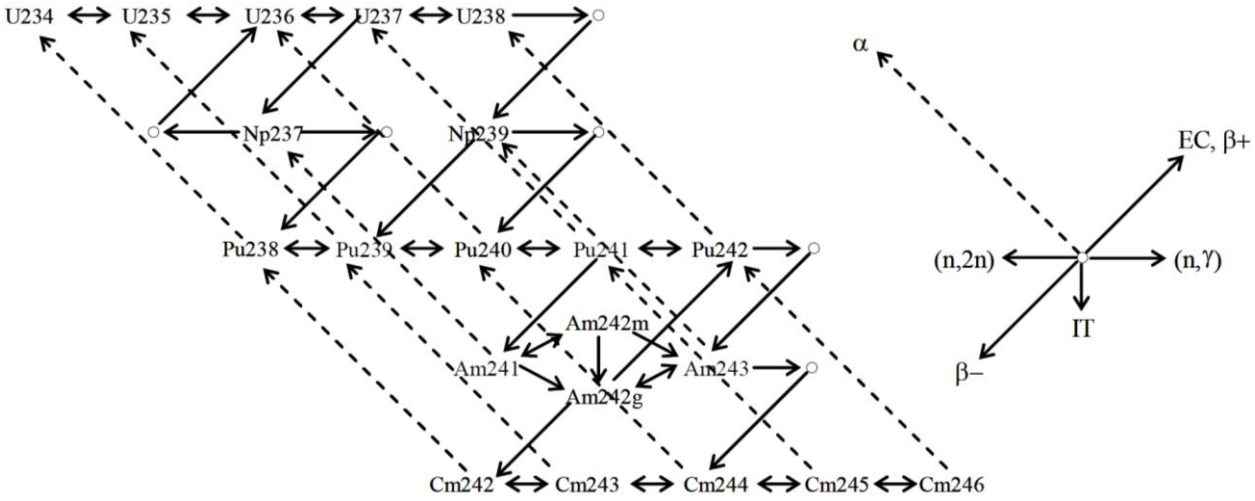

Figure 1.2. Burnup and decay chains for actinides [18].

There are other nuclides important for consequences that are not direct fission products or actinides. An example is Cs-134 ($t_{1/2} \approx 2$ years), which is produced almost entirely by neutron transmutation of Cs-133, a stable fission product with high fission yield. There is also no production of Cs-134 due to decay since Xe-134 is stable. ORIGEN-S calculations for Cs-134 production therefore depend on the flux-weighted cross section for neutron absorption by Cs-133. Another example is Ag-110m ($t_{1/2} \approx 250$ days), which is also produced by neutron activation of other fission/decay products (e.g. Ag-109, which is stable, accumulates to high inventories) and in silver structural materials. Ag-110m is also not a direct decay product since Pd-110 is stable. Such nuclides can be accounted for using standalone ORIGEN-S analyses with adequate cross section libraries–this is demonstrated in Section 4.3 and Section 5.2.3 in this report.

Through careful generation of cross section libraries, standalone ORIGEN-S calculations can provide fast and accurate inventory and decay heat information for severe accident models. The use of other SCALE modules, such as the Automatic Rapid Processing (ARP) module, can facilitate this process. ARP estimates problem-dependent cross sections by interpolating between data libraries available at discrete levels of enrichment, burnup, and void fraction. The use of ARP with ORIGEN-S allows burnup-dependent cross sections such as Pu-240 absorption to be considered in the depletion analysis. The ORIGEN-S/ARP data libraries must still be generated by a coupled depletion analysis, such as the TRITON sequence in SCALE. If simple 2D lattice models are used in the TRITON calculations, such as NEWT models, then the generation of the ORIGEN-S/ARP libraries from TRITON can be completed on desktops or workstations. Depending upon the number of enrichments, void fractions (for BWRs), and the range of burnups considered, this process may take a few hours to a couple days to complete. Much of this effort can be accelerated by distributed processing, and codes like NEWT have some capability for shared memory (openMP) parallelism to further reduce CPU time.

1.2 SNL Historical Treatments of Decay Heat and Inventory

The SNL treatments for decay heat and inventories in MELCOR have not been reevaluated with rigorous, documented analyses since 1985. These methods and any assumptions involved are therefore reviewed in this work to support the new SNL methodology for automated inventory and decay heat processing of MELCOR inputs. Such a review is commonsense considering the advances in modern neutronic codes, nuclear data, and computing capabilities.

Large gains in CPU speed and memory, and the prevalence of massively distributed/parallel systems, over the past three decades has enabled reasonably-detailed depletion calculations to be performed with minimal CPU time. Standalone ORIGEN-S calculations can be completed for hundreds to thousands of regions of a core (assuming adequate data libraries are available) – i.e. for each fuel assembly in a large LWR (150 to 700 assemblies) and for several axial levels – in about 1 hour on a modern processor. For example, for the results presented in Section 4.3, 548 ORIGEN-S/ARP calculations are performed to generate a complete radionuclide inventory for Fukushima Unit 3, which amounts to 1 input model per assembly. Each ORIGEN-S/ARP simulation entails up to 40 irradiation cycles (for burnup-dependent cross sections) and several decay calculations. The entire process, including post-processing for MELCOR/MACCS inputs, takes roughly 30 minutes on one thread of a 3.30 GHz Intel Xeon E5-2667-v2 processor. Since each calculation is essentially decoupled and independent, distributed processing could be used

to reduce the CPU expenditure to a few minutes. Burnup calculations with codes like ORIGEN-S are only time-consuming when executed for millions of regions of a very high-fidelity neutronic model–even then, distributed processing is typically used to drastically reduce the CPU time of the depletion calculations since each regional depletion is independent. The spatial interdependence between burnable regions is usually treated wholly by the steady state transport calculations.

Some key assumptions involved in the historical SNL formulations for inventories and decay heat in MELCOR/MACCS are reviewed in Section 6. The class abstractions necessary for 1980s computing capabilities are compared to calculations by modern codes (SCALE6) and nuclear data (ENDF-B/VII.1). It is confirmed that the historical assumptions required for source term and consequences are largely valid for severe reactor accidents of proper simulation times, which are typically less than seven days after shutdown. There exist other assumptions and simplifications, such as radiation effects on radionuclide speciation and parent/daughter decay heat partitioning, which require further analyses to confirm or refute. These topics are also discussed briefly in Section 6.

1.3 Report Structure and Purpose

In addition to documenting the new SNL methods for decay heat and inventory analysis, this report is intended to act as a rudimentary reference guide for users who need to implement consistent inventories and decay power inputs for MELCOR and MACCS. It seeks to guide users to the appropriate sections of the more detailed reference manuals for MELCOR and SCALE, while providing sufficient material to assist new users in analyzing SCALE outputs for streamlined creation of MELCOR and MACCS inputs.

A review of the input records in MELCOR and MACCS necessary for user-defined inventories and decay heating is presented in Section 2. The new SNL methodology for automated input creation, execution, and post-processing of ORIGEN-S/ARP models is discussed in Section 3. The application of the tool for generation of unit-specific Fukushima inventories and decay powers is presented in Section 4. Application of the tool to historical SNL MELCOR models, such as the Peach Bottom and Surry reactors, is given in Section 5. The review of historical SNL approximations required for MELCOR and MACCS inventories and decay power is given Section 6. Section 7 provides a summary of the new SNL tools and of the various findings in the report.

2 OVERVIEW OF MELCOR AND MACCS INPUTS FOR INVENTORIES AND DECAY HEAT

Three fundamental but separate sets of input records are used by MELCOR and MACCS to account for radionuclide inventory and decay heating. It is the user responsibility to ensure consistency between the separate inputs. These inputs are:

1. Chemically and physically lumped inventories used by the MELCOR radionuclide (RN) package. These are called RN classes.
2. RN class specific decay powers and overall core decay power in MELCOR. Decay power inputs are specified mostly in the MELCOR decay heat (DCH) package.
3. MACCS isotopic inventories (via MELMACCS) to decompose the lumped MELCOR source term.

The input for lumped MELCOR RN inventories is discussed in Section 2.1. MELCOR decay heat input is described in Section 2.2. Lastly, the isotopic inventory input for MELMACCS and MACCS is reviewed in Section 2.3.

2.1 MELCOR Input for User-defined RN Inventories

MELCOR performs radionuclide transport calculations using a handful of RN classes to reduce the computational effort of the simulation. MELCOR was initially developed in the 1980s; hence 1980s computational capabilities precluded the distinct transport and tracking of hundreds or thousands of unique RN species. The problem domain can quickly become intractable for serial computing of many species, aerosol bins, and reactions over hundreds of control volumes and flow paths – plus such calculations need to be performed for millions of time steps for severe accident source term calculations. Therefore, MELCOR lumps the fission products, actinides, activation products, and decay daughters based on the elemental classifications shown in Table 2-1.

Table 2-1. Element compositions for base MELCOR RN classes

Class Name	Representative	Member Elements
1. Noble Gases	Xe	He, Ne, Ar, Kr, Xe, Rn, H, N
2. Alkali Metals	Cs	Li, Na, K, Rb, Cs, Fr, Cu
3. Alkaline Earths	Ba	Be, Mg, Ca, Sr, Ba, Ra, Es, Fm
4. Halogens	I	F, Cl, Br, I, At
5. Chalcogens	Te	O, S, Se, Te, Po
6. Platinoids	Ru	Ru, Rh, Pd, Re, Os, Ir, Pt, Au, Ni
7. Early Transition Elements	Mo	V, Cr, Fe, Co, Mn, Nb, Mo, Tc, Ta, W
8. Tetravalent	Ce	Ti, Zr, Hf, Ce, Th, Pa, Np, Pu, C
9. Trivalents	La	Al, Sc, Y, La, Ac, Pr, Nd, Pm, Sm, Eu, Gd, Tb, Dy, Ho, Er, Tm, Yb, Lu, Am, Cm, Bk, Cf
10. Uranium	U	U
11. More Volatile Main Group	Cd	Cd, Hg, Zn, As, Sb, Pb, Tl, Bi
12. Less Volatile Main Group	Sn / Ag	Ga, Ge, In, Sn, Ag
13. Boron	B	B, Si, P

The user must specify input on the DCH_CL, DCH_EL, and RN1_FPN records for user-defined inventories that do not use any pre-generated data in MELCOR. MELCOR contains some limited internal capabilities to estimate RN inventories and decay powers; these internal models, which are discussed more in Section 5.1, are not applicable to best-estimate severe accident simulations of modern nuclear plants.

2.1.1 MELCOR DCH_CL and DCH_EL Inputs

The DCH_CL record specifies the names of the user-defined class and its constituent elements. The elements are given masses and specific decay power curves (W/kg) on the DCH_EL records. The class mass for the DCH package is therefore the summation of its element masses over the appropriate DCH_EL records. If no elements are specified on DCH_CL for a class ('DEFAULT' instead of a 'USER' class), then MELCOR searches for DCH_EL records for the default elements in the class (Table 2-1); this only works correctly if the user-defined class is one of the following default character strings listed in Table 2-2, which are case-sensitive:

Table 2-2. MELCOR RN class default names on DCH_CL

Class Name	Representative	Default DCH_CL string
1. Noble Gases	Xe	'XE'
2. Alkali Metals	Cs	'CS'
3. Alkaline Earths	Ba	'BA'
4. Halogens	I	'I2'
5. Chalcogens	Te	'TE'
6. Platinoids	Ru	'RU'
7. Early Transition Elements	Mo	'MO'
8. Tetravalent	Ce	'CE'
9. Trivalents	La	'LA'
10. Uranium	U	'UO2'
11. More Volatile Main Group	Cd	'CD'
12. Less Volatile Main Group	Sn / Ag	'AG'
13. Boron	B	'BO2'
16. Cesium iodide	Cs and I classes	'CSI'
17. Cesium molybdate	Cs and Mo classes	'CSM'

In MELCOR 2.1, it is currently required to specify user-defined RN classes using the class names from Table 2-2 as they appear exactly, even if the element constituents are entirely redefined by the user. The cesium iodide class is a combination of the alkali metal and halogen groups; hence it reflects CsI in addition to other combinations of the classes' member elements, such as RbBr; i.e., over 10% of the alkali metal (Cs) class is rubidium (mostly Rb-87), and about 10% of the halogen (I_2) class is composed of bromine isotopes (namely Br-81). The same logic applies to the cesium molybdate (Cs_2MoO_4) class, which is a combination of the alkali metal and transition metal classes–some of the mass for the combination class is rubidium and technetium (about 20% of the transition metal (Mo) mass is technetium isotopes). A more detailed

discussion on isotopic compositions of the classes is given by Section 6.2. Class numbers 14 and 15 are reserved for water and concrete aerosols that can be modeled by the RN package.

Both user-defined and 'DEFAULT' RN classes must use the DCH_CL names listed in Table 2-2. The input records below demonstrate acceptable and unacceptable input records for the less volatile main group (Sn/Ag). MELCOR and MELGEN may be able to process 'unacceptable' input, but the processed input model will not match the user's actual input specifications. The class names must be exactly specified in MELCOR, while the elements names are rather flexible:

```
DCH_CL 'AG' DEFAULT ! acceptable –class is totally default

DCH_CL 'AG' USER 1  ! acceptable –user defined class with proper name
            1 'Ag'

DCH_CL 'AG' USER 1  ! acceptable –proper class name, element name is flexible
            1 'AG'

DCH_CL 'AG' USER 1  ! acceptable –proper class name, element name is flexible
            1 'Sn'

DCH_CL 'AG' USER 1  ! acceptable –proper class name, element name is flexible
            1 'SN'

DCH_CL 'Ag' DEFAULT ! unacceptable – class name must be AG, not Ag

DCH_CL 'Ag' USER 1  ! unacceptable – class name must be AG, not Ag
            1 'Ag'

DCH_CL 'SN' USER 1  ! unacceptable – class name must be AG
            1 'Ag'

DCH_CL 'Sn' USER 1  ! unacceptable – class name must be AG
            1 'Sn'
```

The element members of the user-defined classes can be the actual default elements, as listed in Table 2-1, or the user can simply specify a single 'fictitious element' that actually represents all of the elemental mass and decay heating for the class. For example, the SOARCA-style input for RN inventories redefined each RN class from Table 2-2 and assigned each a single lumped element; each element's DCH_EL input has mass and decay power that actually represents all of the elements in the class. This method allows for shorter and more legible MELCOR input records, but it does require some more post-processing of ORIGEN outputs–i.e. the ORIGEN-predicted masses and decay power over the elements can be readily extracted using OPUS in SCALE6, but then this elemental data requires summation into the RN classes from Table 2-1. Alternatively, if the user does not mind lengthier MELCOR input records, the user can input DCH_EL tables for each element from Table 2-1 individually. In this case, the elements should be linked to the appropriate classes manually via DCH_CL 'USER' input records or by specifying 'DEFAULT' for each DCH_CL record; either way MELCOR will simply add up the elemental data to create overall class masses and decay powers.

2.1.2 RN Spatial Distribution Input in Fuel

The spatial distributions of each RN class are specified on the RN1_FPN card. MELCOR allows this input to be rather flexible: the user may specify absolute masses for each class over each COR cell, or the user may specify simple radial and axial multipliers to be used for all classes. The use of the radial and axial multipliers facilitates capturing the exact desired decay power distribution with less input. When specifying the absolute RN masses over all COR cells, the user must be careful to preserve the total class masses while also allocating the nodal masses appropriately to create the desired decay power distribution. Since modern MELCOR models may contain 50 or more COR cells for the active fuel region, the specification of nodal masses for 15 (or more) RN classes results in rather lengthy input records that probably requires user-automation to ensure input consistency.

2.1.3 RN Spatial Distribution Input in Fuel-cladding Gap

The RN1_GAP record specifies the RN class masses that are initially in the fuel-cladding gap. The user can specify unique mass fractions for each class and each COR cell. Most MELCOR models simply specify global values for the fuel-cladding gap inventories for a single COR cell; the global values are then copied over to the entire COR nodalization by usage of 'CELL' inputs on RN1_GAP, followed by the appropriate index (ring, level) of the reference COR cell. Unique gap fractions may be specified for different core rings, but the axial distributions are rather inconsequential since MELCOR releases the gap inventory for all levels in a ring simultaneously after clad rupture. RN1_GAP input is demonstrated below for a core model with 3 rings and 6 axial levels and with gap inventories informed by NUREG-1465 [19]:

```
RN1_GAP 22! r, z input class  refindex frac1  frac2
         1  1  6 CLASS  'XE'            0.05   1.0 ! 5% noble gas in gap
         2  1  6 CLASS  'CS'             1.0   1.0 ! all CsOH is in gap
         3  1  6 CLASS  'BA'            0.01   1.0 ! 1% barium class in gap
         4  1  6 CLASS  'TE'            0.05   1.0 ! 5% Te in gap
         5  1  6 CLASS 'CSI'            0.05   1.0 ! 5% of CsI in gap
         6  1  7  CELL          1 6      1.0
         7  1  8  CELL          1 6      1.0 ! all cells use cell(1,6) inputs
         8  1  9  CELL          1 6      1.0
         9  1 10  CELL          1 6      1.0
        10  1 11  CELL          1 6      1.0
        11  2  6  CELL          1 6      1.0
        12  2  7  CELL          1 6      1.0
        13  2  8  CELL          1 6      1.0
        14  2  9  CELL          1 6      1.0
        15  2 10  CELL          1 6      1.0
        16  2 11  CELL          1 6      1.0
        17  3  6  CELL          1 6      1.0
        18  3  7  CELL          1 6      1.0
        19  3  8  CELL          1 6      1.0
        20  3  9  CELL          1 6      1.0
        21  3 10  CELL          1 6      1.0
        22  3 11  CELL          1 6      1.0
```

2.1.4 MELCOR RN Masses and Radioactive Decay

MELCOR does not account for time-dependent RN masses with respect to radioactive decay. Thus the RN inventories are notionally a snapshot of the core inventory at a particular time, which is usually chosen to be the moment of shutdown for reactor analyses. As discussed more in Section 6.2, lumped RN masses do not vary considerably *soon* after shutdown, so the approximation of constant RN masses is valid for severe accident simulations of reactors that are typically 1 week after shutdown. However, this approximation may not be appropriate for spent fuel pool (SFP) source term analysis, whereby RN masses can vary significantly due to the long cooling times involved.

2.2 MELCOR Input for User-defined Decay Heat

MELCOR requires input records for the specific decay powers of the constituent elements in each class. These inputs are specified on the DCH_EL records, where class decay power (W) is normalized to the initial class inventory (kg). The mass inventories are constant with respect to decay time after shutdown, and they include the masses of stable fission products and decay daughters. The inventory summation calculations and assumptions are discussed more in Section 3.3 and Section 6.2.

In general, the total power derived from the class inventories and specific decay powers equals the overall core decay heat curve that the user should also specify on a tabular function (TF) and link to the DCH_DPW record. To allow for scram at any time during the transient, the user should actually link a control function (CF) to DCH_DPW that determines the appropriate time-dependent decay power as a function of time since shutdown; this is accomplished by using a trip CF that monitors other logical CFs that signal reactor scram. A simple example of the input records required to accomplish this is given below:

```
CF_ID 'T>SCRAM' 801 TRIP          ! this CF is the time (s) since shutdown
CF_SAI 1.0 0.0 0.0
CF_ARG 1
       1 CF-VALU('CF_900.SCRAM') ! 'CF_900.SCRAM' = logical SCRAM signal CF

CF_ID 'decayPower' 999 TAB-FUN    ! this is the total power given to DCH_DPW
CF_SAI 1.0 0.0 1.4987e+08         ! steady state decay power = 149.87 MW
CF_MSC 'tf_DECAY'                 !'tf_DECAY' = the TF for overall decay power
CF_ARG 1
       1 CF-VALU('T>SCRAM') 1.0 0.0 ! time since scram

DCH_DPW CF  'decayPower'          ! DCH package input
```

Ideally, the decay powers from the DCH_EL and DCH_CL inputs will sum to the total decay power on the CF/TF input (i.e. `'decayPower'` in the above example) linked to DCH_DPW. However, certain MELCOR simulations may call for quick and dynamic modification of the overall core decay heat. An example is uncertainty analysis that may treat the decay heat as an uncertain parameter–the overall decay heat curve on the CF/TF input can be quickly varied by simple multipliers from other control functions. To facilitate such analyses, the DCH_NRM record can be specified to ‘YES’ to force the total decay power from DCH_EL and DCH_CL inputs to equal the total decay power supplied to DCH_DPW via CF/TF input. The DCH_NRM

option equally scales each class decay power (but not the masses) in order to force consistency between DCH_EL, DCH_CL, and DCH_DPW inputs.

With the RN package active in MELCOR, the decay power distribution is not automatically identical to the operating power distributions specified on COR_ZP and COR_RP records. The decay power distribution is instead determined by the RN1_FPN, DCH_CL, and DCH_EL inputs. The DCH_CL and DCH_EL records determine the total mass and specific decay power of each class, and RN1_FPN defines the spatial distribution of RN masses in the fuel for each COR cell. By default, this forces decay power to conform to the spatial allocations of RN class masses–this assumption is further discussed in Section 6.1. Some decay power and mass may also be apportioned to the fuel-clad gap by the RN1_GAP input record.

2.3 MELMACCS Input for MACCS Inventory

MACCS requires isotopic breakdowns of the RN classes present in the MELCOR source term output. It accomplishes this task through a pre-processing program called MELMACCS, which takes user-inputted masses and activities for nuclides separated by ORIGEN-S output libraries (i.e. light elements, actinides, and fission products) and reactor model type. MELMACCS does not contain nuclear decay data such as decay constant so it requires both nuclide mass and activity. The nuclide masses were historically used to linearly scale the activities for each nuclide by comparing the appropriate class mass from the MELCOR plot file to the class mass in MELMACCS, which is calculated by summing the applicable user-specified nuclide masses. This process allowed for rough usage of inconsistent source terms and nuclide inventories, if desired. However, the SNL process for automatic generation of consistent MELCOR and MACCS inventories directly from ORIGEN-S output supersedes the need for the scaling algorithm. After summation over the appropriate elements and over the ORIGEN-S libraries, the isotopic masses in the MELMACCS input correspond perfectly with the RN class masses in the MELCOR input and output files (i.e. the MELCOR plot file).

3 METHODS FOR AUTOMATED GENERATION OF SEVERE ACCIDENT INVENTORIES AND DECAY HEAT

Best-estimate analyses of severe nuclear accidents and consequences using MELCOR and MACCS require radionuclide inventories at shutdown and decay heat curves as a function of radionuclide class and time after shutdown. SNL has developed automated processes that use ORIGEN-S/ARP in the SCALE6 code package in conjunction with Perl automation scripts to efficiently create input records for MELCOR and MACCS. TRITON may optionally be used in this process to generate ARP data libraries for specific fuel assembly geometry, radial core location (e.g. assemblies adjacent to the reflector), axial core location (for void fraction considerations), and fuel/poison zoning. The SNL method creates, executes, and post-processes ORIGEN-S/ARP models to automatically generate consistent input records in MELCOR and MACCS. The SNL scripts are versatile enough to allow for different user options concerning spatial allocation of MELCOR RN mass and decay power, summation algorithms of RN inventories, and MELCOR input printing.

The SNL methods use ORIGEN-S/ARP to analyze the whole core (i.e. a single input model) or several regions of the core (i.e. several input models) in order to provide MELCOR with spatial distributions of RN mass and decay power. Even with proper usage of TRITON to supply the ARP libraries, this process does not 'predict' core behavior as a more system-level neutronic simulation would–there are no predictions of reactivity and core-wide neutron balance. The real core performance information comes from the plant data that is used to as input for the ORIGEN-S/ARP models. The plant data may be from the plant process computer and/or from core neutronic simulations, which naturally include depletion calculations of some kind that are performed by the operator, vendor, or a contractor. The SNL processes use ORIGEN-S/ARP to simply 'infer' the radionuclides inventories associated with known reactor operation. Moreover, the analysis of several core regions is only intended to supply MELCOR with spatially resolved inputs for decay heat and inventory, and is not meant to improve overall predictions compared to simpler whole-core calculations.

Some prerequisite processing of plant data is required for the Perl scripts; this pre-processing is discussed in Section 3.1. The automated creation of ORIGEN-S/ARP input files is presented in Section 3.2. The execution and automated post-processing of ORIGEN-S output quantities is given in Section 3.3.

3.1 Pre-processing of Plant Data

The SNL method assumes plant data is available for each fuel assembly and for a sufficient number of cycles. A particular cycle or a 'generalized' equilibrium cycle may be chosen to be the time of the severe accident initiator. Sufficient irradiation history for all fuel assemblies present in the core for this cycle is required by the SNL method. In modern LWR cores, fuel assemblies may be irradiated for up to three or more cycles. For example, typical US PWRs irradiate most fuel assemblies for three cycles–some assemblies may be burned for less time for various reasons (e.g. fuel depletion, cladding corrosion, CRUD) while others may be stored in the SFP and used in later cycles. The Fukushima Daiichi reactors contained several high burnup fuel assemblies that were irradiated in more than three cycles.

The SNL method uses a Perl script to generate unique ORIGEN-S/ARP input files for each fuel assembly in the cycle of interest, i.e. the cycle that experiences the severe accident. The Perl script reads an ASCII input file that contains the following information for each fuel assembly:

- The fuel assembly type and enrichment;
- The location of the fuel assembly in the core relative to the radial nodalization of the MELCOR COR model;
- The axially-integrated relative power fraction of the assembly for the final irradiation period. This is assumed to be the average of the BOC and the EOC power fractions, where EOC is the time of scram just before the accident (the BOC and EOC values are nearly the same for most assemblies);
- The number of previous irradiation cycles for fuel assemblies that are not fresh at BOC of the cycle of interest;
- Overall irradiation history in the form of BOC, MOC, and EOC burnups, which is especially necessary if the exact number of previous cycles and cycle-dependent power histories are unknown for each assembly.

The type of the fuel assembly determines the appropriate ARP data library to use in the ORIGEN-S input models for each fuel assembly. Most of the reactor physics pertaining to geometry and spectral effects on burnup behavior, such as spatial and energy self-shielding effects, are captured by the flux-weighted cross sections in the ARP library, which can be a function of burnup. The TRITON sequence in SCALE can generate ARP libraries for ORIGEN-S. The TRITON sequence allows for integrated lattice physics and burnup analysis by automatically coupling cross section processing modules (e.g. CENTRM), neutron transport modules (e.g. NEWT), and the depletion modules (e.g. COUPLE and ORIGEN-S) for the user. Several TRITON models can be executed for a range of enrichments, void fractions (for BWRs), and burnup level to provide a general-use ARP library for variable reactor operation.

For the Fukushima and Surry calculations presented in this report, plant data on a fuel assembly basis is available and mapped over the unique MELCOR core nodalizations for each model. The plant data was originally in the form of Excel spreadsheets; thus simple Visual Basic scripts can be used to pre-process and map the data onto MELCOR COR rings, as shown by Figure 3.1.

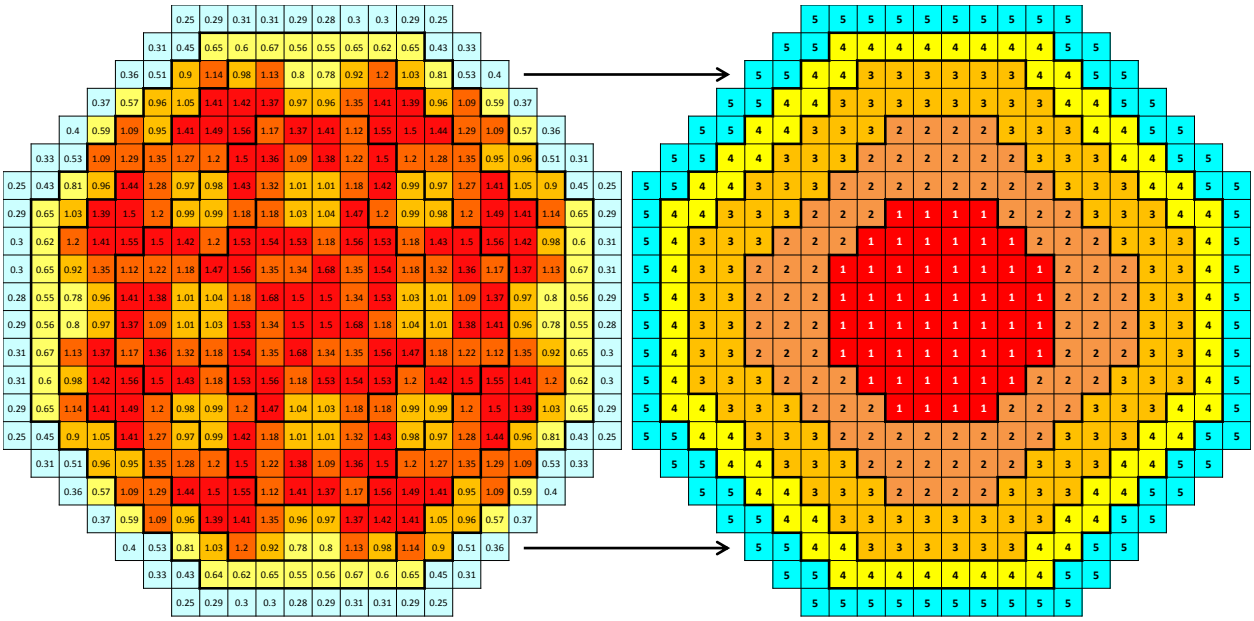

Figure 3.1. Mapping of plant data and ORIGEN-S predictions to MELCOR COR rings.

3.2 Automated Creation and Execution of ORIGEN-S/ARP Input Files

The distinct information for each fuel assembly is used to populate ORIGEN-S/ARP template input files that are pre-generated manually with some assistance from the ORIGEN-ARP GUI. The template files contain simple character strings that are replaced with fuel assembly data by the SNL Perl script. Currently five template input files are available for fresh fuel and for fuel that has been irradiated in one to four prior cycles, and one template input file is available for MOX fuel. Each complete cycle is subdivided into ten ORIGEN-S irradiation sub-cycles to allow for burnup-dependent cross sections. Each sub-cycle is further divided into ten timesteps. Each complete cycle is also separated by a 30 day decay cycle, which can be easily modified by the user if necessary. The final complete cycle in each template is always assumed to be the cycle that experiences the severe accident. After the final shutdown, which is variable and specified by user input for the Perl script, the template file has ORIGEN-S/ARP input for a final decay period extending to 300 hours and with a sufficiently detailed time-mesh for accurate decay heat information for MELCOR. Additionally, each template file has input that prints the radionuclide inventory in units of mass and activity at the moment of final shutdown, and the decay power curves for each element.

3.2.1 Input Creation

An ASCII data file is read by the Perl script that contains the fuel assembly data from the plant. The text data file currently specifies the fuel quantities denoted by the character variables in Table 3-1. The Perl script reads the data fields adjacent to the variable strings to generate the ORIGEN-S/ARP input files. The script is versatile enough such that the information in Table 3-1 can be for the whole core, lumped batches, each fuel assembly, or for each fuel assembly at several axial nodes. No matter the desired level of spatial resolution, the Perl script will create the necessary number of ORIGEN-S/ARP input files to represent the input data. The process assumes the appropriate ARP data libraries exist to properly characterize each region of the core.

Some other important user-specified quantities for the creation of ORIGEN-S/ARP input files, such as the final cycle operating time and total thermal power level, are currently specified directly in the Perl script by the Perl variables listed in Table 3-2.

Table 3-1. ASCII input fields to provide plant data to the Perl script.

Variable string	Description
n	Arbitrary fuel assembly or region index
x,y or ID	2D coordinates or fuel assembly ID
FAtype	Indicates the ORIGEN-S/ARP data library to use and the fuel assembly fuel loading (i.e. metric tons of heavy metal)
CORring	MELCOR COR ring location
BurnupBOC	BOC burnup (GWd/t) for the last cycle
BurnupEOC	EOC burnup (GWd/t) for the last cycle
diffBurnup	Cycle differential burnup (GWd/t) for the last cycle
BOCpower	BOC power fraction for the last cycle
EOCpower	EOC power fraction for the last cycle
priorBOCburnTime or Ncycle	Previous total irradiation time (days) or number of cycles

Table 3-2. User options for ORIGEN-S/ARP input creation using the SNL Perl script.

User input Perl variable	Description
$finalIrradiation	The final irradiation time (days) for the primary cycle of interest, which should be the cycle that experiences the severe accident initiator
$totalMTHM	Total metric tons of heavy metal (U+Pu+Am) initially loaded in the core; used to derive a core-average specific power level
$power	Thermal power level (MW), which is currently treated as constant for all cycles
$nAssemblies	Number of fuel assemblies in the core. The script will also count the number of fuel assemblies listed in the $dataFile file (Table 3-1) and report an error if these two values are not equivalent
$dataFile	File name for the ASCII input file containing the information listed in Table 3-1

A listing of the template input files for the Fukushima reactors is given in APPENDIX A. The templates for the Surry reactor are essentially the same, excluding modification of the assumed light element loadings that are of secondary importance for severe accident inventories. MELCOR and MACCS currently do not model radioactive releases from activated structural materials such as Co-60. The release models in MELCOR (e.g., CORSOR-Booth) treat RN releases from fuel as a diffusion process through spherical fuel grains. Vapor and aerosol masses from structural releases can be roughly approximated by the fuel release models through clever implementation of release multipliers (which are user-specified), but the structural releases are still treated as ‘nonradioactive’ and are only considered for their contribution to the radionuclide transport calculations for the RN classes emanating from the fuel. Light element masses for fuel structures can be optionally included in the ORIGEN-S/ARP models and later sifted out of the RN class masses by the Perl script–this ensures that the RN masses in MELCOR and MACCS only represent the inventory of radionuclides residing in the fuel or fuel-cladding gap.

3.2.2 Execution of Many ORIGEN-S/ARP Input Files

ORIGEN-S/ARP can be executed for all input files in a working directory by using SCALE6 in batch mode (in Linux or Windows):

```
batch6.1 *inp
```

The runtime involved for a single ORIGEN-S/ARP model is quite reasonable, even for cases with 30-40 irradiation cycles and several other decay cycles. Thus serial processing can execute 548 ORIGEN-S/ARP simulations for a Fukushima unit 2/3 calculation in about 30 minutes to 1 hour, depending upon the quality of the processor. Nonetheless, distributed processing of the jobs over several cores and/or processors can be used to reduce execution time to a few minutes since each calculation is essentially decoupled and independent. Even with very high fidelity neutronic models, the spatial interdependence between burnable regions is usually treated wholly by the steady state transport calculations. The depletion calculations can therefore be simply parallelized via distributed processing.

3.3 Automated Processing for MELCOR and MACCS Input Generation

After successful execution of all ORIGEN-S/ARP input files, the Perl script locates and reads all ORIGEN-S/ARP output files (i.e., *.out files) and the associated OPUS output files. OPUS is a SCALE auxiliary tool that is used to assist with some post-processing, such as extracting element-based decay powers, which are later lumped into MELCOR RN class decay powers and an overall core decay power.

3.3.1 User Input Options for Perl Script

Located at the top of the Perl script are variables that the user can modify to allow for proper post-processing of different problems. These input options could also be read from an input file with minor script modifications. There are user options for various methods of radial RN mass and power allocation in MELCOR. The radial distributions of lumped RN mass and decay power soon after shutdown are not necessarily similar in LWRs due to modern fuel shuffling techniques. In fact, lumped RN mass and decay power can have inverse radial distributions throughout the core, depending on the operating power distribution, burnup distribution from fuel shuffling and the current cycle burnup, and the chosen radial nodalization of the core. A prime example is given in the next paragraph. The user can request that all RN class masses be radially distributed according to the decay power distribution or according to the exact ORIGEN-S predictions. Alternatively, the user can request a combination of options that is effectively a compromise: the script allocates most RN mass according to the radial power distribution, while preserving the true radial mass distribution for key RN classes such as alkali metal (Cs) and tetravalent (Pu) classes. This way the desired decay power distribution is mostly captured, and the true radial distributions of long-lived nuclides important for consequence effects are also modeled.

The radial distribution of the alkali metal (Cs) class can be opposite the decay power distribution due to the shuffling of high burnup assemblies to the outer core periphery. The alkali metal class mass is dominated by Cs-133 (stable) and Cs-137 ($t_{1/2}$ ~ 30 years); both of these nuclides build continually with burnup, and thus the alkali metal class mass and its key nuclides (Cs-137) can

be concentrated in the outer high burnup regions of the core and not the inner high power regions. Similarly, the tetravalent class mass is mostly comprised of plutonium isotopes (namely Pu-239 and Pu-240) that accrue with burnup, and can also be concentrated in the outer, higher burnup rings of the core. The halogen (iodine) class could also be treated in such a fashion, but its key nuclides for health effects are relatively short-lived (e.g., I-131, I-133, I-135) and are therefore distributed more by recent power density; distributing the halogen class mass by power allows for capturing the spatial distribution of the important nuclides for health effects, but will also result in incorrect radial distributions of I-129, I-127, and Br-81, which are the principle mass contributors in the halogen class that depend more on integral burnup and the number of assemblies in the ring. Basically, all RN-class mass increases monotonically with burnup (excluding uranium of course) and not recent local power density, due to the steady accumulation of long-lived and stable isotopes. Some RN mass must still be distributed according to the decay power due to modeling limitations in MELCOR (see Section 6.1)– otherwise the MELCOR model will exhibit an inverse decay power distribution that can have physically unrealistic effects on thermal-hydraulics, core degradation, and RN release calculations.

The uranium class mass, which generally contributes just 0.3% to 2.0% of the whole-core decay power, is always distributed according to the ORIGEN-S/ARP predictions. Some uranium mass is depleted by neutron absorptions (e.g., fission and transuranic production), but overall uranium mass remains mostly as U-238, and the ring-based totals are essentially proportional to the initial MTU loading and the number of assemblies in the ring. Additional user-options for allocating RN masses will be implemented in future work as the need arises; these may include further control over the radial allocation of each RN class, unique RN classes for each COR ring (to capture local RN compositions due to burnup heterogeneity), and more advanced options for axial modeling of RN masses (e.g., if several axial nodes are considered). A complete listing of all current user input options for the Perl script is given by Table 3-3.

Table 3-3. User input variables for post-processing with SNL Perl script.

User input Perl variable	Description
$unitName	Unit/plant name for printing output and summary files
$Nrings	Number of MELCOR COR rings
$Naxial	Number of axial levels; only used for writing the RN1_FPN and COR_KFU records
$zfuel	Lowermost axial level (BAF) of active fuel in the MELCOR model
$RN1_FPN_option	0 = use RN1_FPN multipliers 1 = absolute RN masses on RN1_FPN
$powerDist_option	0 = allocate classes to match decay power distribution 1 = allocate masses according to ORIGEN-S
$CsDistOption	0 = allocate Cs mass by power both radially and axially 1 = allocate Cs mass radially according to ORIGEN-S (axial distribution is still determined by @FA array input) This option affects all classes with alkali metal (Cs) mass including CsOH, CsI, and Cs_2MoO_4.
$CeDistOption	0 = allocate Ce class by power both radially and axially 1 = allocate Ce class radially according to ORIGEN-S (axial distribution is still determined by @FA array input)

$CRD_type	0 = Ag-In-Cd, i.e. typical PWR control rod poison 1 = B_4C, i.e. typical BWR control rod poison
@FA	Array of axial power/burnup factors for axial RN mass allocation in MELCOR inputs. The array should sum to 1.0.
$fI_inCsI	Mass fraction of halogen class in the CsI class
$fCs_inCsI	Mass fraction of alkali metal class in the CsI class
$fCsinCsM	Mass fraction of alkali metal class in the Cs_2MoO_4 class
$fMoInCsM	Mass fraction of transition metal class in the Cs_2MoO_4 class
$totalCsGapFrac	Total mass fraction of alkali metal class from all species (CsOH, CsI, Cs_2MoO_4) initially residing in the gap
$CsIinGapFrac	Mass fraction of CsI combination class initially in the gap
$iodineNumericalMass	Initial mass of the halogen (I2) MELCOR class. Assuming all iodine exists as CsI immediately after release from the fuel, the initial I2 mass is typically set to a very small value ($1.0x10^{-10}$) to allow for consideration of I_2 transport following subsequent class reactions such as chemisorption.
@RN_ele[class,@element_array]	Asymmetric matrix that defines the RN class component elements based on 2-character element names. The first index corresponds with the RN class names defined on the @RN array. The matrix can contain any number of classes, and each @element_array contains an arbitrary number of user-defined elements.
@RN[class]	Names of the RN classes defined by the @RN_ele matrix for output printing purposes.
@exclude	Array of isotopes to exclude from RN masses (e.g. O-16 in UO_2)

The $powerDist_option, $CsDistOption, and $CeDistOption can be modified in unison for the desired effect: E.g. $powerDist_option set to 0, $CsDistOption set to 1, and $CeDistOption set to 1 will allocate all RN mass according to the decay power distribution excluding the alkali metal and tetravalent classes, which will be allocated according to the ORIGEN-S/ARP predictions. Also, the uranium class is always be distributed according to ORIGEN-S/ARP predictions.

The user also specifies an asymmetric matrix (@RN_ele) that defines the constituent element in each RN class. The RN class definition matrix is versatile with regards to the total number of classes and the number of elements in each class; in fact, the RN class definition matrix depicted in Figure 3.2 is essentially copy and pasted from the MELCOR RN reference manual. The classes defined in the user matrix must be comprised of two-character elements–currently, specific isotopes for an element cannot be separated between classes in an automated fashion, but this is likely an unnecessary feature for LWR severe accident source terms (see Section 6.2). This flexible input record facilitates uncertainty and sensitivity studies that may utilize diverse RN classes and compositions, such as distinct barium and strontium classes, which are usually lumped together as a single RN class.

```
@RN_ele = ( ["He","Ne","Ar","Kr","Xe","Rn","H","N"],
            ["Li","Na","K","Rb","Cs","Fr","Cu"],
            ["Be","Mg","Ca","Sr","Ba","Ra","Es","Fm"],
            ["F","Cl","Br","I","At"],
            ["O","S","Se","Te","Po"],
            ["Ru","Rh","Pd","Re","Os","Ir","Pt","Au","Ni"],
            ["V","Cr","Fe","Co","Mn","Nb","Mo","Tc","Ta","W"],
            ["Ti","Zr","Hf","Ce","Th","Pa","Np","Pu","C"],
            ["Al","Sc","Y","La","Ac","Pr","Nd","Pm","Sm","Eu","Gd","Tb","Dy",
             "Ho","Er","Tm","Yb","Lu","Am","Cm","Bk","Cf"],
            ["U"],
            ["Cd","Hg","Zn","As","Sb","Pb","Tl","Bi"],
            ["Ga","Ge","In","Sn","Ag"],
            ["B","Si","P"] );
```

Figure 3.2. Default RN class definition matrix in the Perl script.

3.3.2 Algorithms for Formation of RN Class Quantities

The current algorithms in the SNL Perl script for calculating RN class quantities from ORIGEN-S outputs are very simple and consistent with historical MELCOR methodologies [10][32][33]. ORIGEN-S/ARP is used to calculate and report the quantities of all isotopes and isomers at the time of shutdown, which is user-specified (see Table 3-2), for fission products, actinides, and light elements (activation products)–these are called ORIGEN 'libraries.' The isotope and isomer quantities are added into elemental quantities over all of the ORIGEN libraries, and the elemental masses are then summed into RN class masses based on the class constituent elements specified by the user in the @RN_ele array (i.e. Figure 3.2). Whole-core and ring-based local RN quantities are preserved in the summation calculations, and axial-node based quantities could also be calculated with minor script additions. ORIGEN-S and the Perl script generate both nuclide masses and RN class masses, and nuclide activities for MACCS (element and class activities are not calculated since such quantities are of limited technical value).

3.3.2.1 Integration of Nuclide Quantities to Form Element Quantities

The information below in Figure 3.3 is ORIGEN-S output data for masses of a few fission products:

```
te135    1.480E-02
 i135    3.828E+01
xe135    1.101E+01
xe135m   3.236E-01
cs135    2.764E+04
cs135m   9.787E-02
ba135    1.319E+01
ba135m   1.527E-02
```

Figure 3.3. Sample ORIGEN-S output data of nuclide masses in grams.

The appropriate arrays for summation of element-based masses are determined by the first two characters from each nuclide record (i.e. the elements highlighted in yellow in Figure 3.3). This simple summation algorithm inherently neglects any attempt to adjust nuclide and class masses based on a-priori knowledge of core damage or release timing; that is, no attempt is made to transfer parent class mass to the daughter class for a specific time after shutdown. As explained

further in Section 6.2, such an effort is likely of limited utility for severe accident source terms. The time scales of severe accidents do not involve considerable class-to-class transfer of lumped RN mass–during such relatively short time frames, the nuclides masses undergoing significant decay are naturally the shorter-lived nuclides, which are intrinsically present in small quantities relative to the lumped RN class masses.

For example, the Te-135 ($t_{1/2}$ ~19 s) mass in Figure 3.3 quickly decays to I-135 ($t_{1/2}$ ~6.6 hr), which subsequently decays to Xe-135 ($t_{1/2}$ ~9.1 hr) and then to long-lived Cs-135 ($2.3x10^6$ years). All of these isotopes are in different RN classes. If desired, the user could manually transfer the Te-135 mass present at shutdown to any of these classes based on the time of interest after shutdown (e.g. the time of release from fuel), since MELCOR does not model time-dependent RN masses with respect to decay time. The fact remains, however, that the inherent short life of Te-135 precludes significant mass accumulation during reactor operation, since decay is always occurring even before shutdown, and thus its mass is quite insignificant compared to the halogen, noble gas, and alkali class masses. In relationship to lumped RN mass, all short lived nuclide mass behaves in an analogous manner despite differences in fission yield, decay in-growth, and production due to neutron absorption. Time-dependent quantities (with respect to decay time) of nuclides that are important for consequences must necessarily be considered by MACCS, but the small changes in overall RN class masses due to decay time are rightly assumed not to strongly influence the RN transport calculations in MELCOR. The more important assumption is likely the choice to limit the RN transport calculations to a handful of classes. Decay and radiation effects on RN speciation are another matter, and are briefly discussed in Sections 6.2 and 6.4.

3.3.2.2 Calculation of Element and Class Decay Powers

The SCALE6 auxiliary code OPUS is used to automatically calculate element-based decay powers for a sufficient number of times steps after shutdown for severe accident simulations with MELCOR (typically 50-100 steps since MELCOR linearly interpolates TF input); this bypasses the need to tally decay powers for many (over 1000) nuclides and for many time steps, which would naturally increase the CPU time associated with post-processing and dramatically increase the size of ORIGEN-S output files. Nuclide-based inventories for mass and activities are necessary for consistent MACCS and MELCOR inputs, and these nuclide quantities are not required at many time steps since these quantities are only required at the moment of shutdown. From the elemental decay powers calculated by OPUS, class specific decay powers are easily derived by the SNL Perl script to generate MELCOR DCH_EL input records. OPUS can also be used to double-check the RN class masses derived from the nuclide data in the ORIGEN-S output files.

3.3.2.3 Algorithms for Unique Combination Classes

The inclusion of combination classes such as CsI and Cs_2MoO_4 requires special attention when calculating the class decay powers and masses. ORIGEN-S, OPUS, and the SNL Perl script calculate masses and decay power curves for the alkali metal (Cs), halogen (I), and molybdenum (Mo) classes. These decay power curves must be appropriately specified to (1) preserve the original total decay power of the three classes, (2) preserve the unique decay powers or the

original (uncombined) classes, and (3) appropriately honor the class decay power contributions to the combination class powers. Because MELCOR notionally uses RN mass to determine RN power allocation, the decay heat curves for the combination classes are derived by mass-weighting the individual decay powers of the constituent classes. The mass distribution of the base classes, particularly the alkali metal class, are determined by the following set of assumptions, which are loosely based off of the Phebus experiments, the VERCORS experiments, and NUREG-1465 [19][20]:

1. All halogen class (I) mass is typically assumed to be in the form of CsI, which therefore allows the corresponding alkali metal mass to be calculated from stoichiometry. The mass fractions can be redefined via $fI_inCsI and $fCs_inCsI in the Perl script, but the default stoichiometric fractions are 4.88444×10^{-1} and 5.11556×10^{-1}, respectively.
2. The mass of the pure alkali metal (Cs) class is treated as CsOH that is entirely in the gap initially. This mass is determined by initial desired gap fractions (the $totalCsGapFrac and $CsIinGapFrac user variables from Table 3-3), and the alkali metal mass determined to be in CsI from step 1. The resulting algorithm in the Perl script is shown below in Figure 3.4. The oxygen and hydrogen mass in CsOH can be added automatically by the MELCOR RN package via sensitivity coefficient 7120(2). The default values for the total cesium gap fraction ($totalCsGapFrac) and the gap fraction of CsI ($CsIinGapFrac) are both 0.05.

```
$CsI_mass  = $RN_core_mass[4] / $fI_inCsI; # $RN_core_mass[4] = I2 class mass
$mCs_inCsI = $CsI_mass - $RN_core_mass[4];
$mCs_gap   = $RN_core_mass[2]*$totalCsGapFrac; #$RN_core_mass[2] = Cs class
$mCs_gap_fromCsI = $mCs_inCsI * $CsIinGapFrac;
$mCs_inCsOH = $mCs_gap - $mCs_gap_fromCsI; # all of this Cs is in the gap
```

Figure 3.4. Algorithm to determine CsOH mass.

3. The remaining alkali metal mass after distributing mass as CsI and CsOH is assumed to be entirely in the form of Cs_2MoO_4. Hence, the alkali metal mass in Cs_2MoO_4 is calculated by subtracting the alkali metal masses in the pure alkali metal (CsOH) class and the CsI combination class from the initial alkali metal mass predicted by ORIGEN-S. The associated early transition element (Mo) class mass in Cs_2MoO_4 is determined by stoichiometry; these mass fractions can be optionally varied by the user via $fCsinCsM and $fMoInCsM in the Perl script, which have default stoichiometric values 7.34789×10^{-1} and 2.65211×10^{-1}, respectively. The pure Mo class mass is then determined by subtracting the Mo mass in Cs_2MoO_4 from the initial Mo mass predicted by ORIGEN-S. The algorithm in the Perl script is depicted in Figure 3.5. The oxygen mass in Cs_2MoO_4 can be added automatically by MELCOR using the 7120(2) sensitivity coefficient.

```
# mass Cs in CsM = all Cs mass - Cs mass in CsI - Cs mass as CsOH
$mCs_inCsM = $RN_core_mass[2] - $mCs_inCsI - $mCs_inCsOH;
$CsM_mass  = $mCs_inCsM/$fCsinCsM;
$mMo_inCsM = $CsM_mass - $mCs_inCsM;
# Mo-only mass remaining after CsM class construction
$onlyMoClass_mass = $RN_core_mass[7]-$mMo_inCsM; #$RN_core_mass[7] = Mo mass
```

Figure 3.5. Algorithm to determine Cs_2MoO_4 and Mo masses.

4. Based on the calculations in steps #1-3, class decay powers are calculated for the combination classes CsI and Cs_2MoO_4. The specific decay power curves for the 'pure' classes such as the alkali metal class (CsOH), the halogen (I) class, and the early transition element (Mo) class can be derived directly from the ORIGEN-S predictions of element masses and powers. Notionally, the total power curves of the pure classes are modified congruently with the lumped RN masses that are reapportioned amongst the classes; hence the specific decay power (W/kg) curves of the pure classes remain the same after formulation of the combination classes (the shuffled masses preserve the total decay powers). The specific decay power curves for CsI and Cs_2MoO_4 are determined by the stoichiometric fractions that comprise combination classes in conjunction with the specific power curves of the pure constituent classes. This simple approach conserves the initial total decay power for all of the base classes involved.

3.3.3 Perl Script Output: Auxiliary Summary Files

The SNL scripts generate a host of auxiliary output files by post-processing ORIGEN-S and OPUS output data. These files are not used directly for MELCOR and MACCS inputs, but nonetheless provide more comprehensive information of nuclide and RN-class quantities for inventory and decay power, including the dependence of decay time after shutdown. The auxiliary summary files are listed and described in Table 3-4.

Table 3-4. Auxiliary summary files generated by Perl post-processor.

Summary file name*	Contents
$unitName_burnupSummary.txt	• Number of assemblies in each ring • Ring-averaged BOC and EOC burnups • Whole-core BOC and EOC burnups • Fuel assembly ID, location, BOC and EOC burnups
$unitName_element_mass_power.txt	• Whole-core and ring-based element masses separated by ORIGEN-S libraries. • Element-based decay heat curves for 100 time steps up to 300 hours after shutdown • Whole-core and ring-based decay heat curves for 100 time steps up to 300 hours after shutdown • RN class masses as a function of decay time
$unitName_inventory_wholeCore.txt	Whole-core nuclide inventories-masses and activities
$unitName_nuclide_summary.txt	Whole-core and ring-based nuclide masses separated by ORIGEN-S libraries
$unitName_RNclasses_mass.txt	Whole-core and ring-based RN class masses, which are further broken down by the relative masses of the constituent elements. Each element is further decomposed by the top isotopic masses.
$unitName_RNclasses_specificDCH.txt	Whole-core and ring-based RN class masses, total RN class decay powers at a few times after shutdown, and specific decay powers (W/kg) for 100 time steps up to 300 hours after shutdown.
$unitName_selectNuclideMasses_decay.txt	Masses of key nuclides for health-effects as function of decay time.

*Note: each file is appended with the $unitName Perl variable (see Table 3-3).

3.3.4 Perl Script Output: MELCOR Input Records

The Perl script directly generates all pertinent MELCOR input records by post-processing outputs from ORIGEN-S and OPUS. Information for the DCH_EL, RN1_FPN, and COR_KFU input records are created and require no further processing to implement into MELCOR. A tabular function of total core decay power is also supplied for linking to the DCH_DPW record. Currently, RN distribution input is only written for the fuel, and inventories in the fuel-cladding gap (RN1_GAP input) are not generated. Nevertheless, RN1_GAP input is based on simple multipliers that are usually uniform over the entire core, and therefore do not really necessitate automated creation. The files created by the Perl script that contain MELCOR input records are listed and described in Table 3-5.

Table 3-5. Files generated by Perl post-processor that containment MELCOR inputs.

File name*	Contents
$unitName_melcorInp_DCH_EL.txt	RN class masses and specific decay powers. The specific decay powers have units of W/kg and are a function of time after shutdown. MELCOR RN class masses are constant with respect to decay time.
$unitName_melcorInp_RN1_FPN.txt	Spatial distribution of RN class masses over MELCOR COR cells. This input determines the decay power distribution in conjunction with DCH_EL inputs.
$unitName_melcorInp_COR_KFU.txt	UO_2 fuel component masses for the MELCOR COR package.
$unitName_melcorInp_decaypowerTF.txt	Tabular function of total decay power for all classes; links to DCH_DPW.

*Note: each file is appended with the $unitName Perl variable (see Table 3-3).

MELCOR requires that the fuel mass for UO_2 specified in the COR package (via COR_KFU) be consistent with the mass specified for the uranium class in the RN and DCH packages. It accomplishes this by modifying the RN mass for the uranium class according to the following expression:

$$M_{U,RN} = f_U \, M_{UO2,COR} - \sum_{all\ classes} m_i$$

Where,
$M_{U,RN}$ = The mass of the uranium class in the RN and DCH packages;
f_U = The mass fraction of uranium in UO_2, which is simply assumed to be 238/270 in MELCOR, no matter the enrichment level;
$M_{UO2,COR}$ = The mass of UO2 in the COR package determined by the COR_KFU record;
$\sum_i m_i$ = The total mass of all other RN classes excluding water and concrete.

MELCOR also automatically modifies the specific decay power of the uranium RN class to preserve the class decay power that was originally specified by the user. Although the uranium class is usually of secondary importance for severe accident source terms, the user needs to ensure consistency between the COR UO_2 mass and the uranium mass in the RN and DCH packages in order to prevent automatic input modification by MELCOR. The $unitName_melcorInp_COR_KFU.txt file generated by the Perl script (Table 3-5) can be

optionally used for this purpose. Currently, it allocates UO_2 mass over MELCOR COR rings according to ORIGEN-S predictions–this accounts for the uranium mass burned by neutron absorptions, but the radial distribution of UO_2 mass remains essentially dependent upon the number of assemblies in the rings and the initial fuel loading. Axially, the Perl script distributes UO_2 mass uniformly, which neglects partial fuel rods in BWRs and axial depletion profiles. Most uranium mass remains as U-238 for typical LEU-fueled LWRs, even after high burnups. Future work can consider axial distributions of uranium and the other RN classes with minor additions to the Perl script; these additional features would also require axial burnup calculations by ORIGEN-S/ARP.

3.3.5 Perl Script Output: MACCS Input Records

The Perl script creates MELMACCS input records that are necessary for MACCS to decompose MELCOR source terms; this input is in a file created by the Perl script named $unitName_melmaccs.inv. The MELMACCS file contains nuclide masses and activities that are totally consistent with the lumped MELCOR RN inventories. The nuclide inventories in the MELMACCS file are separated by ORIGEN-S libraries (actinides, light elements, and fission products), which are summed together by MELMACCS to derive whole-core nuclide and RN class inventories. The RN class inventories calculated by MELMACCS are used for comparison to the RN class masses in the MELCOR source term (via the MELCOR plot file). These two sets of RN class inventories are guaranteed to be consistent with the new SNL tools, since the MELMACCS and MELCOR inventories come from the same ORIGEN-S calculations.

A complete MELMACCS input file requires several other input records that are not presently generated by the SNL Perl script. Besides the inventories, MELMACCS input entails user-specification of coefficients for dry deposition velocity, select nuclides to consider for the consequence calculations, and the definition of elemental compositions of the RN classes (similar to Figure 3.2).

4 APPLICATION TO FUKUSHIMA MELCOR MODELS

The SCALE6 code package, namely the ORIGEN-S and ARP modules, are used in conjunction with SNL script tools to analyze the Fukushima reactors. The SNL tools automate the process of ORIGEN-S/ARP input generation and post-processing of ORIGEN-S/ARP output. Input records for MELCOR and MACCS are directly generated for each Fukushima unit. This section describes the application of the SNL tools for decay heat and inventory analysis to the Fukushima reactors.

4.1 Need for SNL Capabilities to Quantitatively Assess Inventory and Decay Heat

As shown in Table 4-1, the Fukushima reactors are of sufficiently different core design, power rating, assembly type, and burnup level to warrant unit-specific core models for the MELCOR core (COR), hydrodynamic (CVH/FL), radionuclide (RN), and decay heat (DCH) packages. Fukushima unit-specific structural and hydrodynamic models of the fuel assemblies, channel boxes, control blades, core support structure, coolant channels, bypass regions, and lower plenum were completed in the joint DOE/NRC Fukushima analysis project [2]. However, this project did not perform depletion calculations to create radionuclide inventory and decay heat information for each unit.

Table 4-1. Reactor core design information for Fukushima reactors.

Parameter	Fukushima Unit 1	Fukushima Unit 2	Fukushima Unit 3
Reactor type	BWR/3	BWR/4	BWR/4
Rating (MWt)	1380	2381	2381
Fuel mass (tHM)	68	94	94
# fuel assemblies	400	548	548
# control blades	97	137	137
Fuel assemblies – type (quantity)	8x8 (68), 9x9B (332)	9x9B (548)	9x9A (516), 8x8MOX (32)
Fuel height, core diameter (m)	3.66 / 3.7	3.71 / 4.4	3.71 / 4.4
Avg. core burnup at shutdown (GWd/t)*	25.8	23.2	21.4
Peak fuel assembly burnup at shutdown (GWd/t)	41.3	42.4	41.7

*For the Fukushima reactors, this is the whole-core average burn-up at the time of scram due to the seismic event (3/11/2011 14:46). It is TEPCO data from the plant process computer.

Late in the development of the Fukushima MELCOR models, TEPCO-calculated core decay power and radionuclide inventories were made available for each unit. The TEPCO decay powers were incorporated into the SNL MELCOR models for each unit [2], but the TEPCO inventories were not implemented. Rather, a power-scaled inventory was adopted from SNL's Peach Bottom model. The TEPCO-supplied inventory was not implemented due to the following reasons:

- The inventory was generated by an ORIGEN2 calculation that was separate from the overall core decay heat and power distribution calculations. ORIGEN2 is a deprecated code, and the use of separate analyses for inventory and decay power data reduces the consistency and scrutability of the MELCOR/MACCS models. ORIGEN-S in SCALE is the current US-NRC code of choice for inventory and decay power calculations. It also has access to the latest ENDF/B-VII nuclear data for cross sections, fission yields, and decay data.
- The inventory only reflected the whole core inventory and lacked spatial distribution details. Radial distributions of radionuclides are especially important for cores where older, high burn-up fuel assemblies are shuffled predominately to the periphery of the core, which was the case for 1F1.
- The TEPCO inventory specified nuclide activities for actinides, fission products, and light activation products, which are indeed necessary information for MELCOR and MACCS. However, by nuclide masses, a large portion of the initial core inventory of fission products and decay daughters are actually stable–the activity of a stable nuclide is zero and is no longer much concern once a source term calculation is complete. (In fact, MACCS only models the consequence effects of select radioactive nuclides.) Still, the stable nuclide masses are important for the accurate formation of MELCOR radionuclide (RN) inventories and the subsequent transport simulation. Initial inventories for MELCOR RN classes require lumped elemental masses, and the isotopic breakdowns of these classes are also required input for MACCS (i.e., MELMACCS input). Upon core heat-up and oxidation, fuel temperatures rise and volatile radionuclide classes are rapidly released from the fuel. These radionuclides transport throughout the plant as vapors and aerosols. Overall vapor and aerosol mass are important for accurate radionuclide transport calculations in MELCOR for each RN class. Hence, it is imperative to include stable radionuclide masses that reside in the fuel, such as Cs-133 (~40% of all core cesium) and I-127 (~20% of all core iodine). These stable nuclides are released with the appropriate RN classes and contribute to overall vapor and aerosol masses for the transport calculations.

In light of these discrepancies, the automated SNL methodology is used to generate accurate and consistent MELCOR inventories, overall core decay power, MELCOR RN class specific decay powers, and MELMACCS isotopic inventories for each Fukushima unit. This capability provides best-estimate information for MELCOR and MACCS, which is also required for integrated MELCOR/MACCS uncertainty analyses that may treat radionuclide inventory and decay heating as uncertain parameters.

4.2 Fukushima Plant Data for Use in SCALE Input Models

The necessary Fukushima plant data used as SCALE6 input is mostly available publically via the Tokyo Electric Power Company (TEPCO) website. Some of the information used is proprietary, such as the more detailed design information for the fuel assemblies. The following sections that originally contained proprietary information in the Official Use Only version of this report (SAND2014-3966) have figures and data removed for this unlimited release document. Plant information that is considered publically available is listed below and summarized in Table 4-2, since this information is available from the TEPCO website [21]:

- Overall BOC and EOC burnups, power levels, and cycle operating times;
- General fuel assembly design (e.g. BWR 9x9) and average enrichments;
- Core and assembly fuel loading, i.e. metric tons of uranium;
- Two-dimensional layouts of the core fuel assemblies;
- Axial void fraction distribution for full-power operation.

Table 4-2. Fukushima plant data for use in SCALE6 models.

	Fukushima Unit 1	Fukushima Unit 2	Fukushima Unit 3
Final operating time before accident (days) (1)	191	113	169
Core-avg. BOC burnup (GWd/t) (2)	21.95	20.17	17.22
Core-avg. EOC burnup (GWd/t) (2)	25.78	22.95	21.41
Peak fuel assembly burnup at shutdown of final cycle (GWd/t) (2)	41.3	42.4	41.7
Specific power (MW/t)	20.3	25.6	25.6
Fuel assemblies – type (quantity)	8x8 (68), 9x9B (332)	9x9B (548)	9x9A (516), 8x8MOX (32)
Average enrichment (w/o)	8x8: 3.4 9x9B: 3.6	3.8	9x9A: 3.8 8x8MOX: 1.2 ^{235}U 8x8MOX: 3.9 Pu(3)

(1) Fukushima units 1-3 appear to have operated on cycle ranging from 300 days to 520 days, according to publically available outage and fuel offload histories.
(2) This burnup data is from the plant process computer, which is publically available.
(3) This is the total plutonium weight percent in the MOX fuel rods. The plutonium vector is currently unknown, but is likely proprietary.

4.2.1 Assumptions for Current Fukushima Analyses with ORIGEN-S/ARP

Most of the data required for ORIGEN-S and ARP input can be obtained directly from the raw TEPCO core data, which is in the form of 3D power and burnup data. Some core design information is also available including number of fuel rods per assembly, number of water rods, basic geometry information (e.g. fuel diameter and lattice pitch), assembly masses, compositions (i.e. U-235 and total Pu enrichment in MOX), and the number of fuel assembly types in each core (see Table 4-2). The Fukushima core data provided by TEPCO is sufficient for the calculation of reasonably detailed and consistent information for MELCOR and MACCS. However, some approximations were necessary to perform the depletion calculations. For

example, Fukushima-specific ARP cross section libraries have not yet been implemented into the Fukushima analyses presented in this report. The original plant data available to SNL lacked sufficient geometry and material information to perform an honest modeling effort with TRITON. Instead, existing ARP libraries are utilized as surrogates that are provided with the SCALE6 distribution; the pre-generated LWR libraries were generated using TRITON with ENDF/B-V data [12]. Some of these approximations and assumptions may be considered for Fukushima uncertainty analyses. A summary of the assumptions used to supplement the unknown information for the current depletion analysis approach is given in Table 4-3.

Table 4-3. Major assumptions and approximations for burnup calculations to provide MELCOR and MACCS input.

Unknown information	Approximations/assumption utilized until more detailed information become available
1. Exact fuel assembly design information detailed enough to create discrete ordinate (NEWT) or Monte Carlo (KENO-VI) models in SCALE. Coupled neutron transport and depletion simulations are required to create problem-dependent ORIGEN-ARP libraries.	Use the ORIGEN-ARP libraries provided with SCALE6 as surrogates. Judging by basic data such as rod diameter, lattice pitch, number of fuel rods, and number of water rods, the following pre-generated ARP libraries appear to be reasonable temporary proxies for the Fukushima fuel assemblies: Fukushima 9x9A ≈ ge9x9-7 SCALE6 library Fukushima 9x9B ≈ atrium9-9 SCALE6 library Fukushima 8x8 (unit 1) ≈ ge8x8-4 SCALE6 library
2. Detailed power history of fuel assemblies burned in previous cycles.	Each assembly with greater than zero BOC burnup is assumed to have been irradiated in one to four previous cycles, depending upon the BOC burnup level. Since the specific (i.e. local) power level is not known for each fuel assembly for the previous cycles, the before-BOC burnup level is attained by appropriately setting the total irradiation time at the core-average specific power level. In effect, the before-BOC irradiation time is artificially modified to yield the exact BOC burnup, assuming every previously irradiated fuel assembly burnup received the core-average specific power level for the derived time.
3. Location of each fuel assembly type in the Fukushima cores.	Infer/guess fuel assembly locations for 'minority' fuel assembly types (i.e. MOX and unit 1 8x8 fuel) based on available TEPCO data. For example, all MOX in unit 3 was fresh at BOC, hence their locations in the core can be roughly guessed given the BOC burnup distribution.
4. MOX fuel assembly data including geometry and plutonium vector.	Until better information becomes available, the use of the 'mox8x8' ARP library in SCALE and plutonium isotope concentrations for a typical MOX 8x8 fuel assembly [12] are assumed to be reasonable approximations. Given that only about 6% of the unit 3 fuel assemblies were MOX, these assumptions may not likely have a large impact on overall core inventories.
5. Average moderator density for ARP library used in ORIGEN-S calculations.	Currently treated as constant for all fuel assemblies based on axially-integrated plant data.

More detailed and proprietary data has recently become available that will reduce the number of necessary assumptions for future work, which is discussed in Section 4.5. This new plant data is available as part of the Benchmark Study of the Accident at the Fukushima Daiichi (BSAF) effort, which is an OECD/NEA project. Most importantly, the use of surrogate ENDF/B-V ARP libraries, which are pre-shipped with SCALE6, for the Fukushima fuel assemblies will no longer be necessary after generation of new Fukushima ARP libraries using the TRITON sequence in SCALE6. The detailed fuel assembly information is given in Section 4.2.3.

Concerning item #2 in Table 4-3, previously irradiated fuel assemblies are treated in an approximate manner. The number of previous irradiation cycles can be roughly inferred from the plant data, and each fuel assembly in the cycle of interest (i.e., the operating cycle of the accident) is assumed to have been irradiated in one to four previous cycles. The resulting irradiation batches are given in Table 4-4. In reality, some fuel assemblies may have been irradiated in over 4 previous cycles, and others may have skipped cycles by cooling in the spent fuel pool before being reinserted into the cores. The exact burnup histories for the previously irradiated assemblies can be readily implemented into updated analyses by the automation scripts once the data becomes available. If the exact information does not become readily available, future SNL research such as Fukushima UA efforts may treat the decay heat and inventories as uncertain parameters that use the SNL tools to inform uncertain distributions and bounds. Such an approach could examine how burnup history and other operating characteristics affect radionuclide inventories and decay heating for MELCOR and MACCS.

Table 4-4. Inferred Fukushima irradiation batches for ORIGEN-S/ARP models.

Assumed burnup batch	Unit 1 (# of assemblies)	Unit 2 (# of assemblies)	Unit 3 (# of assemblies)
Fresh at BOC	64 (16.0%)	116 (21.17%)	148 (27.01%)
1 prior irradiation cycle BOC burnup < 15 GWd/t	64 (16.0%)	116 (21.17%)	112 (20.44%)
2 prior irradiation cycles BOC burnup < 25 GWd/t	80 (20.0%)	92 (16.79%)	96 (17.52%)
3 prior irradiation cycles BOC burnup < 33 GWd/t	76 (19.0%)	116 (21.17%)	110 (20.07%)
4 prior irradiation cycles BOC burnup ≥ 33 GWd/t	116 (29.0%)	108 (19.71%)	82 (14.96%)

4.2.2 3D Power and Burnup Distributions

TEPCO data for three-dimensional distributions of relative power and burnup are post-processed in Excel with Visual Basic in order to generate 2D radial (assembly-wise) distributions and axial distributions for MELCOR inputs. The ORIGEN-S/ARP calculations are currently performed on the assembly-level basis with no consideration of axial variations. Eventually, ARP libraries are to be generated at several void fractions and ORIGEN-S/ARP calculations will subsequently be performed for several axial nodes. The SNL tools collapse the 2D radial data created by the distinct ORIGEN-S/ARP simulations onto the 1D MELCOR COR rings. The 2D Fukushima plant information for BOC/EOC power and BOC/EOC burnup are provided by Figure 4.1, Figure 4.2, and Figure 4.3. The COR ring nodalizations for the MELCOR models are shown by

Figure 4.4 and Figure 4.5. The sizes of each ring, in terms of the number of fuel assemblies, are summarized in Table 4-5.

This image is available in the Official Use Only (OUO) version of this report (SAND2014-3966).

Figure 4.1. Core data for Fukushima unit 1: BOC power (top left), EOC power (top right), BOC burnup (bottom left), and EOC burnup (bottom right).

This image is available in the Official Use Only (OUO) version of this report (SAND2014-3966).

Figure 4.2. Core data for Fukushima unit 2: BOC power (top left), EOC power (top right), BOC burnup (bottom left), and EOC burnup (bottom right).

This image is available in the Official Use Only (OUO) version of this report (SAND2014-3966).

Figure 4.3. Core data for Fukushima unit 3: BOC power (top left), EOC power (top right), BOC burnup (bottom left), and EOC burnup (bottom right).

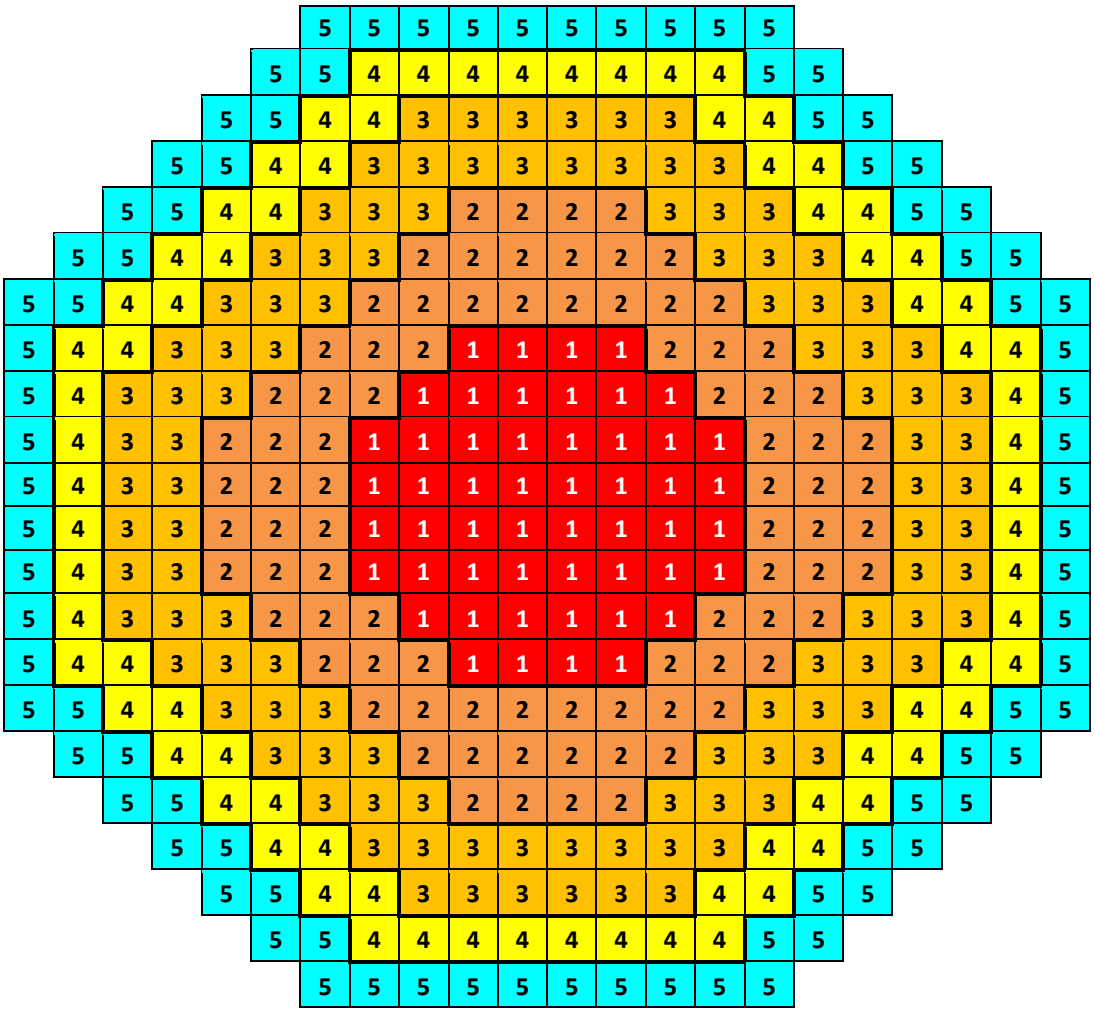

Figure 4.4. COR 5-ring nodalization scheme of MELCOR RN, COR, CVH, and FL packages for unit 1. The bypass volumes and flow paths are not represented.

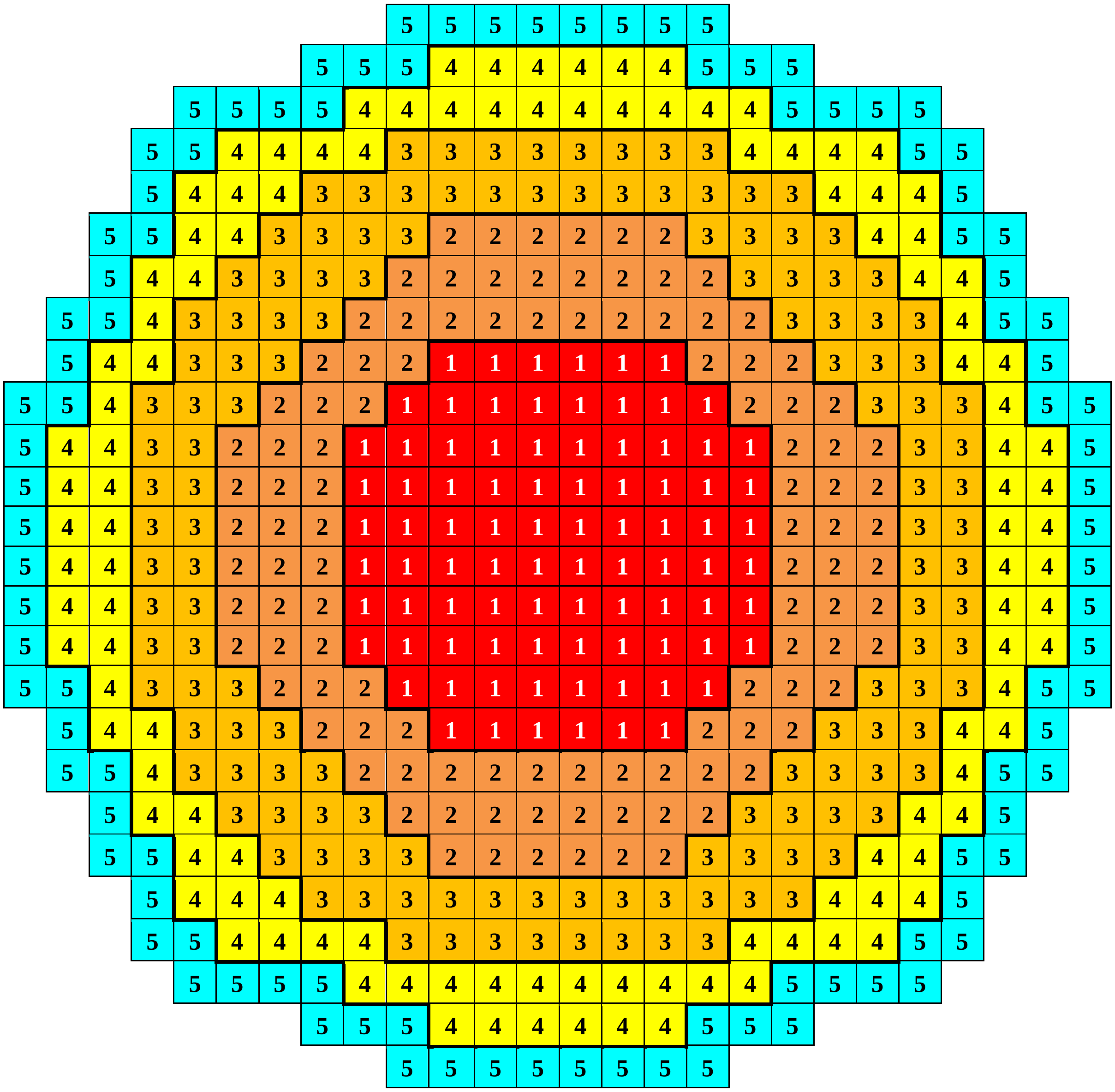

Figure 4.5. COR 5-ring nodalization scheme of MELCOR RN, COR, CVH, and FL packages for unit 2 and unit 3. The bypass volumes and flow paths are not represented.

Table 4-5. Core ring sizes (numbers of assemblies) for MELCOR Fukushima models.

Ring index	Unit 1	Unit 2 and unit 3
1	52	88
2	84	108
3	104	136
4	76	116
5	84	100

Axial distributions of power and burnup for each Fukushima unit are depicted in Figure 4.6, Figure 4.7, and Figure 4.8. The 3D Fukushima plant data exists for each assembly over 24 axial nodes. Also shown in these figures are nodal-averaged power and burnup factors over the 10 axial nodes in the MELCOR COR models. The current Fukushima analyses do not directly calculate axial variations in RN masses and decay powers. The ORIGEN-S/ARP models only consider 2D radial distributions over the fuel assemblies. Hence, RN masses and inventories must be apportioned axially by user-specified scaling factors for each axial node of the active core region in the MELCOR model. The SNL Perl script allows for the user to specify the desired number of axial nodes and the scaling factor for each node, normalized to the nodal totals (i.e. the scaling factors should sum to 1.0).

In contrast to the radial distributions, the axial distributions of RN masses and decay powers are intrinsically similar; this similarity is due to comparable operating power and burnup distributions along the axial core dimension, which are the natural results of the axial symmetry of the core and the lack of axial fuel shuffling. The decay power soon after shutdown follows the operating power distribution, since high power regions of the core contain higher concentrations of short-lived nuclides. RN class masses are dominated by long-lived and stable nuclides that intrinsically build with burnup. The axial power and burnup distributions for unit 1 and unit 2 (Figure 4.6 and Figure 4.7) are quite similar, facilitating the selection of the axial scaling factors for RN masses and decay powers. The unit 3 power and burnup distributions (Figure 4.8) exhibit a slight divergence. Therefore, averages of the axial power and burnup distributions are implemented as the axial scaling factors for each unit.

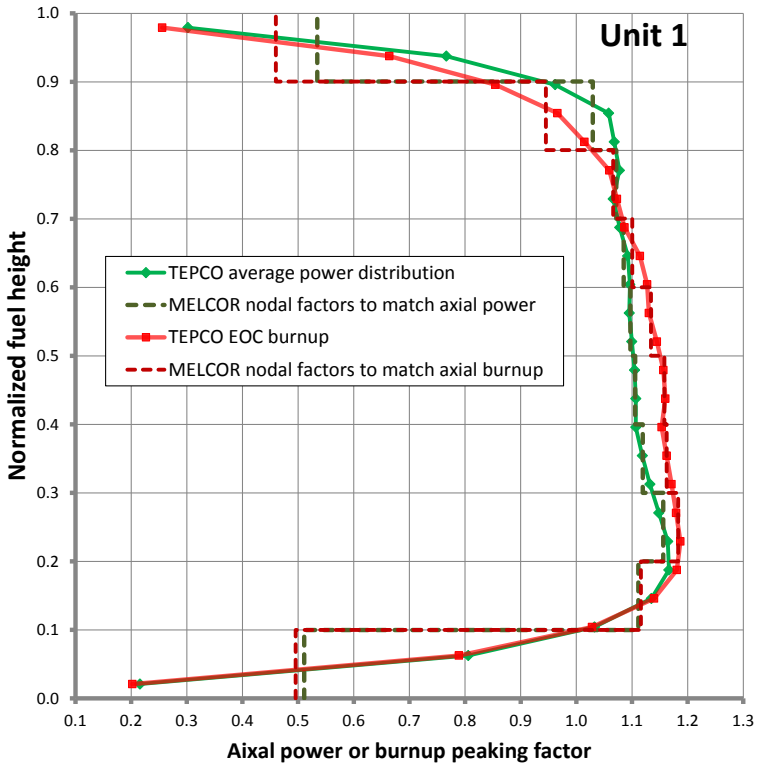

Figure 4.6. Fukushima unit 1 axial power and burnup distributions.

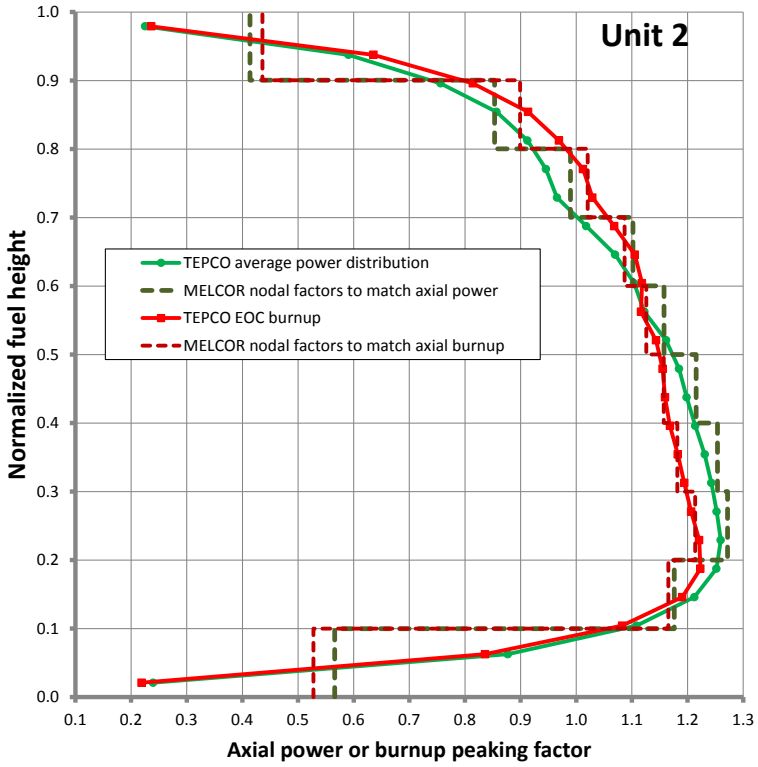

Figure 4.7. Fukushima unit 2 axial power and burnup distributions.

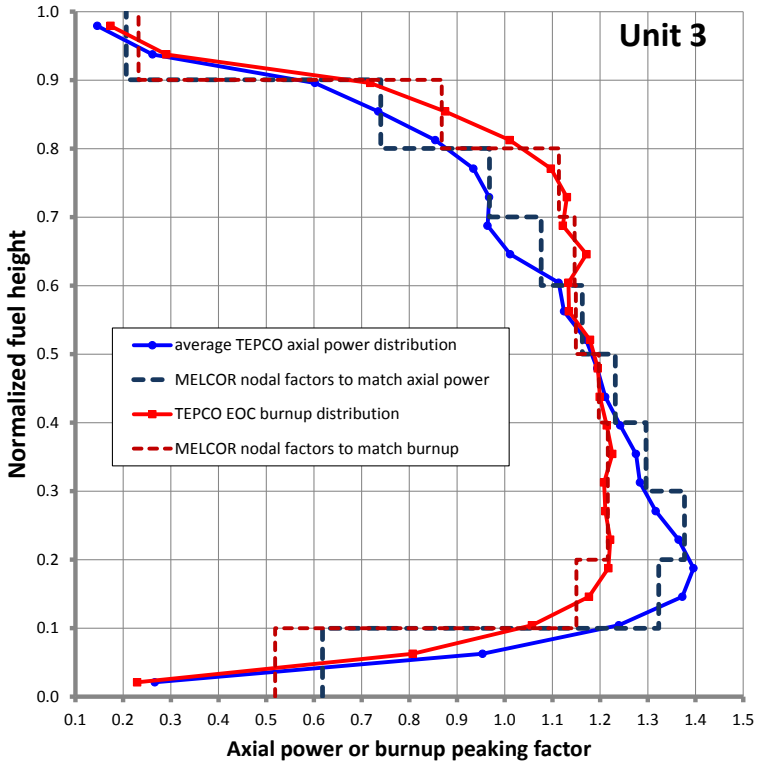

Figure 4.8. Fukushima unit 3 axial power and burnup distributions.

4.2.3 Fuel Assembly Geometry and Design Details

Fuel assembly geometry information for the major fuel assemblies in Fukushima Daiichi units 1-3 was made available to SNL via the BSAF project. The information is likely sufficient to generate ORIGEN-S and ARP data libraries using TRITON that are more representative of the fuel used in each Fukushima reactor. However, the intricacies of the fuel and poison zoning in the major fuel types, as well as the existence and nature of any fuel subtypes (i.e., small variations in fuel and poison placement/loading), remain unknown. Such fine details are usually considered unnecessary for the generation of core-wide nuclide inventories, decay power, and radionuclide class characteristics for severe accident simulations.

Fukushima Daiichi unit 1 contained two major fuel types according to TEPCO (see Table 4-2): the 9x9B assembly (i.e. STEP3B) and older 8x8 (i.e. STEP2) assemblies. Fukushima unit 2 is comprised entirely of the 9x9B/STEP3B assemblies, except possibly at greater axial length compared to unit 1. The geometry of the fuel lattice for STEP3B (9x9B) fuel is shown by Figure 4.9, and the control blade details are depicted by Figure 4.10. The dimensions of the STEP3B fuel assembly for unit 1 and unit 2 are listed in Table 4-6. The lattice geometry for STEP2 (8x8) assemblies in unit 1 is depicted in Figure 4.11, and the control blade is given by Figure 4.12. The dimensions of the STEP2 assemblies in unit 1 are listed in Table 4-7.

This image is available in the Official Use Only (OUO) version of this report (SAND2014-3966).
Figure 4.9. STEP3B (9x9B) fuel assembly in unit 1 and unit 2 – lattice detail.

This image is available in the Official Use Only (OUO) version of this report (SAND2014-3966).
Figure 4.10. STEP3B (9x9B) fuel assembly in unit 1 and unit 2 – control blade detail.

Table 4-6. STEP3B (9x9B) dimensions.
This table is available in the Official Use Only (OUO) version of this report (SAND2014-3966).

This image is available in the Official Use Only (OUO) version of this report (SAND2014-3966).
Figure 4.11. STEP2 (8x8) fuel assembly in unit 1 (MOX in unit 3) – lattice detail.

This image is available in the Official Use Only (OUO) version of this report (SAND2014-3966).
Figure 4.12. STEP2 (8x8) fuel assembly in unit 1 (MOX in unit 3) – control blade detail.

Table 4-7. 8x8 dimensions for unit 1.
This table is available in the Official Use Only (OUO) version of this report (SAND2014-3966).

Fukushima Daiichi unit 3 contained two major fuel types according to TEPCO (see Table 4-2): the 9x9A assembly, also referred to as STEP3A, and 8x8 MOX fuel assemblies, which are similar to the STEP2 (non-MOX) assemblies used in unit 1 except some rods contain MOX fuel. The geometry of the fuel lattice for STEP3A (9x9A) fuel is shown by Figure 4.13, and the control blade details are depicted by Figure 4.14. Table 4-8 provides the quantities for the dimensional variables defined in Figure 4.13 and Figure 4.14. The geometric depictions of the lattice and control blade arrangement for the MOX fuel are given by Figure 4.11 and Figure 4.12, respectively, which have identical geometry to the 8x8 fuel in unit 1. The quantitative dimensions for the MOX fuel are listed in Table 4-9.

This image is available in the Official Use Only (OUO) version of this report (SAND2014-3966).

Figure 4.13. STEP3A (9x9A) fuel assembly in unit 3 – lattice detail.

This image is available in the Official Use Only (OUO) version of this report (SAND2014-3966).

Figure 4.14. STEP3A (9x9A) fuel assembly in unit 3 – control blade detail.

Table 4-8. STEP3A (9x9A) dimensions.

This table is available in the Official Use Only (OUO) version of this report (SAND2014-3966).

Table 4-9. MOX dimensions.

This table is available in the Official Use Only (OUO) version of this report (SAND2014-3966).

4.2.4 Core Maps

As discussed in Section 4.2.1 and Table 4-3, the details of the fuel assembly zoning throughout the core is unknown for each unit. The radial locations of the 8x8 high burnup assemblies in unit 1 and the MOX assemblies in unit 3 are unknown. Furthermore, the cores likely have various subtypes of assembly designs with different burnable poisons (e.g. gadolinia) configurations, partial fuel rods (to reduce two-phase pressure drop and enhance moderation in the upper core), and enrichment zoning depending on the location of the assembly in the core. Hence, even though unit 2 is comprised of one major assembly type, there are core design details that are not being considered due to a lack of data. These nuances are necessarily neglected unless more information is made available, but they likely do not have first-order effects on overall inventories and decay powers.

Currently the locations of the distinct fuel assembly designs are inferred from the BOC burnup distribution. For example, it is known from plant data that the 8x8 fuel assemblies in unit 1 were of the greatest burnups and longest total irradiation times. The burnup distribution (Figure 4.1) can be used to make an educated guess of the locations of the high burnup 8x8 fuel assemblies in the unit 1 core. This tends to concentrate the 8x8 assemblies in the outer ring of the core. Likewise for unit 3, it is known that the MOX assemblies where fresh at BOC; the MOX assemblies are therefore assumed to be located at positions of zero BOC burnup, and are further assumed to be nearly uniformly distributed over the MELCOR COR rings that contain fresh fuel assemblies. The exact core layouts for each unit can be readily implemented into the ORIGEN-S/ARP models via the Perl script if the information becomes available.

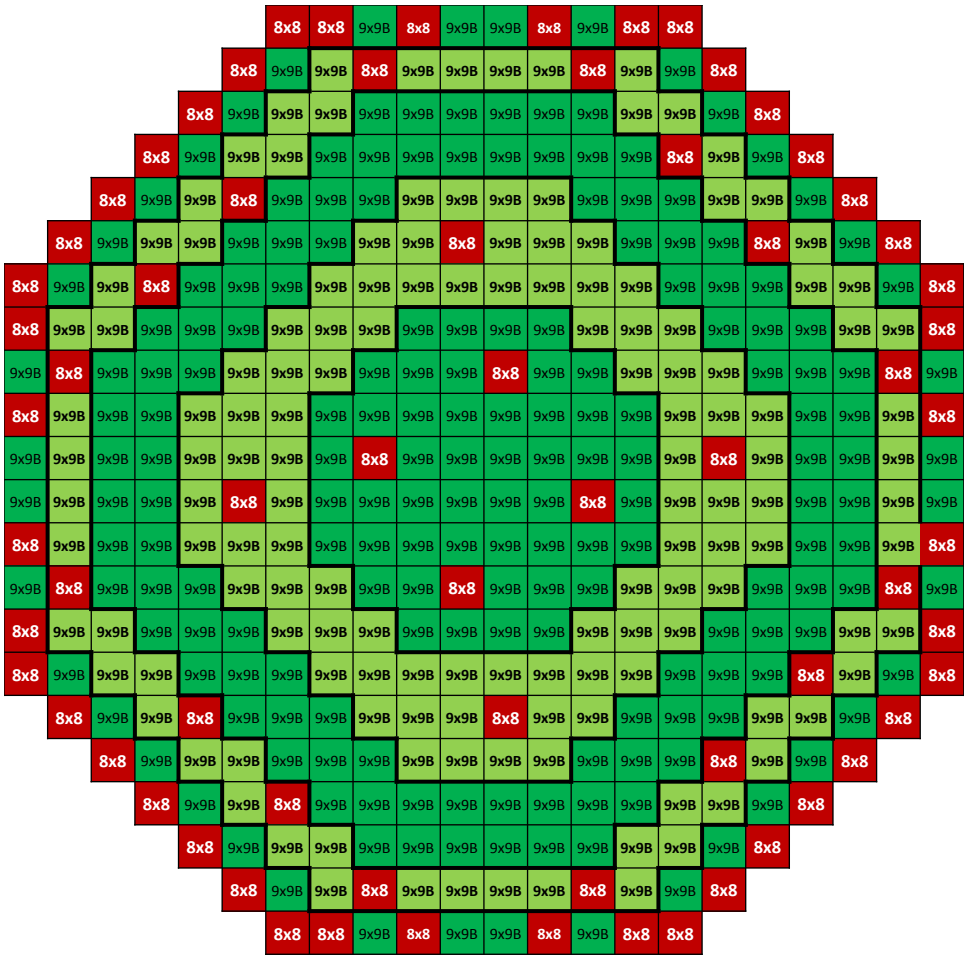

Figure 4.15. Fukushima unit 1 fuel assembly map.

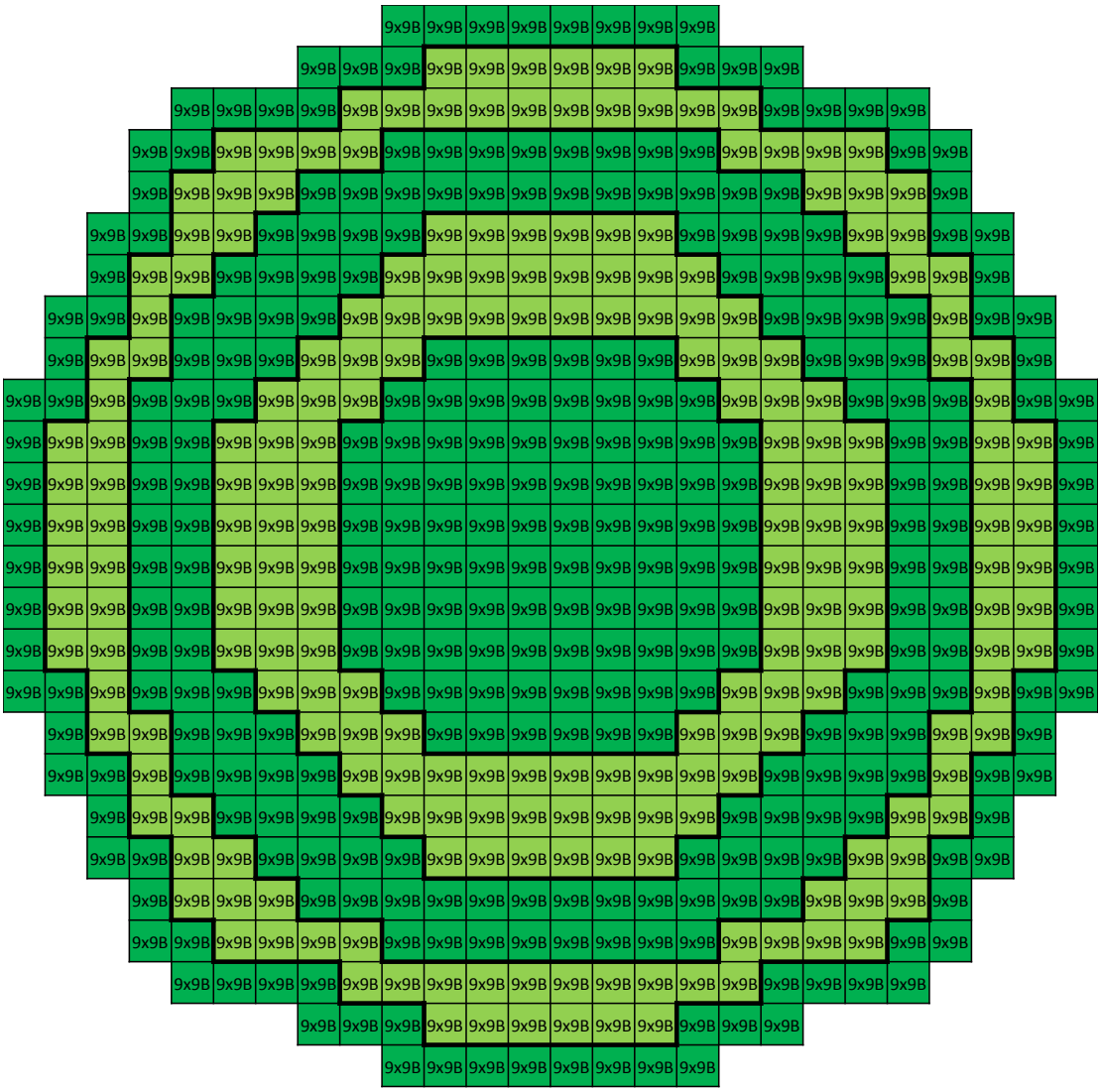

Figure 4.16. Fukushima unit 2 fuel assembly map.

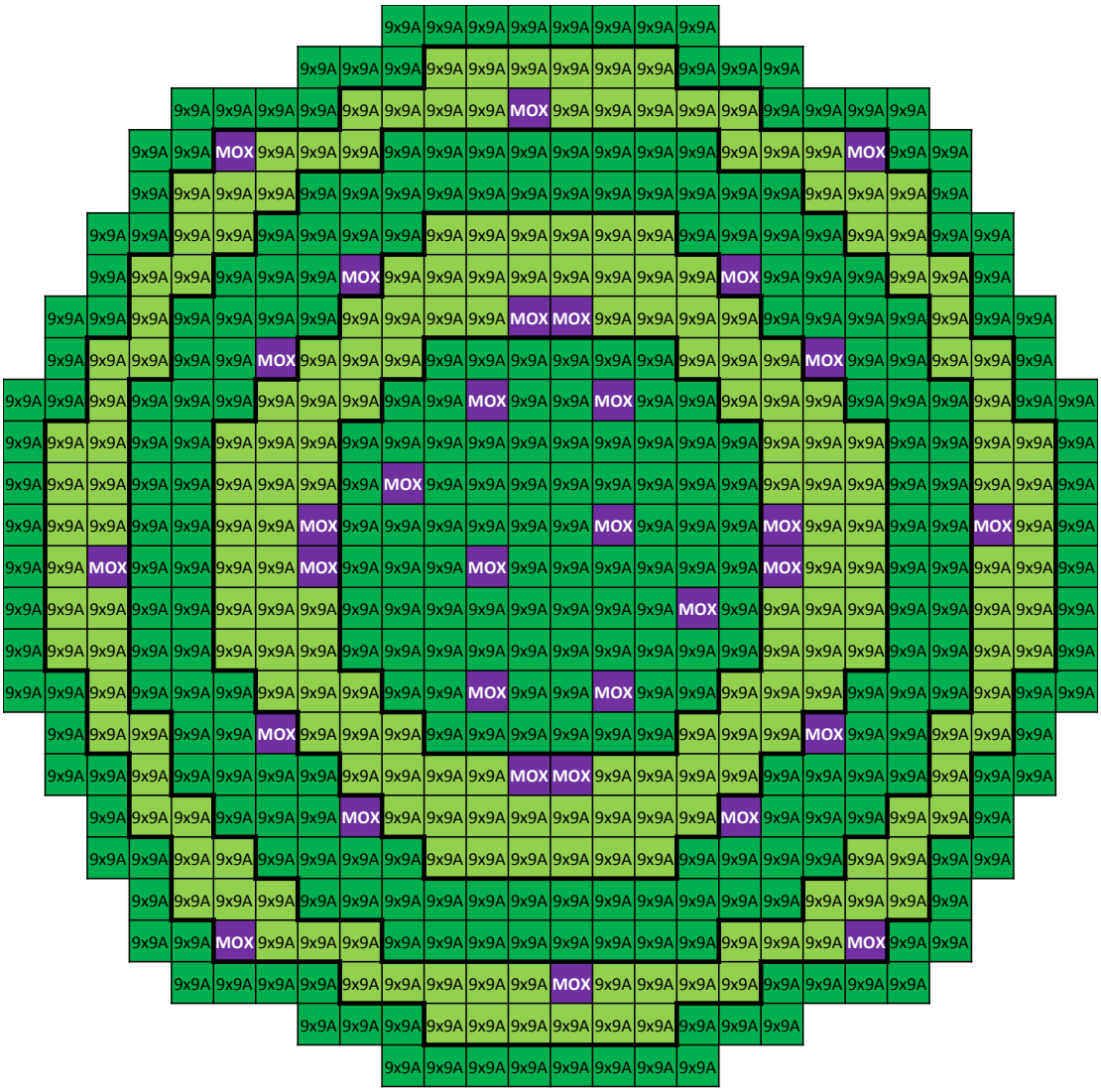

Figure 4.17. Fukushima unit 3 fuel assembly map.

4.2.5 Axial Void Distributions

BWRs are designed for two-phase flow through the active region of the core. Coolant enters the bottom of the core in a subcooled state. The coolant temperature increases up to the bulk saturation temperature after traversing about 10% of the active fuel length of the core. After saturation, additional heat is transferred to the coolant by increased void formation as the coolant rises and exits the core. Steam voids affect the bulk density of the coolant/moderator, and therefore significantly influence the spatial and spectral characteristics of neutron reaction rates. These effects need to be captured by the spatially-integrated, one-group cross sections given to ORIGEN-S for a fuel assembly depletion simulation.

The radially integrated void fraction ranges from 0.0 at the inlet to about 0.7 at the core exit. A typical BWR at full power, steady state operation exhibits a core-averaged void fraction of about 0.4. The fuel assembly-level burnup simulations in Section 4.3 do not consider axial variations in

power, materials, void fraction, or one-group reaction rates for the ORIGEN-S/ARP calculations; RN mass and decay power are simply allocated over the axial levels in the MELCOR model via user-specified multipliers informed by the axial burnup and power distributions from full-power operation. Hence an axially-integrated void fraction of 0.4 is used to calculate an average moderator density for the analyses using:

$$\rho_{avg} = \alpha\rho_v + \rho_l(1-\alpha)$$

Where,

ρ_{avg} = Bulk average density of the two-phase mixture

α = Average void fraction

ρ_v = Vapor (i.e., steam/void) density at saturation temperature

ρ_l = Liquid density at saturation temperature.

A typical axial distribution for void fraction for a BWR is demonstrated by Figure 4.18. It depicts the operating void distribution for Fukushima unit 3 during its final cycle before the severe accident, and is publically accessible from the TEPCO website [21]. Such information will be used in the current ORIGEN-S/ARP analyses in an axially-integrated form, and in future TRITON analyses that examine several core regions to generate axially-refined ARP libraries.

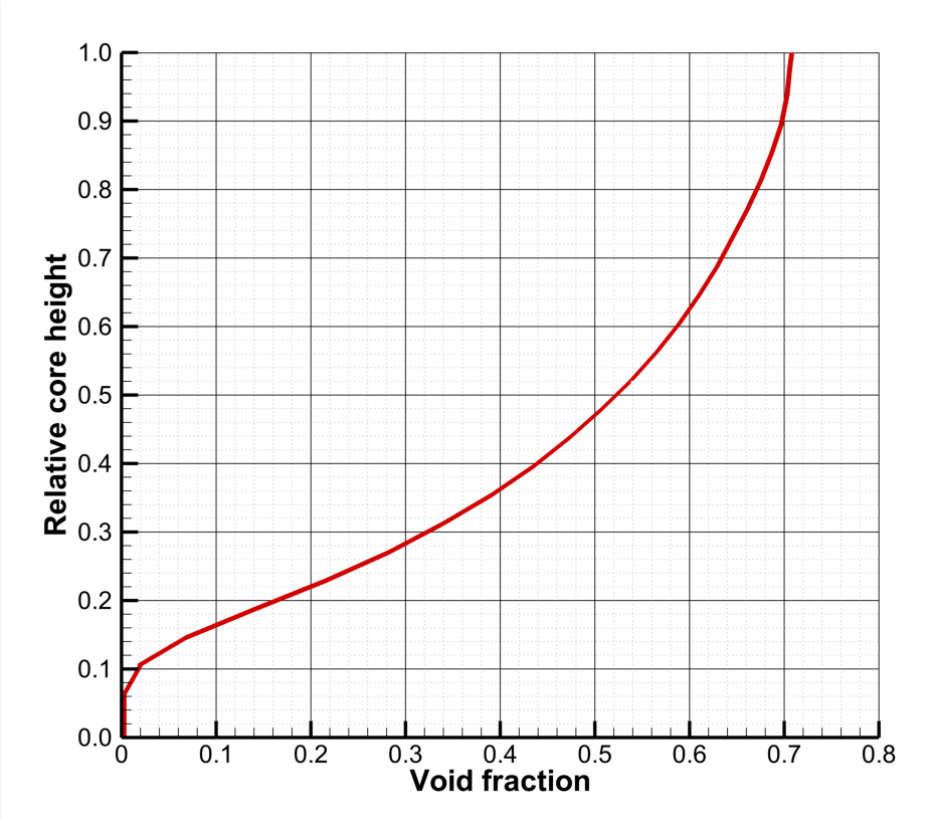

Figure 4.18. Axial void fraction distribution for Fukushima unit 3.

4.3 Fukushima Unit 1-3 Analyses and Results

This section documents the analysis of units 1-3 at Fukushima using ORIGEN-S/ARP in conjunction with the SNL tools. The results for lumped RN class inventories are described in Section 4.3.1. Calculated class inventories are compared to downscaled inventories from the Peach Bottom MELCOR model. Section 4.3.2 discusses the total decay heat curves for each unit. The calculated decay powers are compared to decay heat curves that were estimated from analytical formulas, ANS standards, and by power-scaling information from the Peach Bottom model. Comparisons to TEPCO-calculated decay heat curves are also provided. In Section 4.3.3, the radial distributions of decay power over MELCOR COR rings are presented. Since the ORIGEN-S/ARP analyses of the Fukushima units consider each fuel assembly individually, it is easy to calculate radial distributions of decay power after shutdown. The SNL Perl script reads the OPUS output files for each fuel assembly in order to derive these radial power distributions. Decay power distributions could be also estimated from the operating power distributions if whole-core ORIGEN simulations were performed instead of assembly-wise calculations.

The calculated isotopic inventories for the Fukushima units are presented in Section 4.3.4, Section, 4.3.5, and Section 4.3.6. The calculated activities are compared to inventories estimated by a power-scaling the RN class masses from Peach Bottom SOARCA. Since MELMACCS attempts to scale each isotope inventory by the relevant RN class inventory derived from MELMACCS input to the RN class inventory in the MELCOR plot file, the isotopic inventories derived by MELMACCS from power-scaled RN masses would also be, naturally, scaled by the power ratio. The power-scaled nuclide inventories are deemed to be inadequate for best-estimate and rigorous uncertainty analyses of the Fukushima accidents using MELCOR and MACCS. The calculated inventories and are also compared to TEPCO calculations that used ORIGEN2.

4.3.1 Lumped RN Class Inventories

The calculated RN class masses for Fukushima units 1-3 are listed in Table 4-10. These quantities are extracted and derived directly from ORIGEN-S nuclide outputs, and these values are used in the DCH_EL and RN1_FPN input records. Since the absolute masses of RN classes are important for various radionuclide transport physics (aerosol dynamics, deposition, etc.), the RN masses include stable fission products and decay products in the fuel. Stable light elements in the fuel, including burnable poisons (e.g. Gd) and trace impurities, are also included in RN masses. Obviously, the RN masses also include radioactive fission products, actinides, activation products in the fuel, and decay daughters.

Table 4-10. RN class inventories for Fukushima MELCOR models.

#	Class (representative)	SNL 1F1 (kg)	SNL 1F2 (kg)	SNL 1F3 (kg)
1	Noble Gases (Xe)	299.96	372.45	346.46
2	Alkali Metals (Cs)	8.13	9.86	9.41
3	Alkaline Earths (Ba)	128.89	159.06	149.26
4	Halogens (I)	all in CsI	all in CsI	all in CsI
5	Chalcogens (Te)	27.59	33.91	31.71
6	Platinoids (Ru)	203.73	247.10	229.01
7	Early Transition Elements (Mo)	171.70	212.45	197.95
8	Tetravalent (Ce)	798.33	994.50	1157.95
9	Trivalents (La)	639.40	811.83	778.83
10	Uranium (U)	65706.83	90335.23	91072.32
11	More Volatile Main Group (Cd)	6.98	8.81	8.29
12	Less Volatile Main Group (Sn)	6.19	7.46	6.95
13	Boron (B)	3.46E-5	4.22E-5	3.86E-5
16	Cesium Iodide (CsI)	23.35	28.86	27.02
17	Cesium Molybdate (Cs_2MoO_4)	210.29	255.02	243.26
	Total cesium class mass	174.59	212.01	201.98
	Total iodine class mass	11.40	14.09	13.20
	Total molybdenum class mass	227.47	280.08	262.47

It is interesting to compare the calculated RN masses with the inventories that were initially used in the Fukushima MELCOR models, which were simply downscaled quantities from the Peach Bottom SOARCA model–the thermal power ratios between the reactors (1380 MW to 3511 MW for unit 1, and 2381 MW to 3511 MW for units 2 and 3) were used to downscale the RN masses in Peach Bottom. These scaled inventories are listed Table 4-11. This table also includes the percent difference between the calculated inventories and the scaled inventories, where a percentage less than zero denotes an over-estimation by the scaled inventories. Lumped RN masses *should* scale reasonably well by thermal power if the reactors are of roughly comparable design (i.e. geometry, neutron spectrum, fuel loading) and overall burnup level. However, as shown in Table 4-11, the scaled inventories under-estimate the true RN masses for unit 1 by 30% or more for several key classes, likely owing to significantly different burnup between unit 1 and the core used in the Peach Bottom model. As shown previously in Table 4-1, Table 4-2, Table 4-4, and Figure 4.1, unit 1 at Fukushima contained a large number of high burnup assemblies (particularly the 8x8 assemblies), some of which were irradiated in four or more previous cycles. Lumped RN inventories are strongly affected by the accumulation of stable and long-lived nuclides that accumulate monotonically with burnup. In contrast, the power-scaled inventories estimate the actual RN inventories relatively well for units 2 and 3, with percent differences of 2% to 16% for the most important classes. Larger differences in other classes, like the trivalent (La) class, could be due to the assumed amounts of Gd burnable poison in the core. Also, unit 3 exhibits increased tetravalent (Ce) mass due to additional Pu in the MOX assemblies.

Table 4-11. Comparison to estimated RN inventories downscaled by thermal power.

#	Class (representative)	1F1 Scaled (kg)	1F2/3 Scaled (kg)	% diff 1F1	% diff 1F3
1	Noble Gases (Xe)	208.80	362.49	30.39	-4.63
2	Alkali Metals (Cs)	5.93	10.94	27.05	-16.28
3	Alkaline Earths (Ba)	92.53	161.10	28.21	-7.93
4	Halogens (I)	all in CsI	all in CsI	NA	NA
5	Chalcogens (Te)	19.29	33.39	30.06	-5.29
6	Platinoids (Ru)	134.60	238.45	33.93	-4.12
7	Early Transition Elements (Mo)	116.48	202.18	32.16	-2.14
8	Tetravalent (Ce)	610.88	1066.79	23.48	7.87
9	Trivalents (La)	704.43	1222.75	-10.17	-57.00
10	Uranium (U)	52150.18	88314.08	20.63	3.03
11	More Volatile Main Group (Cd)	2.59	4.54	62.87	45.22
12	Less Volatile Main Group (Sn)	3.78	6.39	38.90	8.09
13	Boron (B)	2.34E-5	4.04E-5	32.32	-4.76
16	Cesium Iodide (CsI)	16.03	27.72	31.34	-2.57
17	Cesium Molybdate (Cs_2MoO_4)	153.41	266.43	27.05	-9.52
	Total cesium class mass	126.86	220.89	27.34	-9.36
	Total iodine class mass	7.83	13.54	31.34	-2.57
	Total molybdenum class mass	157.17	272.84	30.91	-3.95

MELCOR contains pre-generated SANDIA-ORIGEN data (see Section 5.1) that may be used to approximate the lumped RN inventories by extrapolating internal data by thermal power. The internal inventory data for BWRs is based on the SANDIA-ORIGEN analysis of a 3578 MWt BWR. The inventory calculated for Fukushima unit 1 using ORIGEN-S/ARP is compared to the MELCOR estimations in Table 4-12. As expected, the internal MELCOR models poorly predict the lumped RN masses for unit 1, as they under-predict the mass of important classes by 30-50%. This probably indicates that the internal MELCOR data does not appropriately consider the burnup of the unit 1 core, since lumped RN masses increase monotonically with burnup. The interpolated inventories out of MELCOR are quite similar to the linear power-scaled inventories from Table 4-11. Neither of the approximated inventories are suitable for best-estimate severe accident and consequence analyses, but are nonetheless useful for quickly obtaining grossly-reasonable RN information.

Table 4-12. Comparison of unit 1 inventories to MELCOR RN inventories extrapolated from SANDIA-ORIGEN data for a 3578 MW BWR.

#	Class (representative)	SNL (kg)*	MELCOR (kg)	% difference
1	Noble Gases (Xe)	299.96	203.99	47.05
2	Alkali Metals (Cs)	8.13	6.16	32.02
3	Alkaline Earths (Ba)	128.89	90.56	42.32
4	Halogens (I)	all in CsI	all in CsI	--
5	Chalcogens (Te)	27.59	18.78	46.89
6	Platinoids (Ru)	203.73	134.06	51.97
7	Early Transition Elements (Mo)	171.70	113.84	50.83
8	Tetravalent (Ce)	798.33	599.16	33.24
9	Trivalents (La)	639.40	688.05	-7.07
10	Uranium (U)	65706.83	66655.94	-1.42
11	More Volatile Main Group (Cd)	6.98	2.56	172.72
12	Less Volatile Main Group (Sn)	6.19	3.60	71.96
12	Boron (B)	3.46E-5	0.0	--
16	Cesium iodide (CsI)	23.35	15.59	49.75
17	Cesium molybdate (Cs_2MoO_4)	210.29	149.78	40.40
	Total cesium class mass	174.59	124.19	40.58
	Total iodine class mass	11.40	7.61	49.75
	Total molybdenum class mass	227.47	153.56	48.13

*These are the inventories calculated by ORIGEN-S/ARP.

4.3.2 Total Decay Power Curves

The total decay powers that are calculated for each unit are depicted in Figure 4.19 on a logarithmic time scale and in Figure 4.20 on a severe accident (linear) time scale. Since these decay heat curves are calculated using ORIGEN-S with ENDF/B-VII decay data and burnup-dependent (albeit ENDF/B-V) cross sections, they are considered sufficiently accurate for use in best-estimate severe accident simulations with MELCOR. These decay heat curves may also be used as 'base' curves to derive uncertainty distributions for each unit, which is discussed more in Section 4.4. The decay power for unit 1 is significantly less than those for units 2 and 3, owing to the lower power rating of unit 1; decay power is always generally 6-7% of the operating power for any significant amount of reactor operation, due to the short-lived nuclides that drive decay power reaching quasi-equilibrium concentrations. The equilibrium concentrations of short-lived nuclides can vary slightly with reactor operation due to changing effective yields, actinide buildup, and cross section variations with burnup. The time-dependence of the decay heat curve after scram can vary significantly with burnup, fuel loading, and reactor operation. Such effects are quantified for the Surry reactor in Section 5.2, but the Fukushima analyses presented here only consider the 'known' reactor operation using the best available plant data. The decay powers for unit 2 and unit 3 are very similar despite the MOX fuel in unit 3.

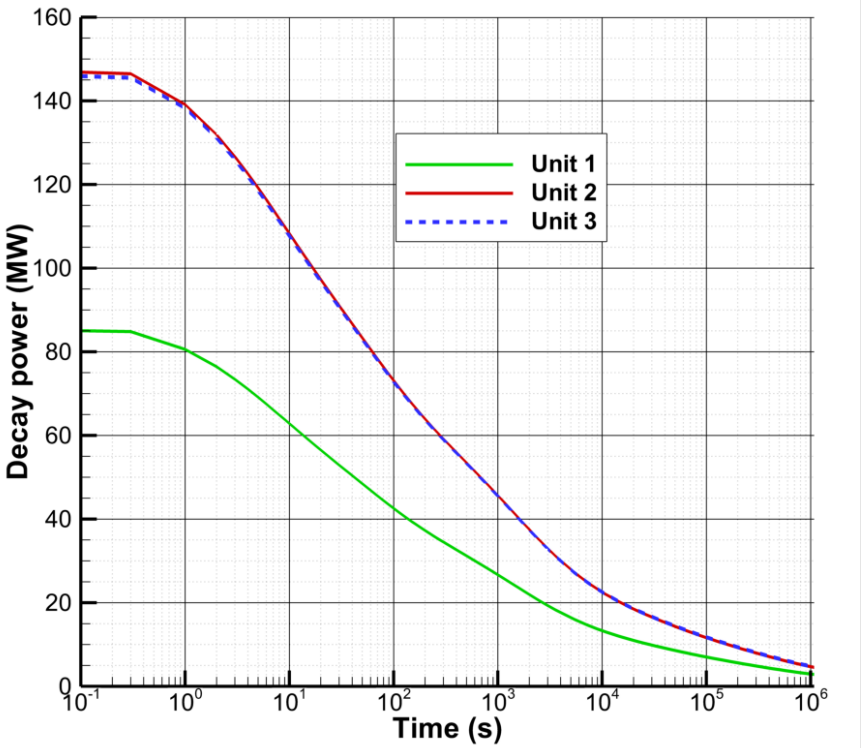

Figure 4.19. Calculated decay power curves for each Fukushima unit, log scale.

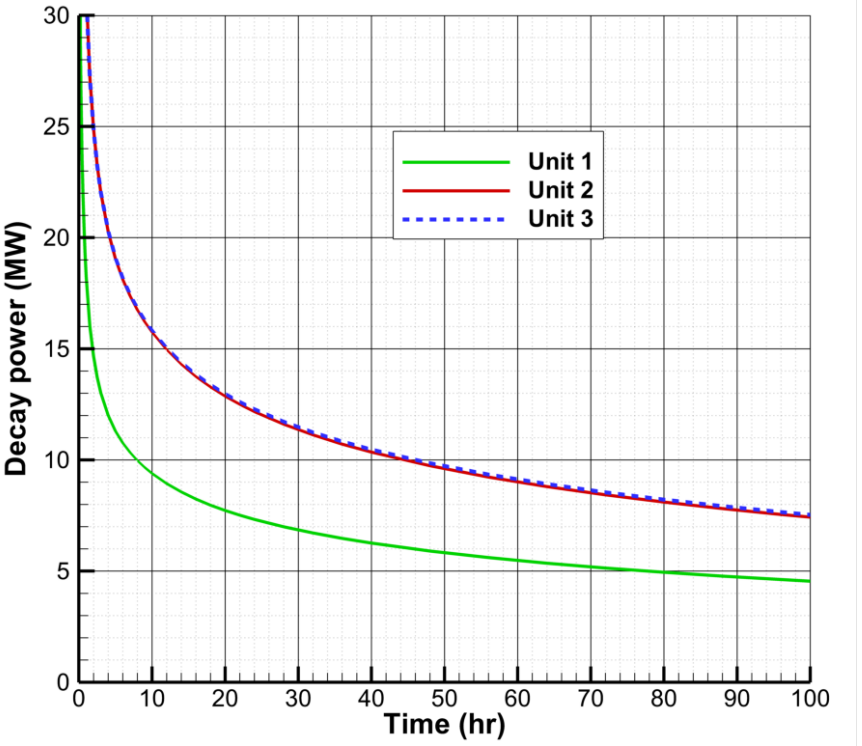

Figure 4.20. Calculated decay power curves for each Fukushima unit, linear scale.

In Figure 4.21 and Figure 4.22 the calculated decay heat curves for unit 1 and unit 3 are compared to TEPCO calculations using ORIGEN2 with unknown data libraries. Comparisons for unit 2 are not presented since the decay power for unit 2 is very similar to unit 3. The SNL calculations are also compared to the thermal power-scaled decay heat curves from the Peach Bottom model and to analytical formulas from reference [22]. Being an integral quantity, decay heat should be relatively well-predicted by both integral methods (e.g. ANS standards) and isotope summation codes (e.g. ORIGEN-S and CINDER90). The total core decay powers predicted by SNL and TEPCO are very similar for all units: the curves are within 1-10% of each other for all times after scram. The decay powers from scaled Peach Bottom data are substantially different from the SNL- and TEPCO-calculated values. The scaled decay powers overestimate the decay powers for units 1-3 by 5-25%, judging by the SNL and TEPCO calculations. The analytical formula is only accurate to within a factor of two for decay time greater than 100 seconds [22]; this is readily evident in Figure 4.21 and Figure 4.22, as the analytical approximations provide excessive over-predictions of decay power soon after scram. The analytical formula seems reasonable several hours after shutdown. These comparisons give justification for implementing best-estimate decay heat curves in severe accident models that are calculated by mechanistic codes such as ORIGEN-S.

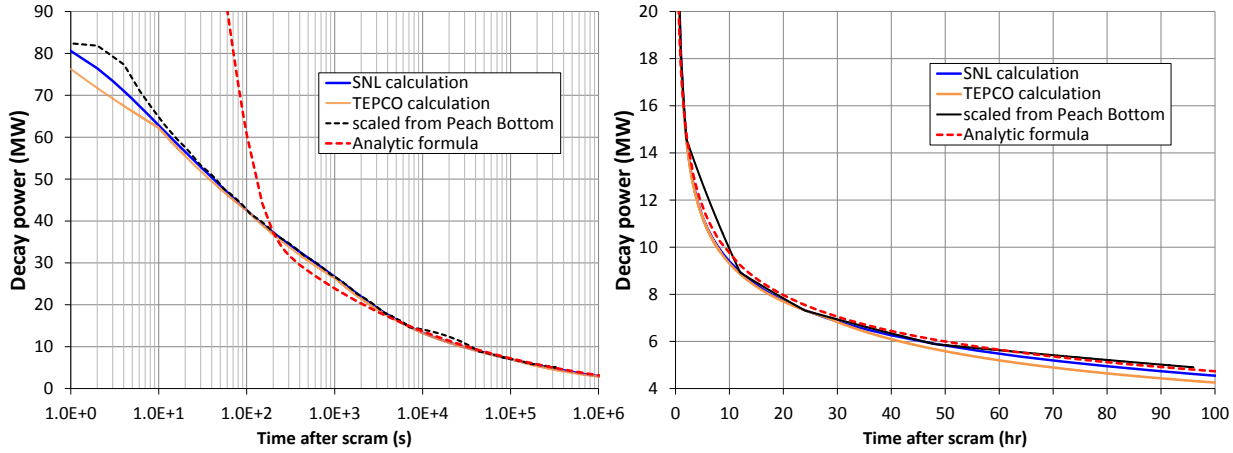

Figure 4.21. Unit 1 decay heat comparisons on log (left) and linear (right) scales.

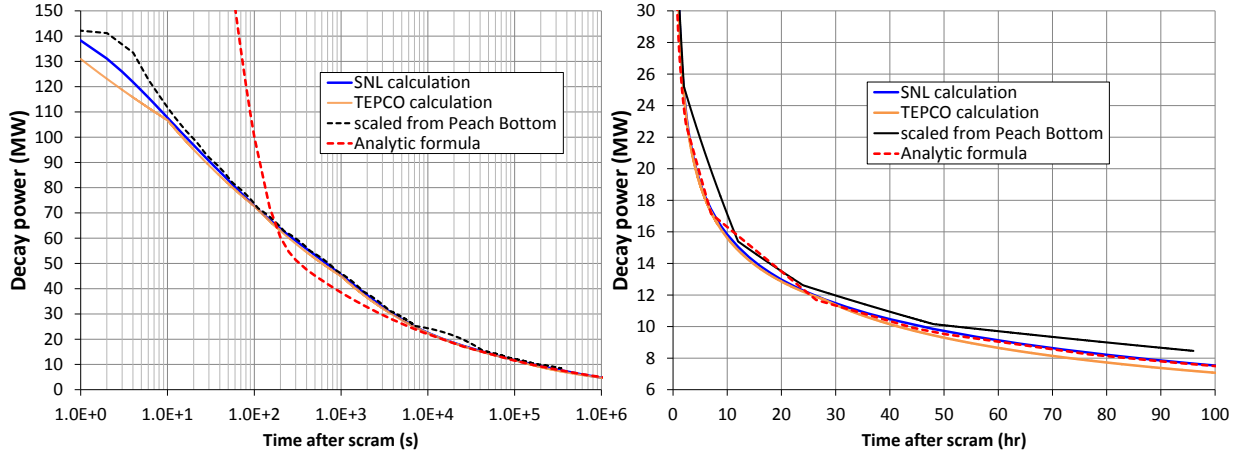

Figure 4.22. Unit 3 decay heat comparisons on log (left) and linear (right) scales.

The decay heat curves calculated by SNL and TEPCO for unit 1 are further compared against the internal models in MELCOR: MELCOR can estimate decay power using the ANS1979 standard or by extrapolating from internal SANDIA-ORIGEN data. These comparisons are depicted in Figure 4.23. Both of the MELCOR estimations over-predict decay power relative to the SNL and TEPCO calculations soon after scram. Later in time, the ANS1979 curve is in good agreement with the SNL and TEPCO curves, but exhibits a few questionable discontinuities. The SANDIA-ORIGEN estimation by MELCOR under-predicts decay power by 15-30% after about 100 seconds of decay time, compared to the SNL and TEPCO curves. The internal SANDIA-ORIGEN data likely does not capture the increased burnup of the unit 1 core. Given the good agreement between the mechanistic SNL and TEPCO calculations, these curves are better indicators of best-estimate decay power for severe accident simulations.

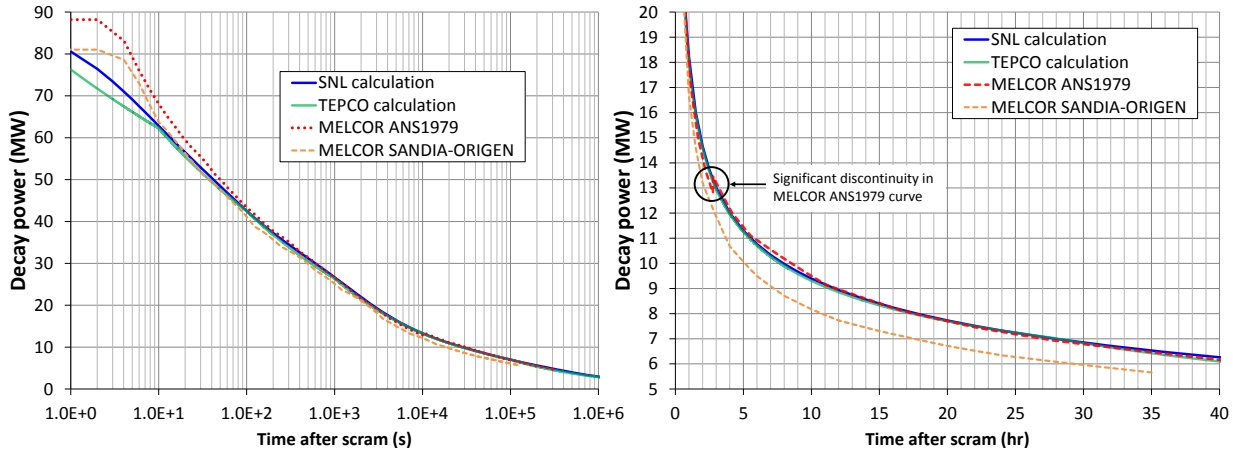

Figure 4.23. Decay heat curves for unit 1 based on different methods.

4.3.3 Radial Distributions of Decay Power

The assembly-wise ORIGEN-S/ARP calculations yield the total decay power produced in each COR ring, which can then be used to derive radial power distributions for MELCOR inputs. Because MELCOR COR rings can be (and usually are) different sizes, it is important to make a distinction between the 'absolute' and 'relative' decay power distributions over the rings. The absolute decay power fraction in a ring is directly proportional to the size of the ring (i.e., number of assemblies) in addition to the local concentration of short-lived nuclides that drive decay power soon after shutdown. In contrast, the relative power distribution inversely accounts for the size of the COR ring, i.e. ring powers are normalized by the number of assemblies or the fuel mass (MTU) in each ring (which are essentially the same quantity for LWRs) and are thus indicative of the relative power density in each ring. The absolute power distribution is the appropriate radial scaling factor for apportioning RN masses according to the decay power distribution, if the user desires. The relative power distribution is useful for comparing power densities between different sized rings for thermal-hydraulic considerations. For example, a 5-assembly ring naturally generates less absolute decay power than a 50-assembly ring; however, the smaller ring may well have a significantly higher relative power fraction (i.e. power density) on a W/assembly or W/kg basis, which can increase local temperatures following core uncovering and hence cause enhanced degradation, oxidation, and RN releases in the COR ring.

The true radial mass distributions of for each RN class are also calculated by ORIGEN-S/ARP. As discussed in Section 3.3.1 and further in Section 6.1, the SNL tools have the option to allocate RN masses according to the decay power distribution, while preserving the true radial distribution of key RN classes like cesium. The Fukushima inventories implement the option to allocate all RN mass radially according to the calculated decay power distribution, excluding the alkali metal (Cs), tetravalent (Ce, Pu), and uranium classes, which are distributed radially according to the ORIGEN-S/ARP predictions. Axially, RN masses for the Fukushima models are apportioned according to an average power and burnup distribution, but the uranium class is distributed uniformly over all axial COR nodes in the MELCOR models.

The absolute distributions radial of decay power are used to provide radial scaling factors for RN masses (i.e. RN1_FPN input), since most RN mass must be allocated according to the decay power distribution, as discussed in Section 4.3 (and more in Sections 3.3.1 and 6.1). Normalized (W/kgU or W/assembly) decay power distributions are also calculated to provide insights into the thermal-hydraulic and degradation behavior of the core during the severe accident. Although decay power distributions are essentially static for severe accident time frames, MELCOR does allow for time-varying decay power distributions since each class has its own decay power curve defined by the user. The decay power distributions depicted in this section are for the moment of shutdown. The time-dependence of the decay power distribution over the core (with respect to decay time) is likely unimportant for severe accident simulations due to core deformation, fuel relocation, and radionuclide release from the fuel, which carries decay heat away from the core. The time-dependent relocation of decay heat throughout the plant, on the other hand, is of first-order importance for severe accidents, and MELCOR directly simulates such behavior. Two primary modes of decay heat relocation during severe accidents are radionuclide release from the fuel and corium discharge to the containment following RPV lower head failure.

Figure 4.24 shows the radial distributions of decay power for each unit, as calculated by the ORIGEN-S/ARP simulations and the SNL Perl script. To reiterate, the absolute decay power distributions are directly proportional to the number of assemblies in each ring, and are therefore used as multiplier factors for radial allocation of RN masses. The relative power distributions reflect the power density in each ring, and are therefore more indicative of relative heating rates and collapse timing during core heatup and damage. The relative decay power distributions are nearly the same as the operating power distributions upon collapsing the TEPCO data (Figure 4.1, Figure 4.2, and Figure 4.3). Figure 4.25 demonstrates that decay power is an insignificant function of decay time soon after shutdown–the decay power is initially quite similar to the operating power distribution due to higher concentrations of short-lived nuclides, but slowly shifts to matching the burnup distribution since higher burnup regions contain increased concentrations of medium- and long-lived nuclides.

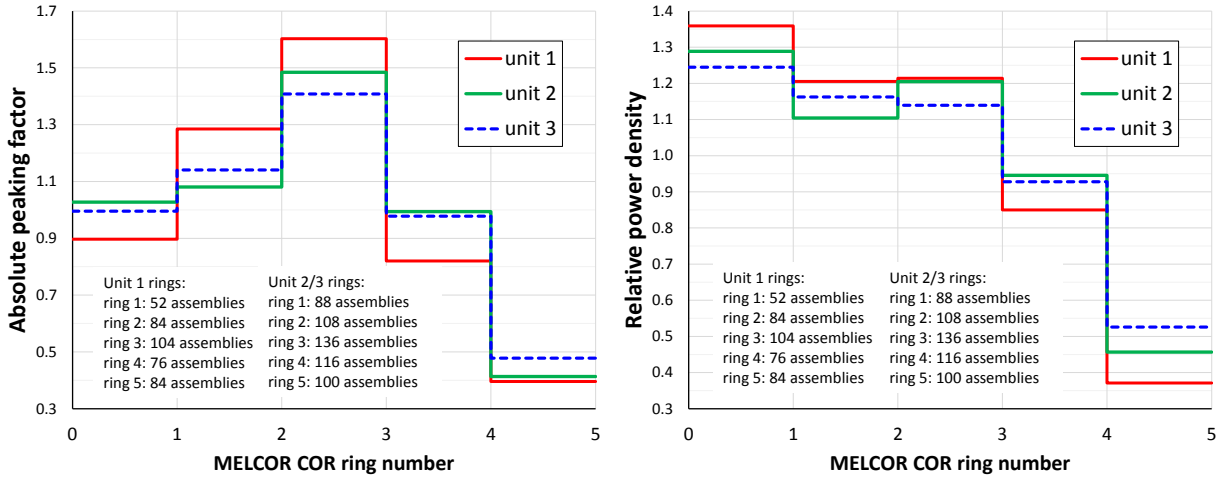

Figure 4.24. Calculated absolute (left) and relative (right) radial decay power distributions.

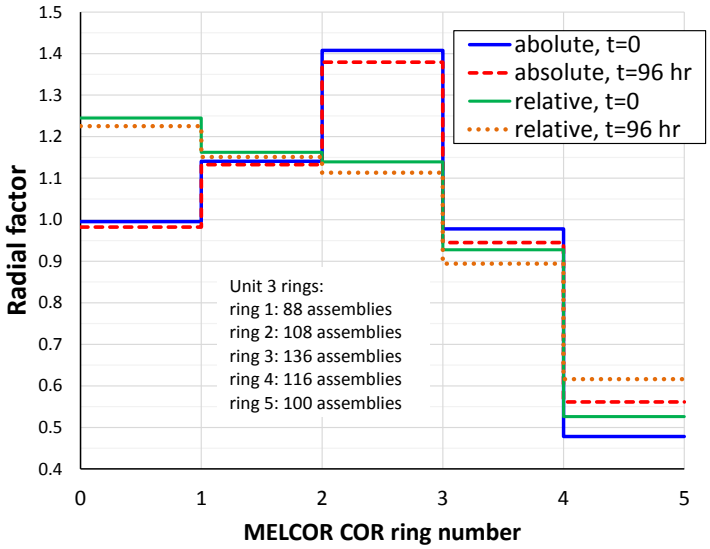

Figure 4.25. Time-dependence of decay power on time after scram for unit 3.

4.3.4 Fukushima Unit 1 Nuclide Inventories

In Table 4-13, Table 4-14, and Table 4-15, the calculated nuclide inventories (in Bq) for unit 1 are compared to scaled inventories from Peach Bottom and to TEPCO calculations that used ORIGEN2. Table 4-13 contains activities for key nuclides in the noble gas, alkali metal, alkaline earth, halogen, and chalcogen classes. Table 4-14 shows key nuclides in the platinoid, early transition metal, and tetravalent classes. Table 4-15 lists nuclide activities in the trivalent class. In general, the scaled inventories are quite inaccurate compared to the SNL and TEPCO calculations. The scaled quantities can be off by a factor of 2 for nuclides of first-order importance for health and consequence effects. Although lumped RN inventories for MELCOR can likely be estimated reasonably well by simple linear scaling (e.g. by burnup or power), accurate nuclide inventories for best-estimate analyses require mechanistic calculations using codes like ORIGEN.

The calculated inventories by SNL are quite comparable to the TEPCO calculations for most of the important nuclides. The SNL to TEPCO calculated ratios for Sr-90, I-131, Te-132, and Cs-137 are 1.10, 1.00, 1.01, and 1.04, respectively. However, there are some considerable differences that call for more comprehensive analyses: the actinides Pu-238 and Pu-241 are under-predicted relative to the TEPCO calculations, with respective ratios of 0.63 and 0.67. There is also a substantial difference in the predicted activity of Cs-134–the SNL to TEPCO ratio is 0.69, which may be indicative of different flux-weighted cross sections (i.e. Cs-133 absorption) and/or other different nuclear data (e.g. fission yields of Cs-133 and Xe-133). The TEPCO nuclide inventories should not be interpreted as 'correct' since they were calculated by ORIGEN2, a deprecated code, with unknown data libraries that likely do not consider cross section variations with burnup. The TEPCO analyses were probably whole-core models that also do not consider the detailed power history of each fuel assembly from previous cycles, based on informal documentation for the BSAF project. Hence, it is equally probable that the SNL calculations (i.e. ORIGEN-S/ARP in SCALE6.1.3, ENDF/B-VII yields and decay data, and burnup-dependent ENDF/B-V cross sections) that consider each fuel assembly individually provide more accurate estimations of Pu-238 and Pu-241.

Quantities of several actinides such as Pu-238, Pu-241, Cm-242, and Cm-244 are relatively complicated to predict compared to the important fission products. As illustrated in Figure 1.2, actinide production can be strongly dependent on numerous factors: flux-weighted cross sections for several neutron reactions, multiple modes of decay, multiple modes of in-growth from parent nuclides, and initial fuel loading (e.g. MOX) can all contribute significantly to a particular actinide's production. Thus, it is no surprise that the SNL predictions for Pu-238, Pu-241, Cm-242, Cm-244, and Am-241 are quite different than the TEPCO predictions. Although the SNL calculations may indeed be more accurate, further investigations that take into account detailed fuel assembly geometry (i.e. use TRITON to create new ARP libraries), irradiation and decay history, and axial void fraction are justified if MELCOR/MACCS predictions are to be benchmarked against real data for releases and dose rates.

Table 4-13. Nuclide inventories (Bq) for unit 1: Xe, Cs, Ba, I, and Te classes.

Isotope	SNL unit 1	Scaled SOARCA	TEPCO 1F1	SNL* to SOARCA ratio	SNL to TEPCO ratio
Noble gases (Xe)					
Kr-85	1.93E+16	1.15E+16	1.76E+16	1.67	1.10
Kr-85m	4.04E+17	3.17E+17	3.75E+17	1.27	1.08
Kr-87	8.05E+17	6.28E+17	7.24E+17	1.28	1.11
Kr-88	1.08E+18	8.40E+17	1.02E+18	1.29	1.06
Xe-133	2.87E+18	2.38E+18	2.78E+18	1.20	1.03
Xe-135	9.08E+17	7.07E+17	1.19E+18	1.28	0.76
Xe-135m	5.76E+17	5.07E+17	5.43E+17	1.14	1.06
Alkali metals (Cs)					
Cs-134	1.90E+17	1.70E+17	2.76E+17	1.12	0.69
Cs-136	5.56E+16	6.17E+16	9.17E+16	0.90	0.61
Cs-137	2.05E+17	1.20E+17	1.97E+17	1.71	1.04
Rb-86	1.54E+15	2.10E+15	2.53E+15	0.73	0.61
Rb-88	1.10E+18	8.48E+17	1.04E+18	1.30	1.06
Alkaline earths (Ba)					
Ba-139	2.58E+18	2.18E+18	2.52E+18	1.19	1.03
Ba-140	2.49E+18	2.11E+18	2.42E+18	1.18	1.03
Sr-89	1.43E+18	1.17E+18	1.36E+18	1.22	1.05
Sr-90	1.56E+17	8.91E+16	1.41E+17	1.75	1.10
Sr-91	1.87E+18	1.47E+18	1.71E+18	1.27	1.10
Sr-92	1.98E+18	1.57E+18	1.84E+18	1.26	1.08
Ba-137m	1.94E+17	1.15E+17	1.86E+17	1.69	1.04
Halogens (I)					
I-131	1.36E+18	1.09E+18	1.36E+18	1.25	1.00
I-132	2.03E+18	1.60E+18	1.97E+18	1.27	1.03
I-133	2.84E+18	2.26E+18	2.80E+18	1.26	1.01
I-134	3.25E+18	2.54E+18	3.08E+18	1.28	1.05
I-135	2.72E+18	2.16E+18	2.62E+18	1.26	1.04
Chalcogens (Te)					
Te-127	1.10E+17	1.02E+17	1.42E+17	1.08	0.78
Te-127m	1.73E+16	1.66E+16	1.86E+16	1.04	0.93
Te-129	3.36E+17	3.06E+17	4.25E+17	1.10	0.79
Te-129m	6.31E+16	5.85E+16	6.33E+16	1.08	1.00
Te-131	1.17E+18	1.00E+18	1.21E+18	1.17	0.97
Te-131m	2.49E+17	2.24E+17	1.95E+17	1.11	1.28
Te-132	1.95E+18	1.68E+18	1.94E+18	1.16	1.01

*This ratio is SNL activity divided by the *scaled* SOARCA activity; the SOARCA values are down-scaled by the power ratio of unit 1 (1380 MW) to Peach Bottom (3511 MW)

Table 4-14. Nuclide inventories (Bq) for unit 1: Ru, Mo, and Ce classes.

Isotope	SNL unit 1	Scaled SOARCA	TEPCO 1F1	SNL to SOARCA ratio	SNL to TEPCO ratio
Platinoids (Ru)					
Rh-105	1.13E+18	1.14E+18	1.30E+18	0.99	0.87
Ru-103	1.93E+18	1.81E+18	2.05E+18	1.07	0.94
Ru-105	1.25E+18	1.23E+18	1.36E+18	1.02	0.92
Ru-106	6.34E+17	5.50E+17	7.47E+17	1.15	0.85
Rh-103m	1.93E+18	1.81E+18	1.85E+18	1.07	1.04
Rh-106	6.81E+17	6.13E+17	7.87E+17	1.11	0.87
Early transition metals (Mo)					
Nb-95	2.17E+18	2.03E+18	2.29E+18	1.07	0.95
Co-58	2.92E+13	1.88E+13	NA	1.55	NA
Co-60	5.93E+15	1.04E+14	NA	57.02	NA
Mo-99	2.61E+18	2.23E+18	2.57E+18	1.17	1.01
Tc-99m	2.30E+18	1.98E+18	2.25E+18	1.17	1.02
Nb-97	2.44E+18	2.06E+18	2.34E+18	1.19	1.05
Nb-97m	2.30E+18	1.94E+18	2.20E+18	1.18	1.05
Tetravalents (Ce)					
Ce-141	2.32E+18	1.91E+18	2.30E+18	1.22	1.01
Ce-143	2.24E+18	1.79E+18	2.14E+18	1.25	1.04
Ce-144	1.63E+18	1.34E+18	1.70E+18	1.22	0.96
Np-239	2.36E+19	2.23E+19	2.81E+19	1.06	0.84
Pu-238	3.70E+15	3.26E+15	5.90E+15	1.13	0.63
Pu-239	5.84E+14	3.75E+14	7.45E+14	1.56	0.78
Pu-240	9.14E+14	4.59E+14	8.77E+14	1.99	1.04
Pu-241	1.76E+17	1.33E+17	2.62E+17	1.32	0.67
Zr-95	2.30E+18	1.95E+18	2.31E+18	1.18	0.99
Zr-97	2.42E+18	1.96E+18	2.32E+18	1.23	1.05

Table 4-15. Nuclide inventories (Bq) for unit 1: La class.

Isotope	SNL unit 1	Scaled SOARCA	TEPCO 1F1	SNL to SOARCA ratio	SNL to TEPCO ratio
Trivalents (La)					
Am-241	3.18E+14	1.35E+14	4.04E+14	2.36	0.79
Cm-242	5.57E+16	4.48E+16	8.27E+16	1.24	0.67
Cm-244	3.18E+15	4.44E+15	5.56E+15	0.72	0.57
La-140	2.55E+18	2.23E+18	2.50E+18	1.14	1.02
La-141	2.35E+18	2.00E+18	2.30E+18	1.17	1.02
La-142	2.28E+18	1.93E+18	2.22E+18	1.18	1.03
Nd-147	9.29E+17	8.01E+17	9.18E+17	1.16	1.01
Pr-143	2.24E+18	1.83E+18	2.11E+18	1.23	1.06
Y-90	1.59E+17	9.39E+16	1.45E+17	1.69	1.10
Y-91	1.83E+18	1.54E+18	1.73E+18	1.19	1.06
Y-92	2.00E+18	1.61E+18	1.85E+18	1.24	1.08
Y-93	2.21E+18	1.81E+18	2.12E+18	1.22	1.04
Y-91m	1.09E+18	8.64E+17	9.92E+17	1.26	1.10
Pr-144	1.64E+18	1.43E+18	1.70E+18	1.15	0.96
Pr-144m	2.29E+16	1.99E+16	2.04E+16	1.15	1.12

4.3.5 Fukushima Unit 2 Nuclide Inventories

The nuclides inventories for unit 2 are shown in Table 4-16, Table 4-17, and Table 4-18. Again, the inventories calculated by SNL with ORIGEN-S/ARP are compared to scaled inventories from Peach Bottom and to TEPCO calculations that used ORIGEN2. Table 4-16 contains activities for key nuclides in the noble gas, alkali metal, alkaline earth, halogen, and chalcogen classes. Table 4-17 shows key nuclides in the platinoid, early transition metal, and tetravalent classes. Table 4-18 lists nuclide activities in the trivalent class. In general, the scaled inventories are quite inaccurate compared to the SNL and TEPCO calculations. The scaled quantities can be off by a factor of 1.4 for nuclides of first-order importance for health and consequence effects.

Similar to unit 1, the calculated unit 2 inventories are in very good agreement with the TEPCO inventories for most key fission products. The SNL to TEPCO calculated ratios for Sr-90, I-131, Te-132, and Cs-137 are 1.10, 1.00, 1.00, and 1.05, respectively. The SNL predictions for Pu-238 and Pu-241 are again quite small compared to the TEPCO predictions, with SNL to TEPCO ratios of 0.65 and 0.70, respectively.

Table 4-16. Nuclide inventories (Bq) for unit 2: Xe, Cs, Ba, I, and Te classes.

Isotope	SNL unit 2	Scaled SOARCA	TEPCO 1F2	SNL to SOARCA ratio	SNL to TEPCO ratio
Noble gases (Xe)					
Kr-85	2.48E+16	1.99E+16	2.26E+16	1.25	1.10
Kr-85m	7.11E+17	5.47E+17	6.94E+17	1.30	1.02
Kr-87	1.42E+18	1.08E+18	1.35E+18	1.31	1.06
Kr-88	1.92E+18	1.45E+18	1.90E+18	1.32	1.01
Xe-133	4.95E+18	4.11E+18	4.87E+18	1.20	1.02
Xe-135	1.40E+18	1.22E+18	1.87E+18	1.15	0.75
Xe-135m	9.86E+17	8.74E+17	9.36E+17	1.13	1.05
Alkali metals (Cs)					
Cs-134	2.48E+17	2.93E+17	3.44E+17	0.85	0.72
Cs-136	7.96E+16	1.06E+17	1.25E+17	0.75	0.64
Cs-137	2.54E+17	2.07E+17	2.43E+17	1.23	1.05
Rb-86	2.40E+15	3.63E+15	3.75E+15	0.66	0.64
Rb-88	1.95E+18	1.46E+18	1.93E+18	1.33	1.01
Alkaline earths (Ba)					
Ba-139	4.48E+18	3.75E+18	4.45E+18	1.19	1.01
Ba-140	4.32E+18	3.64E+18	4.24E+18	1.19	1.02
Sr-89	2.30E+18	2.02E+18	2.32E+18	1.14	0.99
Sr-90	1.96E+17	1.54E+17	1.79E+17	1.28	1.10
Sr-91	3.31E+18	2.54E+18	3.17E+18	1.30	1.05
Sr-92	3.48E+18	2.71E+18	3.38E+18	1.28	1.03
Ba-137m	2.42E+17	1.98E+17	2.30E+17	1.22	1.05
Halogens (I)					
I-131	2.34E+18	1.88E+18	2.34E+18	1.24	1.00
I-132	3.51E+18	2.76E+18	3.42E+18	1.27	1.03
I-133	4.90E+18	3.90E+18	4.91E+18	1.25	1.00
I-134	5.62E+18	4.39E+18	5.42E+18	1.28	1.04
I-135	4.69E+18	3.72E+18	4.59E+18	1.26	1.02
Chalcogens (Te)					
Te-127	1.81E+17	1.76E+17	2.32E+17	1.03	0.78
Te-127m	2.62E+16	2.86E+16	2.82E+16	0.92	0.93
Te-129	5.64E+17	5.28E+17	7.14E+17	1.07	0.79
Te-129m	1.01E+17	1.01E+17	1.02E+17	1.00	0.99
Te-131	2.01E+18	1.73E+18	2.09E+18	1.16	0.96
Te-131m	4.20E+17	3.87E+17	3.32E+17	1.08	1.26
Te-132	3.36E+18	2.91E+18	3.37E+18	1.16	1.00

Table 4-17. Nuclide inventories (Bq) for unit 2: Ru, Mo, and Ce classes.

Isotope	SNL unit 2	Scaled SOARCA	TEPCO 1F2	SNL to SOARCA ratio	SNL to TEPCO ratio
Platinoids (Ru)					
Rh-105	1.92E+18	1.96E+18	2.05E+18	0.98	0.94
Ru-103	3.06E+18	3.12E+18	3.26E+18	0.98	0.94
Ru-105	2.05E+18	2.13E+18	2.16E+18	0.96	0.95
Ru-106	8.98E+17	9.49E+17	1.02E+18	0.95	0.88
Rh-103m	3.05E+18	3.12E+18	2.94E+18	0.98	1.04
Rh-106	9.95E+17	1.06E+18	1.09E+18	0.94	0.91
Early transition metals (Mo)					
Nb-95	3.22E+18	3.51E+18	3.54E+18	0.92	0.91
Co-58	4.39E+13	3.25E+13	NA	1.35	NA
Co-60	7.64E+15	1.80E+14	NA	42.53	NA
Mo-99	4.50E+18	3.85E+18	4.49E+18	1.17	1.00
Tc-99m	3.97E+18	3.41E+18	3.94E+18	1.17	1.01
Nb-97	4.23E+18	3.55E+18	4.12E+18	1.19	1.03
Nb-97m	3.99E+18	3.35E+18	3.88E+18	1.19	1.03
Tetravalents (Ce)					
Ce-141	3.83E+18	3.30E+18	3.87E+18	1.16	0.99
Ce-143	3.90E+18	3.08E+18	3.83E+18	1.26	1.02
Ce-144	2.49E+18	2.32E+18	2.60E+18	1.07	0.96
Np-239	4.00E+19	3.84E+19	4.65E+19	1.04	0.86
Pu-238	4.16E+15	5.63E+15	6.39E+15	0.74	0.65
Pu-239	7.43E+14	6.48E+14	9.21E+14	1.15	0.81
Pu-240	1.10E+15	7.93E+14	1.04E+15	1.39	1.05
Pu-241	2.15E+17	2.30E+17	3.09E+17	0.94	0.70
Zr-95	3.62E+18	3.36E+18	3.78E+18	1.08	0.96
Zr-97	4.20E+18	3.39E+18	4.09E+18	1.24	1.03

Table 4-18. Nuclide inventories (Bq) for unit 2: La class.

Isotope	SNL unit 2	Scaled SOARCA	TEPCO 1F2	SNL to SOARCA ratio	SNL to TEPCO ratio
Trivalents (La)					
Am-241	3.03E+14	2.32E+14	3.72E+14	1.31	0.81
Cm-242	6.38E+16	7.72E+16	8.50E+16	0.83	0.75
Cm-244	3.53E+15	7.66E+15	5.49E+15	0.46	0.64
La-140	4.40E+18	3.84E+18	4.35E+18	1.15	1.01
La-141	4.01E+18	3.46E+18	4.06E+18	1.16	0.99
La-142	3.97E+18	3.33E+18	3.95E+18	1.19	1.00
Nd-147	1.61E+18	1.38E+18	1.60E+18	1.16	1.00
Pr-143	3.89E+18	3.15E+18	3.71E+18	1.23	1.05
Y-90	2.01E+17	1.62E+17	1.84E+17	1.24	1.09
Y-91	2.93E+18	2.66E+18	2.91E+18	1.10	1.01
Y-92	3.52E+18	2.78E+18	3.39E+18	1.27	1.04
Y-93	3.87E+18	3.13E+18	3.85E+18	1.24	1.01
Y-91m	1.95E+18	1.49E+18	1.84E+18	1.30	1.06
Pr-144	2.51E+18	2.46E+18	2.61E+18	1.02	0.96
Pr-144m	3.49E+16	3.43E+16	3.12E+16	1.02	1.12

4.3.6 Fukushima Unit 3 Nuclide Inventories

The nuclides inventories for unit 3 are shown in Table 4-19, Table 4-20, and Table 4-21. The inventories calculated by SNL with ORIGEN-S/ARP are compared to scaled inventories from Peach Bottom and to TEPCO calculations that used ORIGEN2. Table 4-19 contains activities for key nuclides in the noble gas, alkali metal, alkaline earth, halogen, and chalcogen classes. Table 4-20 shows key nuclides in the platinoid, early transition metal, and tetravalent classes. Table 4-21 lists nuclide activities in the trivalent class. In general, the scaled inventories are quite inaccurate compared to the SNL and TEPCO calculations. The scaled quantities can be off by a factor of 1.9 for nuclides of first-order importance for health and consequence effects.

Similar to unit 1 and unit 2, the calculated unit 3 inventories are in very good agreement with the TEPCO inventories for most key fission products. The SNL to TEPCO ratios for predicted quantities of Sr-90, I-131, Te-132, and Cs-137 are 1.08, 0.99, 0.99, and 1.03, respectively. The SNL predictions for Pu-238 and Pu-241 for unit 3 compared quite well to the TEPCO predictions (in contrast to unit 1 and unit 2), with SNL to TEPCO ratios of 0.91 and 0.87, respectively. However, the SNL calculations predict very low Am-241 relative to TEPCO, with a ratio of 0.23. The predicted quantities of Cm-242 and Cm-244 are also quite low. These deviations may suggest that the surrogate MOX data libraries (see Section 4.2.1) used in the SNL analyses do not adequately represent the actual MOX fuel in unit 3.

Table 4-19. Nuclide inventories (Bq) for unit 3: Xe, Cs, Ba, I, and Te classes.

Isotope	SNL unit 3	Scaled SOARCA	TEPCO 1F3	SNL to SOARCA ratio	SNL to TEPCO ratio
Noble gases (Xe)					
Kr-85	2.35E+16	1.99E+16	2.17E+16	1.18	1.08
Kr-85m	6.95E+17	5.47E+17	6.83E+17	1.27	1.02
Kr-87	1.39E+18	1.08E+18	1.32E+18	1.28	1.05
Kr-88	1.88E+18	1.45E+18	1.87E+18	1.30	1.01
Xe-133	4.95E+18	4.11E+18	4.86E+18	1.20	1.02
Xe-135	1.61E+18	1.22E+18	1.90E+18	1.32	0.85
Xe-135m	9.91E+17	8.74E+17	9.47E+17	1.13	1.05
Alkali metals (Cs)					
Cs-134	2.17E+17	2.93E+17	3.18E+17	0.74	0.68
Cs-136	8.20E+16	1.06E+17	1.21E+17	0.77	0.68
Cs-137	2.39E+17	2.07E+17	2.32E+17	1.15	1.03
Rb-86	2.29E+15	3.63E+15	3.56E+15	0.63	0.64
Rb-88	1.90E+18	1.46E+18	1.89E+18	1.30	1.01
Alkaline earths (Ba)					
Ba-139	4.46E+18	3.75E+18	4.44E+18	1.19	1.00
Ba-140	4.32E+18	3.64E+18	4.27E+18	1.19	1.01
Sr-89	2.42E+18	2.02E+18	2.40E+18	1.20	1.01
Sr-90	1.85E+17	1.54E+17	1.71E+17	1.20	1.08
Sr-91	3.24E+18	2.54E+18	3.11E+18	1.28	1.04
Sr-92	3.42E+18	2.71E+18	3.33E+18	1.26	1.03
Ba-137m	2.27E+17	1.98E+17	2.20E+17	1.15	1.03
Halogens (I)					
I-131	2.35E+18	1.88E+18	2.37E+18	1.25	0.99
I-132	3.51E+18	2.76E+18	3.44E+18	1.27	1.02
I-133	4.90E+18	3.90E+18	4.93E+18	1.26	0.99
I-134	5.60E+18	4.39E+18	5.43E+18	1.27	1.03
I-135	4.69E+18	3.72E+18	4.60E+18	1.26	1.02
Chalcogens (Te)					
Te-127	1.86E+17	1.76E+17	2.38E+17	1.06	0.78
Te-127m	2.77E+16	2.86E+16	2.90E+16	0.97	0.95
Te-129	5.81E+17	5.28E+17	7.29E+17	1.10	0.80
Te-129m	1.09E+17	1.01E+17	1.06E+17	1.08	1.03
Te-131	2.01E+18	1.73E+18	2.11E+18	1.16	0.95
Te-131m	4.29E+17	3.87E+17	3.38E+17	1.11	1.27
Te-132	3.37E+18	2.91E+18	3.39E+18	1.16	0.99

Table 4-20. Nuclide inventories (Bq) for unit 3: Ru, Mo, and Ce classes.

Isotope	SNL unit 3	Scaled SOARCA	TEPCO 1F3	SNL to SOARCA ratio	SNL to TEPCO ratio
Platinoids (Ru)					
Rh-105	2.01E+18	1.96E+18	2.13E+18	1.02	0.94
Ru-103	3.27E+18	3.12E+18	3.41E+18	1.05	0.96
Ru-105	2.13E+18	2.13E+18	2.25E+18	1.00	0.95
Ru-106	8.67E+17	9.49E+17	1.00E+18	0.91	0.87
Rh-103m	3.27E+18	3.12E+18	3.07E+18	1.05	1.07
Rh-106	9.56E+17	1.06E+18	1.08E+18	0.90	0.89
Early transition metals (Mo)					
Nb-95	3.56E+18	3.51E+18	3.75E+18	1.01	0.95
Co-58	4.95E+13	3.25E+13	NA	1.53	NA
Co-60	6.79E+15	1.80E+14	NA	37.80	NA
Mo-99	4.50E+18	3.85E+18	4.49E+18	1.17	1.00
Tc-99m	3.97E+18	3.41E+18	3.94E+18	1.16	1.01
Nb-97	4.20E+18	3.55E+18	4.12E+18	1.18	1.02
Nb-97m	3.96E+18	3.35E+18	3.88E+18	1.18	1.02
Tetravalents (Ce)					
Ce-141	3.98E+18	3.30E+18	4.00E+18	1.21	1.00
Ce-143	3.87E+18	3.08E+18	3.82E+18	1.25	1.01
Ce-144	2.49E+18	2.32E+18	2.59E+18	1.07	0.96
Np-239	3.90E+19	3.84E+19	4.57E+19	1.02	0.85
Pu-238	6.88E+15	5.63E+15	7.59E+15	1.22	0.91
Pu-239	9.87E+14	6.48E+14	1.15E+15	1.52	0.86
Pu-240	1.50E+15	7.93E+14	1.44E+15	1.89	1.04
Pu-241	2.91E+17	2.30E+17	3.36E+17	1.27	0.87
Zr-95	3.86E+18	3.36E+18	3.93E+18	1.15	0.98
Zr-97	4.17E+18	3.39E+18	4.09E+18	1.23	1.02

Table 4-21. Nuclide inventories (Bq) for unit 3: La class.

Isotope	SNL unit 3	Scaled SOARCA	TEPCO 1F3	SNL to SOARCA ratio	SNL to TEPCO ratio
Trivalents (La)					
Am-241	3.43E+14	2.32E+14	1.48E+15	1.48	0.23
Cm-242	6.09E+16	7.72E+16	1.72E+17	0.79	0.35
Cm-244	2.79E+15	7.66E+15	4.80E+15	0.36	0.58
La-140	4.39E+18	3.84E+18	4.41E+18	1.14	1.00
La-141	4.06E+18	3.46E+18	4.06E+18	1.18	1.00
La-142	3.95E+18	3.33E+18	3.94E+18	1.18	1.00
Nd-147	1.60E+18	1.38E+18	1.61E+18	1.16	1.00
Pr-143	3.87E+18	3.15E+18	3.72E+18	1.23	1.04
Y-90	1.90E+17	1.62E+17	1.76E+17	1.17	1.08
Y-91	3.10E+18	2.66E+18	3.02E+18	1.16	1.03
Y-92	3.47E+18	2.78E+18	3.35E+18	1.24	1.04
Y-93	3.75E+18	3.13E+18	3.82E+18	1.20	0.98
Y-91m	1.89E+18	1.49E+18	1.81E+18	1.27	1.05
Pr-144	2.51E+18	2.46E+18	2.61E+18	1.02	0.96
Pr-144m	3.49E+16	3.43E+16	3.11E+16	1.02	1.12

4.4 Uncertain Parameter Treatment for Fukushima Uncertainty Analyses

Past severe accident research [1][2][3][4][5][6][7][8][9] has observed considerable variation in accident progression and releases attributable to relatively minor changes in decay power. Furthermore, in conjunction with significant additional uncertainties associated with variability in reactor operation (e.g. burnup history), the associated variation in the decay power and radionuclide inventory input for MELCOR and MACCS can have a first-order impact on key severe accident signatures such as H_2/CO generation, release fractions and absolute source terms, and event timing.

For a given set of reactor conditions the uncertainty in the decay power soon after shutdown may vary between 1-10% according to the "Decay Heat Power in Light Water Reactor" standard (ANS-5.1-2005) [23], which considers the decay heat of fission products, U-239, and Np-239 for LWRs that predominantly involve fission of U-235, U-238, and plutonium isotopes; uncertainties vary with time after shutdown, among other factors. The ANS standard is intended for conservative safety evaluations and is therefore biased to predicting higher overall decay power. Conversely, an ORIGEN-S calculation with modern nuclear data is more aligned with the best-estimate analyses, and the uncertainties inherent to the code's computational methods and approximations are likely less than that of the ANS standard. Nonetheless, the ANS standard provides for readily available quantification of uncertainty in the decay power after shutdown, which would otherwise require random sampling and analysis of uncertain ORIGEN-S inputs, namely nuclear data such as cross sections, fission yields, decay constants, and decay energies

[12][16]–this is probably outside the scope of current Fukushima UA efforts, but should be considered for future work.

Uncertainty in decay heat will therefore be treated using a combined approach with ORIGEN-S and the ANS standard: ORIGEN-S is used to calculate consistent decay heat and inventory information for each unit while uncertainty within each decay heat curve will be derived from ANS-5.1-2005. The uncertainties derived from the ANS standard principally reflect the uncertainties in nuclear decay data for short-lived nuclides. From the ORIGEN-S calculations, fractional fission powers over the previous cycle of important actinides (U-235, U-238, Pu-239, Pu-241) can be extracted for each unit. Using these nuclide specific fission power levels, the time-dependent uncertainties in percentage of total decay heat power can be calculated using the methods described in Section 3 of ANS-5.1-2005. These uncertainties are then applied to the 'base' decay heat curves for each that are calculated by ORIGEN-S/ARP.

Since the integral burnups and shutdown times are well-quantified for the Fukushima units, bulk variations in RN inventories probably do not need to be considered. The inventories of certain nuclides for health effects, particularly isotopes that can be relatively difficult to predict (e.g. Pu-238), will be considered for uncertain parameter treatment if MACCS analyses are to be included. Uncertainty analyses focused on severe accident phenomena with MELCOR do not necessitate the treatment of uncertainties in RN inventory.

4.5 Modeling Improvements and Future Work

Future analyses may take a quasi-3D (i.e. nodal) approach comprised of many SCALE calculations for each fuel assembly at several axial nodes. The 3D TEPCO core data supports such an approach. The SNL automation tools can be easily extended to consider axial variations in power, burnup, fuel assembly geometry and materials (e.g. partial fuel rods and control blades), and void fraction. Standalone use of ORIGEN-S/ARP naturally still requires adequate ARP libraries generated by TRITON–i.e. several TRITON calculations would need to be performed for a range of void fractions. The pre-generated ENDF-B/V libraries available in SCALE6 may be used as a temporary workaround to new TRITON calculations, and this approach was taken for the Fukushima analyses documented in this report. SNL has recently completed TRITON modeling efforts to generate data libraries for each of the fuel assembly types in units 1-3 at Fukushima. Distinct geometric models were created for each fuel assembly and were analyzed over a range of void fractions, enrichments, poison zoning, and burnup levels. Appropriate Dancoff factors were computed for high void fraction cases. These new cross section libraries are much more representative of the Fukushima fuel than the pre-generated ENDF-B/V libraries. The new data will probably have a small influence on the ORIGEN-S/ARP calculations of decay heat and the fission product inventories presented in this report. However, inventories of some actinides and neutron absorption products may change significantly due to the use of different flux-weighted cross sections. Upcoming Fukushima research on source term quantification will utilize updated SCALE calculations that make use of the detailed fuel assembly models.

The nuclide inventories presented in Section 4.3.4, Section 4.3.5, and Section 4.3.6 have revealed some potential areas for improvement. Accurate predictions of several key nuclides

(especially actinides) with ORIGEN-S/ARP hinges on the use of appropriate plant data, such as fuel assembly data and irradiation/decay histories, and nuclear data libraries, which requires neutron transport analysis with codes like NEWT/TRITON. Alternatively, the inventories for key nuclides could just be treated as uncertain parameters; sufficient information from multiple analyses is already available to assist in informing uncertain parameter ranges and distributions.

Finally, further Fukushima analyses may investigate various schemes of decay heat partitioning over the RN classes. The current analyses used ORIGEN-S and OPUS outputs directly to determined RN class power, as done in the Surry and Peach Bottom SOARCA models, which naturally results in separation of certain parent and daughter decay powers between different RN classes. The MELCOR inputs generated by current Fukushima analyses are likely satisfactory for best-estimate and uncertainty analyses, since the issue of parent and daughter decay power is really limited to a few key nuclides and classes. The issue is not necessarily a simple matter of choosing between always retaining daughter decay heat in the parent class and always separated the parent-daughter decay powers. This subject is discussed further in Section 6.3.

5 APPLICATION TO HISTORICAL SNL MELCOR MODELS

The SNL tools for generating MELCOR/MACCS inventory and decay heat information are applicable to historical SNL MELCOR models. SNL MELCOR efforts in the past decade have focused on the Peach Bottom (3511 MWt GE BWR/4) and Surry (2546 MWt 3-loop Westinghouse PWR) plants, mainly due to the NRC's State of the Art Reactor Consequence Analysis (SOARCA) project. These models already have user-defined inventories and decay heat curves that are intended to reflect the unique characteristics of the reactors. Other frequently used MELCOR models include Sequoyah (3411 MWt 4-loop Westinghouse PWR) and Monticello (2004 MWt GE BWR/3). The MELCOR RN and DCH inputs for these models are likely subpar for best-estimate analyses of modern conditions, and the associated MACCS inventory inputs are dated or just nonexistent. The newly developed SNL tools are well-suited to support future MELCOR/MACCS analyses of these plants.

Detailed SCALE6 analyses of the Surry reactor are completed in order to support upcoming best-estimate and uncertainty analyses. The technical justifications for this effort and for future endeavors for the other SNL models are describe in Section 5.1. The results of the Surry analysis and the post-processed information for MELCOR/MACCS inputs are presented in Section 5.2. Preliminary analyses of the Peach Bottom BWR are presented in Section 5.3.

5.1 Justification for Reevaluating Inventory and Decay Heat Information for Future MELCOR Analyses with Historical SNL Models

The decay heat and inventory input records in MELCOR and MACCS are fairly lengthy and time-consuming to develop manually from scratch–at least it is for user-specified and problem-dependent information. In addition to the lengthy MELCOR/MACCS input records themselves, the radionuclide information entails a relatively large amount of data reduction for the ORIGEN outputs. Hence most MELCOR and MACCS users avoid having to define/redefine these inputs if possible. To assist users, MELCOR includes some internal capabilities to estimate RN inventories, RN specific decay heats, and overall core decay heat with minimal user input. The internal models are based on calculations performed by SNL [33] in the 1980s for a representative 3412 MWt PWR and a 3578 MWt BWR, in conjunction with interpolation algorithms that adjust the inventories to the user-specified conditions. The SNL calculations used a deprecated version of ORIGEN (dubbed SANDIA-ORIGEN) and old nuclear data for fission yields, cross sections, and decay data. Nonetheless, this internal capability allows for very quick and grossly realistic population of MELCOR RN information for "representative" accident simulations. The need for best-estimate input information for specific reactor models precludes the use of the internal MELCOR inventories, which cannot realistically describe the new fuel designs and operating characteristics (e.g. higher burnup) of modern LWR cores. Furthermore, internal MELCOR capabilities are incapable of providing the MACCS isotopic inventories to allow for consistent consequence analysis of a MELCOR source term.

Modern MELCOR models used by SNL, such as the Peach Bottom and Surry SOARCA models, tend to be rather large (up to about 50,000 lines) and complicated. Such models have been under nearly-continual development and refinement for decades. Model updates and revisions are typically limited to changes in control systems and boundary conditions to support new analyses

of different accident scenarios. However, the SOARCA project included concentrated efforts to update and improve nearly all aspects of the Peach Bottom and Surry MELCOR models, such as finely nodalized thermal-hydraulic regions in the core and RPV. For the Peach Bottom model, this also included detailed inventory and decay power analyses using modern codes, nuclear data, and realistic plant information. ORNL performed SCALE analyses of the Peach Bottom plant to provide inputs for MELCOR. The ORNL analyses used the TRITON sequence in SCALE to generate spatial distributions of inventories and decay power for several axial and radial nodes of the Peach Bottom core. These efforts are probably the most detailed and accurate to date for MELCOR model input. Unfortunately, a similar effort was not performed for the Surry SOARCA model due to time and budget constraints.

The original Surry SOARCA model used a decay heat curve from ORIGEN analyses of a hypothetical and extrapolated high burnup core for Surry, in conjunction with an inventory scaled from similar analyses of a Sequoyah reactor [24][25]. Thus, the decay heat curve used in the model is quite conservative, and the MELCOR and MACCS inventories lack consistency. In keeping with the best-estimate approach intended for the SOARCA project, consistent sets of decay power, lumped MELCOR RN inventories, and nuclide-level MACCS inventories are calculated using the new SNL process and more realistic operating data from the Surry plant. A new best-estimate decay power and radionuclide inventory is calculated using SCALE6 and implemented into the SNL MELCOR model for the Surry PWR plant. The post-processing tools facilitate the treatment of decay power and inventory as an uncertain parameter for uncertainty analyses. Starting from a truly best-estimate and consistent (between MELCOR and MACCS) set of decay power and inventory input facilitates a technically rigorous treatment of the uncertain parameter. For example, operating time before scram or overall burnup can be treated as a random variable to assess the impact on decay power and inventories, which then influence severe accident progression and source terms predicted by MELCOR.

Several Surry calculations using the SCALE6 and the SNL tools are presented in Section 5.2; these are intended to provide consistent information for MELCOR and MACCS Surry inputs for use in subsequent best-estimate and/or uncertainty analyses of severe accidents. Given the relatively crude decay power and inventory information in the original Surry-SOARCA model, the demonstration of the SNL tools in this report is initially focused on the Surry PWR. A preliminary analysis of the Peach Bottom BWR is given in Section 5.3. More in-depth analyses of Peach Bottom are planned in order to thoroughly benchmark the SNL methods and to provide information for potential MELCOR BWR projects in the near future. For example, future uncertainty analyses or best-estimate calculations of BWR severe accidents may consider variable reactor operation that affects core inventory and decay heat, and the SNL methods could readily support such projects.

5.2 Surry Analysis

An updated decay power and radionuclide inventory is calculated using ORIGEN-S/ARP and implemented into the Surry model in order to support future best-estimate and uncertainty analyses. Similar to the Fukushima UA, decay power and inventory can be treated as an integrated uncertain parameter for uncertainty analysis of the Surry model. The ORIGEN-S/ARP calculations aim to quantify the variability in inventory and decay power due variable reactor

operation, which is chosen to be the time of shutdown in the final operating cycle before the accident initiator. The time of shutdown in the cycle affects the integral core burnup, which could act as a simple surrogate for other variable/uncertain parameters related to reactor operation.

State-of-the-art nuclear data and problem-dependent cross sections are first generated using TRITON with the latest ENDF/B-VII.1 library, as described in Section 5.2.1. TRITON provides the necessary ARP libraries for subsequent (and faster) ORIGEN-S standalone calculations. Further, the libraries contain cross section data that reflect the spatial and spectral characteristics of the Westinghouse 15x15 assemblies used at Surry for cycles 18, 19, and 20 over a range of enrichments and burnups. Using plant operating data from these cycles for each fuel assembly, ORIGEN-S/ARP calculations are performed that consider the burnup history, power fraction, and enrichment of each assembly from cycle 20, which is the cycle chosen to undergo the severe accident initiator. Previously irradiated assemblies at BOC of cycle 20 are modeled from cycles 18 and 19, as is the location of fuel assemblies in the core to ascertain the radial distributions of radionuclide inventory and decay power over MELCOR core rings. The ORIGEN-S/ARP models and calculations are described in Section 5.2.2. The post-processing of these calculations for creation of MELCOR and MACCS inputs is described in Section 5.2.3.

5.2.1 Generation of Problem-dependent Data Libraries for ORIGEN-S/ARP

Problem-dependent cross sections and modern ENDF/B-VII.1 nuclear data are incorporated by generating ORIGEN-S/ARP data libraries using the TRITON sequence in SCALE6.1.3. SCALE has numerous pre-generated data libraries for a variety of fuel assemblies and reactor types, including Westinghouse 15x15 fuel like that used in Surry. However, these data libraries were created using older ENDF/B-V cross section data. Problem-independent decay data from the newer ENDF/B-VII library may still be used with ORIGEN-S and the pre-generated (ENDF/B-V) cross sections. The ENDF/B-VII library contains improved information for fission product yield, gamma emission data, decay constant (particularly for short-lived nuclides), and cross sections which support nuclide summation codes such as ORIGEN in accurately calculating decay heat for short-term applications (e.g. severe accidents) [27]. Since the release of ENDF/B-VI, best-estimate predictions of decay heat soon after shutdown are possible with ORIGEN-S and similar codes [27]. Therefore, the TRITON calculations are performed to provide the ORIGEN-S/ARP analyses of Surry with data libraries that include the latest ENDF/B-VII.1 data.

5.2.1.1 TRITON (NEWT) Models for Surry 15x15 Fuel Assemblies

TRITON models of a Westinghouse 15x15 fuel assembly are created to support the ORIGEN-S/ARP calculations for Surry. Two basic models were created, as shown in Figure 5.1: a full assembly model that depletes all fuel rods uniformly and a quarter-assembly model that takes advantage of geometric symmetry and depletes each fuel rod individually. ORIGEN-S/ARP calculations were performed using the data libraries generated by both models, and the differences caused by the two different TRITON models are quite small–differences are generally less than 1% for key nuclides of interest for MELCOR and MACCS. The data libraries generated for the quarter-assembly TRITON model with multi-rod depletion are used in the final ORIGEN-S/ARP analyses for Surry.

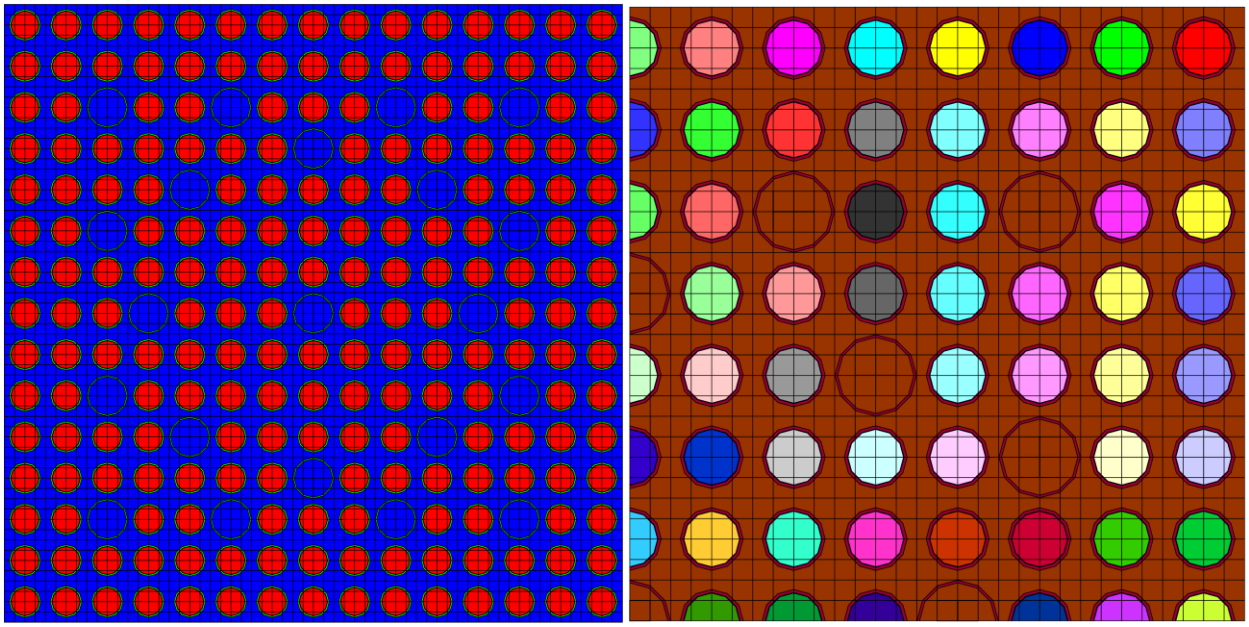

Figure 5.1. TRITON/NEWT Models for full 15x15 assembly (left) and quarter-assembly with multi-rod depletion (right).

The TRITON models burn all fuel material by constant power depletion. The ENDF/B-VII 238 group library is used ("v7-238") along with CENTRM for cross section processing, which is the one-dimensional discrete ordinates option in SCALE for calculating point-wise energy spectra and preparing the problem-dependent, multigroup data library [12]. A constant moderator density of 0.72 g/cm^3 is used, and the soluble boron concentration is also assumed constant at a value of 758 ppm, which is informed by Surry operating data. The soluble boron is not depleted in the TRITON simulations as it is assumed the boron concentration is controlled by the operators.

Using the quarter-assembly TRITON model with multi-rod depletion, data libraries for ORIGEN-S/ARP are generated for the Surry enrichment levels present in cycle 20, which range from 3.8 w/o to 4.25 w/o. The model uses the Surry specific power level (35 MW/MTU) and depletes over a wide range of burnup values – up to about 72 GWd/t.

5.2.1.2 Simplifying Assumptions in TRITON Analyses for Generating ORIGEN-S/ARP Libraries

The Surry core actually contains several different types of fuel assemblies; some assemblies have ZrB_2 Integral Fuel Burnable Absorbers (IFBA), wet annular burnable absorbers (WABA, B_4C/Al_2O_3) in the guide tubes, or flux suppression inserts. These burnable poisons can affect the flux-weighted cross sections generated for ORIGEN-S/ARP. In the TRITON and ORIGEN-S analyses for Surry, however, each fuel assembly is treated as a Westinghouse 15x15 assembly in an infinite lattice with no fixed burnable poison (i.e. ZrB_2 and WABA assemblies are not considered); this also means that unique cross sections for assemblies adjacent to the reflector are not considered. The letdown curve for the soluble boron in the moderator is not modeled, but the

letdown curve is typically not modeled for lattice physics calculations for generating ORIGEN-S/ARP data libraries [12].

5.2.1.3 Examination of One-group Cross Sections for ORIGEN-S

Accurate predictions of radionuclide inventories by ORIGEN-S/ARP are predicated on the one-group cross sections that are calculated by reactor analysis codes like TRITON. Some one-group cross sections calculated by TRITON and the 15x15 Surry model are briefly reviewed here.

The TRITON cross sections (Table 5-1) are compared to MCNP6 [34] calculations with continuous ENDF/B-VII data (Table 5-2). The geometry for the MCNP6 model is depicted by Figure 5.2. This comparison between TRITON and MCNP6 is not intended to be a rigorous benchmark, since numerous minor differences exist between the input models (e.g., boric acid density). Instead, this simple comparison roughly validates the Surry TRITON model, the data libraries generated for ORIGEN-S/ARP, and thus the calculations of radionuclide inventories for MELCOR/MACCS. The collapsed cross sections calculated by TRITON and MCNP6 for a 15x15 PWR assembly are very similar, as shown by Table 5-1 and Table 5-2. The predicted eigenvalues are also roughly comparable (around 1.31). The MCNP6 relative errors associated with the collapsed cross sections are negligible, due to the integral nature of these values and the use of a sufficient number of batches and neutron histories (150 million active histories after fission source convergence).

Table 5-1. Collapsed cross sections (barns) calculated by TRITON (CENTRM/NEWT) with 238-group ENDF/B-VII.

Energy group	$\sigma_{n,gamma}$ U-235	$\sigma_{fission}$ U-235	$\sigma_{n,gamma}$ U-238	$\sigma_{fission}$ U-238
$1x10^{-5}$ to 0.625 eV	47.065	266.625	1.371	0.000
0.625 eV to 1 MeV	5.228	10.868	1.069	0.001
1 MeV to 20 MeV	0.056	1.226	0.050	0.408
Total spectrum	8.886	38.706	0.851	0.102

Table 5-2. Collapsed cross sections (barns) calculated by MCNP6 with ENDF/B-VII.

Energy group	$\sigma_{n,gamma}$ U-235	$\sigma_{fission}$ U-235	$\sigma_{n,gamma}$ U-238	$\sigma_{fission}$ U-238
$1x10^{-5}$ to 0.625 eV	47.191	268.277	1.380	0.000
0.625 eV to 1 MeV	5.211	10.768	1.049	0.001
1 MeV to 20 MeV	0.053	1.228	0.046	0.426
Total spectrum	9.224	40.610	0.853	0.101

The three energy groups listed in Table 5-1 and Table 5-2 correspond to the groups used to generate cross sections for ORIGEN-S in SCALE5 [28]. In SCALE5, three-group cross sections were specified in ORIGEN-S libraries, which were reduced to one-group values by use of energy group weighting factors; these factors were [12][28]:

- THERM: the thermal cross-section value for a 1/v absorber,
- RES: the ratio of intermediate flux to thermal group flux, and
- FAST: is the ratio of fast flux to thermal flux.

These factors are listed in Table M6.5.1 in the SCALE manual [12] but are no longer used in SCALE6.

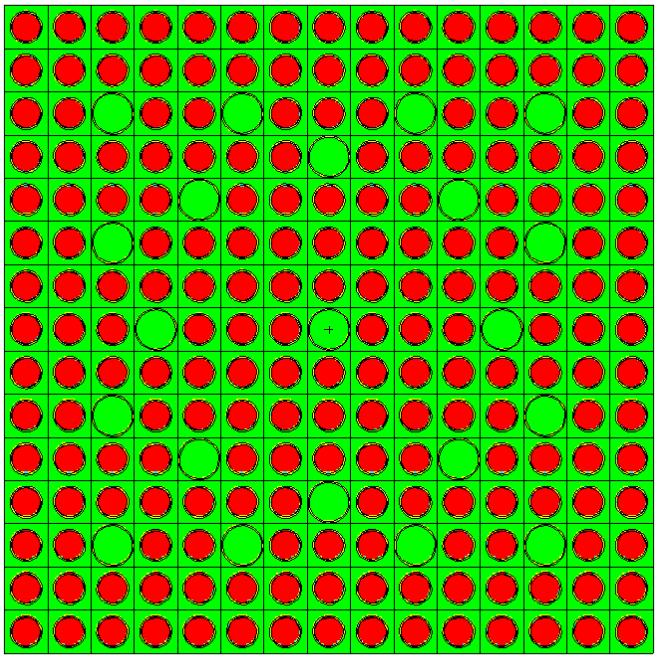

Figure 5.2. MCNP6 model of Surry 15x15 PWR assembly.

The current default behavior of TRITON in SCALE6 is to generate one-group cross sections for the ORIGEN-S/ARP libraries (i.e., the ft33f001.cmbined file) that are weighted by the whole-problem neutron spectrum, which would correspond to the 'Total spectrum' entries in Table 5-1 and Table 5-2. Therefore if cross sections normalized by thermal flux are desired in the ARP libraries, the user may have to manually specify the appropriate COUPLE input. The NORM record (the 17th entry) on the \$1 input array for COUPLE will weight cross sections for ORIGEN-S by the thermal flux for all energy groups less than 0.625 eV [12]. In order to preserve consistency with the historical SCALE LWR data libraries for ORIGEN-S/ARP, thermal flux-weighted cross sections are used in the ORIGEN-S/ARP analyses of the Surry reactor.

5.2.2 Calculation Process under the SNL Framework

ORIGEN-S/ARP is executed for each fuel assembly in the core from cycle 20 at Surry using the pre-generated data libraries and Surry operation data from cycles 18, 19, and 20–this includes each fuel assembly's power fraction, burnup, enrichment, and the number of times each was irradiated. The ORIGEN-S/ARP analyses are intended to have a similar level of detail as the TRITON analyses performed by ORNL for the Peach Bottom SOARCA model [29]. The ORNL analyses generated spatial distributions of inventories and decay power for several axial and radial nodes of the Peach Bottom core. Hence, the analyses for the Surry core consider each fuel assembly individually, since plant data exists on this scale, and the results are lumped over the MELCOR radial nodalization.

5.2.2.1 Surry Plant Operating Data

The ORIGEN-S/ARP simulations use proprietary operating information from the Surry plant for cycles 18-20. This includes fuel design details, enrichments, power/burnup distributions, and fuel shuffling schemes. The analyses take into account the numbers of fresh assemblies, once-burned, and twice-burned assemblies at the beginning of cycle 20.

The raw plant data is pre-processed and mapped onto the COR ring nodalization in the Surry MELCOR model, as shown by Figure 5.3. This facilitates later post-processing of the ORIGEN-S output to create radial distributions of decay power and/or MELCOR RN mass.

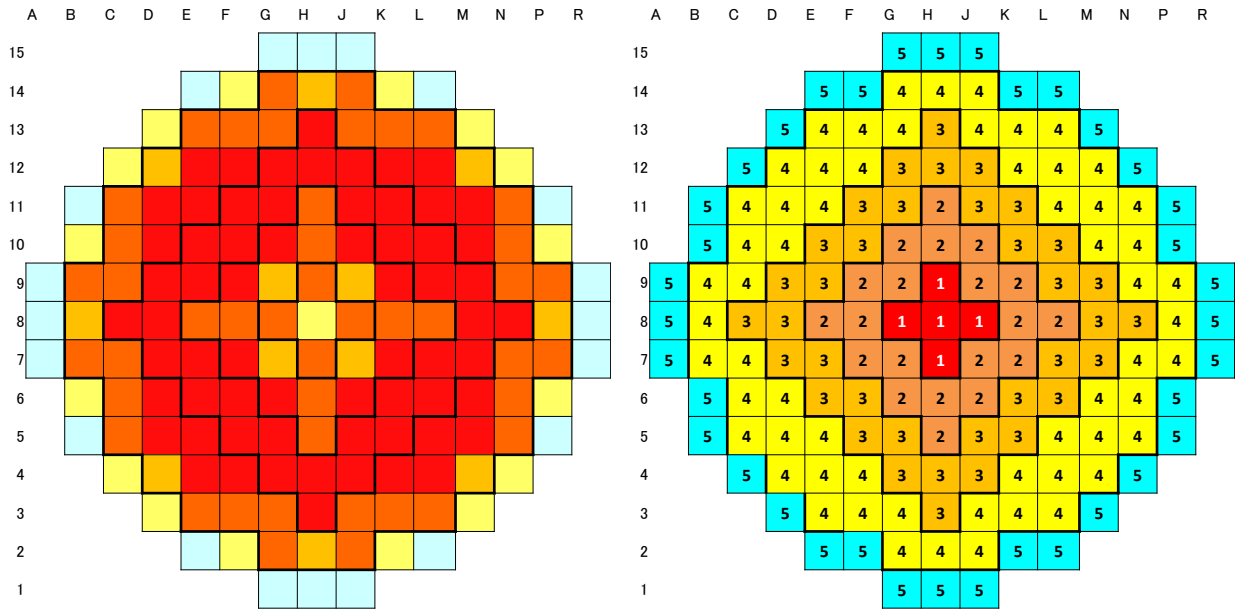

Figure 5.3. Processed Surry data (left) mapped over to MELCOR COR rings (right).

Table 5-3 lists a summary of fuel assembly and core information used for the decay power and inventory calculations for Surry. All of the previously irradiated assemblies in cycle 20 can be traced back to cycles 18 and 19, excluding just one assembly (probably from the SFP), which is just treated as an assembly from cycle 18 since its burnup history is not known.

Table 5-3. Surry reactor information used for ORIGEN-S/ARP analyses.

Quantity	Value for Surry Cycle 20
Total fuel loading (MTU)	72.58
Power rating (MWt)	2546
Specific power level (MW/MTU)	35.1
Total fuel assemblies in core	157
Number of fuel assemblies in COR ring 1	5 (3.2% of core)
Number of fuel assemblies in COR ring 2	20 (12.7% of core)
Number of fuel assemblies in COR ring 3	36 (22.9% of core)
Number of fuel assemblies in COR ring 4	60 (38.2% of core)

Number of fuel assemblies in COR ring 5	36 (22.9 % of core)
Core average burnup at BOC (GWd/t)	17.7
Core average burnup at EOC (GWd/t)	35.4
Cycle differential burnup (GWd/t)	17.7
Burnup in COR ring 1: BOC, EOC (GWd/t)	24.3, 41.3
Burnup in COR ring 2: BOC, EOC (GWd/t)	15.7, 36.6
Burnup in COR ring 3: BOC, EOC (GWd/t)	9.73, 32.7
Burnup in COR ring 4: BOC, EOC (GWd/t)	9.22, 29.6
Burnup in COR ring 5: BOC, EOC (GWd/t)	39.9, 46.3
Approximate full cycle operating time (days)	505

5.2.2.2 Automated Creation of ORIGEN-S/ARP Input and Analysis Execution

A Perl script generates the ORIGEN-S/ARP input files for each fuel assembly using the processed Surry plant data. An input file is generated for each fuel assembly present in the core for cycle 20. The Perl script populates template input files with Surry data for fresh, once-irradiated, and twice-irradiated fuel assemblies at BOC for cycle 20. ORIGEN-S/ARP is then executed for all input files using SCALE6.1.3 in batch mode.

The CPU time involved with the ORIGEN-S analyses is rather trivial compared to MELCOR runtimes–execution of the 157 ORIGEN-S jobs for a whole-core calculation requires less than 30 minutes on a 3.30 GHz Intel Xeon E5-2667-v2 processor. Nonetheless, distributed processing of the jobs over several cores and/or processors can be used to reduce execution time to a few minutes.

5.2.2.3 Simplifying Assumption for ORIGEN-S/ARP Analyses

The ORIGEN-S/ARP calculations only consider the radial variations of burnup, enrichment, and power distributions. Due to modern fuel shuffling strategies, radial distributions of burnup, radionuclide inventories, and decay power can differ greatly from each other. High burnup assemblies in the inner core are typically allocated in a checkerboard-type pattern, which would simply be homogenized over the inner MELCOR COR rings. In the outer core regions, however, modern fuel shuffling tends to concentrate high burnup assemblies in a ring around the periphery of the core; this acts to concentrate high burnup inventories (e.g., more Cs-137) in the outer MELCOR COR ring (ring 5). The operating and decay power distributions are generally still peaked around the inner regions of the core, indicating higher concentrations of shorter-lived fission products and actinides that drive decay power soon after shutdown. Conversely, enhanced quantities of stable and long-lived nuclides are present in the relatively higher burnup regions of the core, such as in the outer ring(s) of assemblies. The new SCALE6 analyses provide insights into such details for MELCOR and MACCS inputs in the Surry model. Additional discussions on these effects are presented in Sections 6.1.1 and 6.1.2.

Since there is no axial fuel shuffling, the post-processor for the ORIGEN-S outputs (see Section 3.3) axially allocates radionuclide mass and power according to a time-integrated axial power distribution from nominal reactor operation. General agreement between axial power and burnup distributions permits this simple approach to axial partitioning of the decay power and

inventories; i.e. the RN mass and decay power distributions are quite similar. The ORNL TRITON/ORIGEN analyses for Peach Bottom SOARCA considered axial effects, but this is more relevant for a BWR given the enhanced axial variation of moderator density/void fraction and the associated influence on local neutron spectrum and flux-weighted cross sections [12][30][29].

The exact power histories from the two previous cycles (18 and 19) are also not currently modeled. For example, there were a few brief unplanned outages in these cycles that are neglected. However, the number of previous irradiations for each fuel assembly and the refueling outages are modeled. The BOC burnup distribution for cycle 20 is recreated in this process. Uncertainty analyses may treat the operating time before the accident initiator as variable. The time of shutdown in cycle 20 has gross effects on the decay heat and inventory used in the severe accident models. Therefore, unplanned outages or variations in operating power in cycle 20 that create small perturbations in decay heat and inventory are also neglected in the ORIGEN-S models.

5.2.3 Consistent MELCOR and MACCS Inputs

A Perl script post-processes outputs from ORIGEN-S and directly generates consistent MELCOR inputs of decay heat and lumped RN-class inventories (including class specific decay heats), along with consistent nuclide-detail input for MACCS. The Perl script reads ORIGEN-S and OPUS outputs directly for each fuel assembly. OPUS is a SCALE auxiliary tool that is used to assist with some post-processing, such as extracting element-based decay powers, which are later lumped into MELCOR RN class decay powers and an overall core decay power. The generation of ring-based and whole-core values of RN class masses and decay power is a simple matter of summation over the output files for each fuel assembly–no ambiguous scaling or normalization schemes are necessary.

5.2.3.1 Selection of New Base Case Condition for Best-estimate MELCOR and MACCS Models

The decay power and inventory calculated for reactor shutdown near MOC of cycle 20 are taken to be the new ‘base case’ inputs for the MELCOR and MACCS models of Surry. The base case models for Peach Bottom SOARCA also used near-MOC conditions. A scoping study using ORIGEN-S/ARP is performed to determine how decay power varies with the final cycle operating time; this assists the selection of the new base inputs for MELCOR and MACCS, and helps inform the development of the distribution and bounds for the uncertain parameter treatment in the UA. The scoping study examines decay power after scram as a function of the final cycle (20) operating time on logarithmic (Figure 5.4) and severe accident time scales for Surry STSBOs (Figure 5.5).

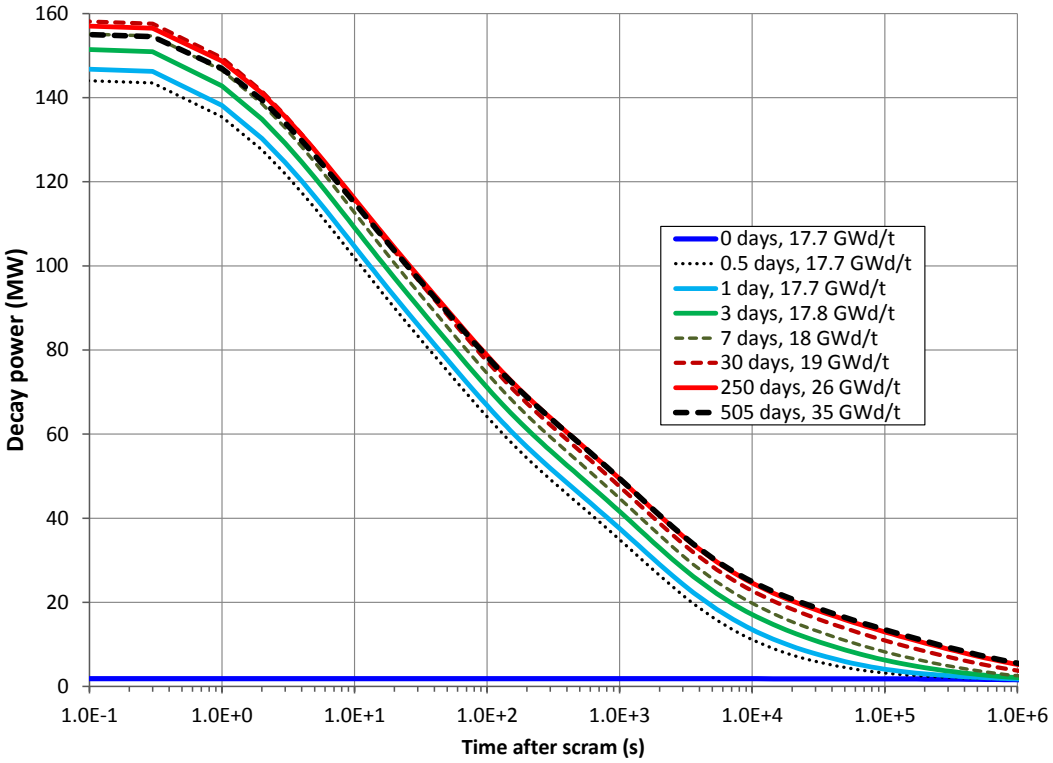

Figure 5.4. Decay power on logarithmic time scale for several shutdown times in cycle 20.

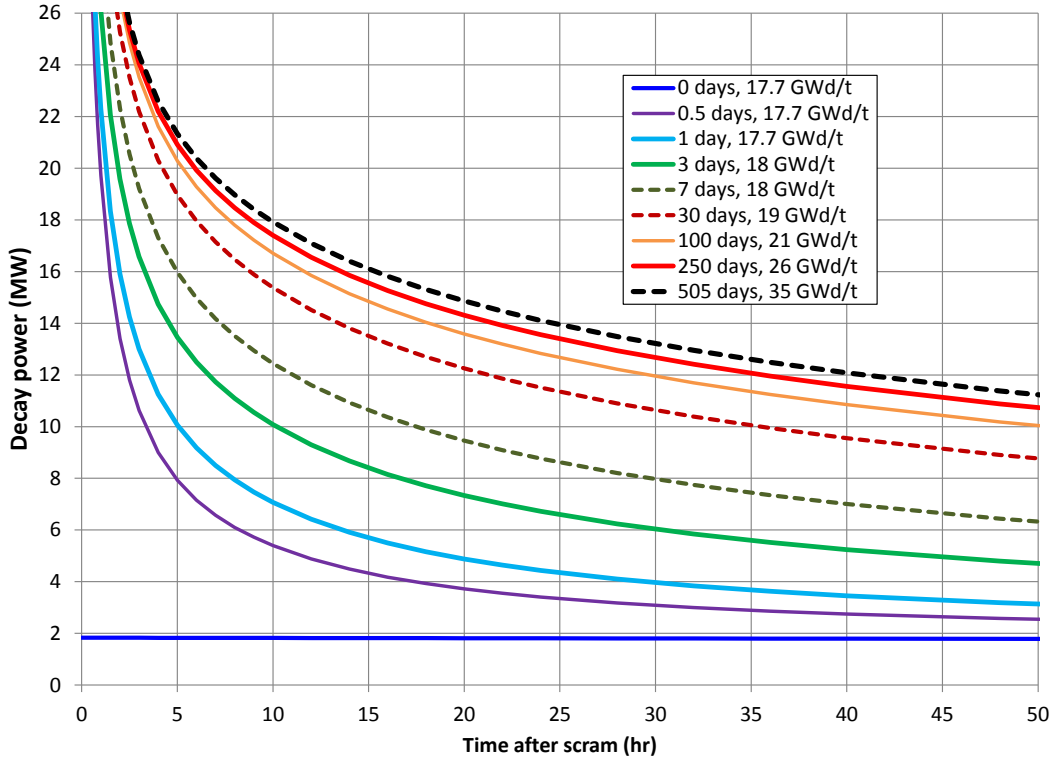

Figure 5.5. Decay power on severe accident time scale for shutdown times in cycle 20.

Any significant reactor operation results in a decay power of 6-7% operating power immediately at shutdown due to quasi-equilibrium levels of short lived nuclides that drive decay power. Concentrations for these nuclides saturate rather quickly with full power operation due to short half-life and possibly significant neutron cross section; later in the cycle, the concentrations of these short lived nuclides are mainly influenced by changes in production rate–such as changes in power level, fission yields, and/or reaction rates due to evolving neutron spectrum and flux-weighted cross sections. After 10 to 1000 seconds, the decay power for BOC conditions (1 to 30 days operating time) ranges from 30% to 90% of the EOC decay power, as shown in Figure 5.6 and Figure 5.7. These two figures depict decay power curves for several operating times, but normalized to the EOC decay power. Near-MOC conditions (100 to 250 days) exhibit decay power curves that are very similar to the EOC decay power for times near shutdown; after a few hours, MOC decay power is 90% to 95% of the EOC decay power. Differences in decay power hours after scram are indicative of different concentrations of medium and longer-lived fission products that are the result of varying burnup levels.

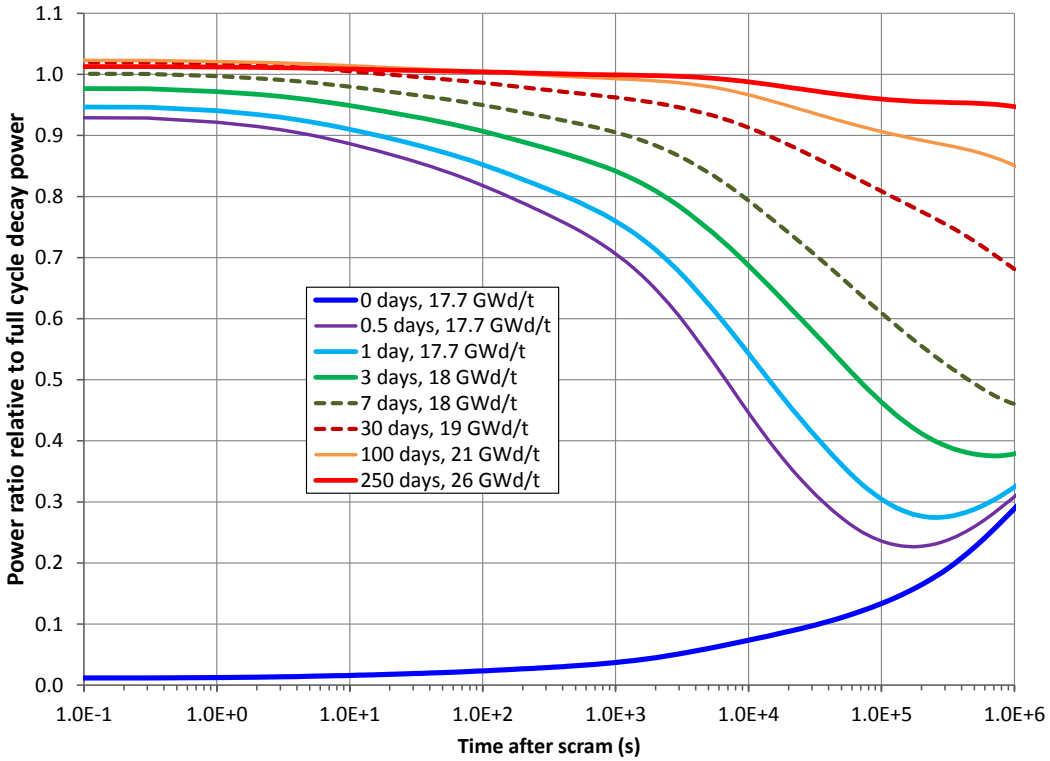

Figure 5.6. Decay power on logarithmic time scale relative to full-cycle EOC power.

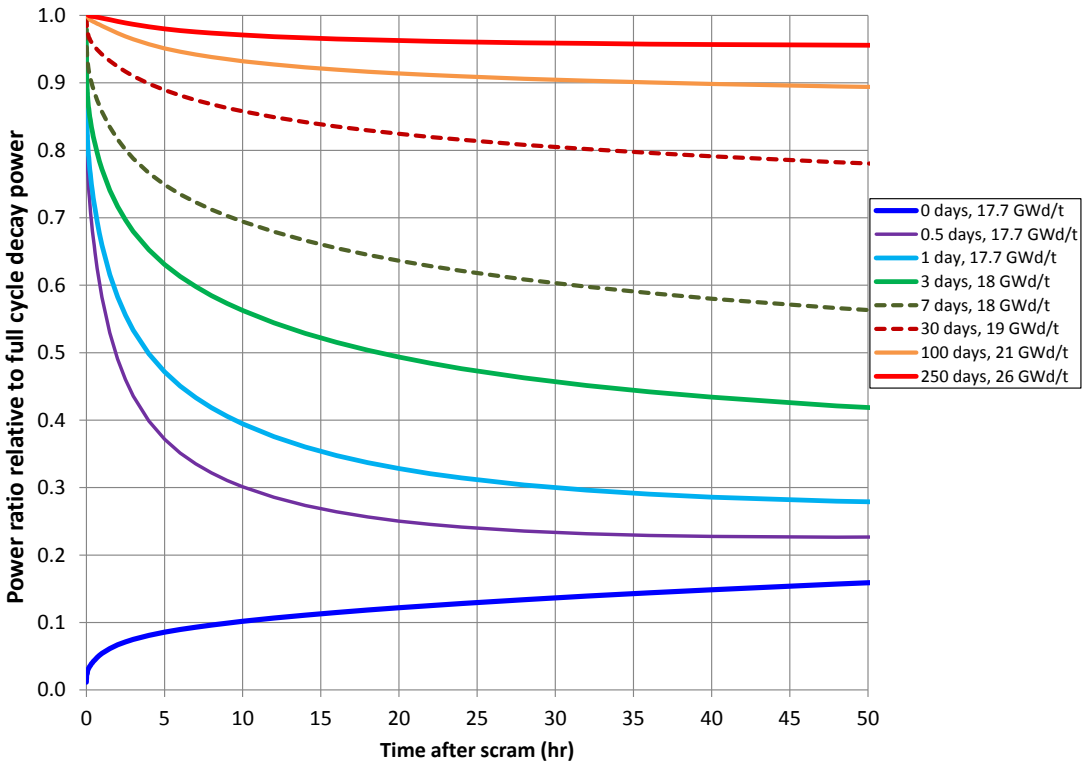

Figure 5.7. Decay power on severe accident time scale relative to full-cycle EOC power.

Using the information from these calculations, uncertainty analysis of Surry can rigorously quantify the effects of shutdown time over cycle 20, including the effects of varied decay power later after shutdown during severe accident phenomena such as core degradation/oxidation, RPV failure, and MCCI. The differences between MOC and EOC decay power support such analyses. Therefore, an MOC operating time of 200 days is selected to provide the decay power and inventory for the new base case MELCOR model–the resulting decay power is about 95% of the EOC decay power after about 18 hours since shutdown, as depicted in Figure 5.8. This MOC condition is also one of the realization values for the decay heat and inventory uncertain parameter in the UA. The new base-case decay power for the Surry MELCOR model at MOC conditions is shown on a logarithmic time scale by Figure 5.9. The base MOC curve is compared to the SOARCA decay heat curve, which is quite conservative given that it reflects an extrapolated high burnup state. The SOARCA decay heat exhibits 'lumps' in its curve since it used a very coarse time-mesh for the tabular function in the MELCOR model–MELCOR linearly interpolates between tabular functions entries.

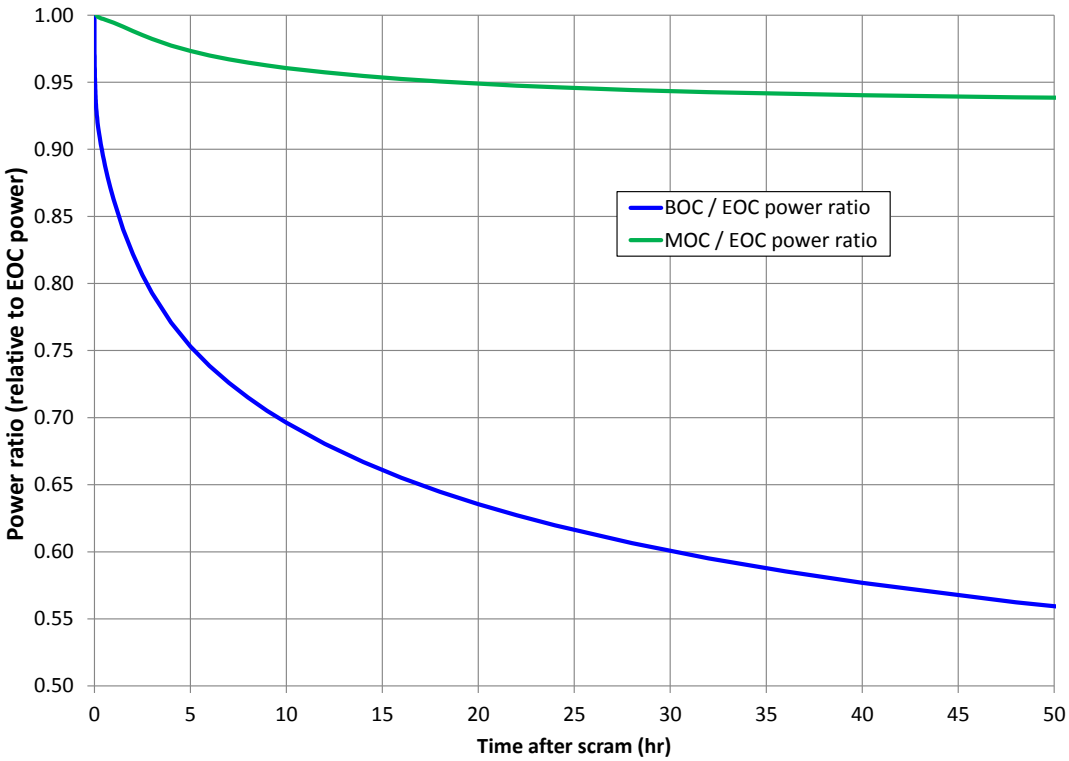

Figure 5.8. BOC and MOC decay powers relative to full-cycle EOC decay power.

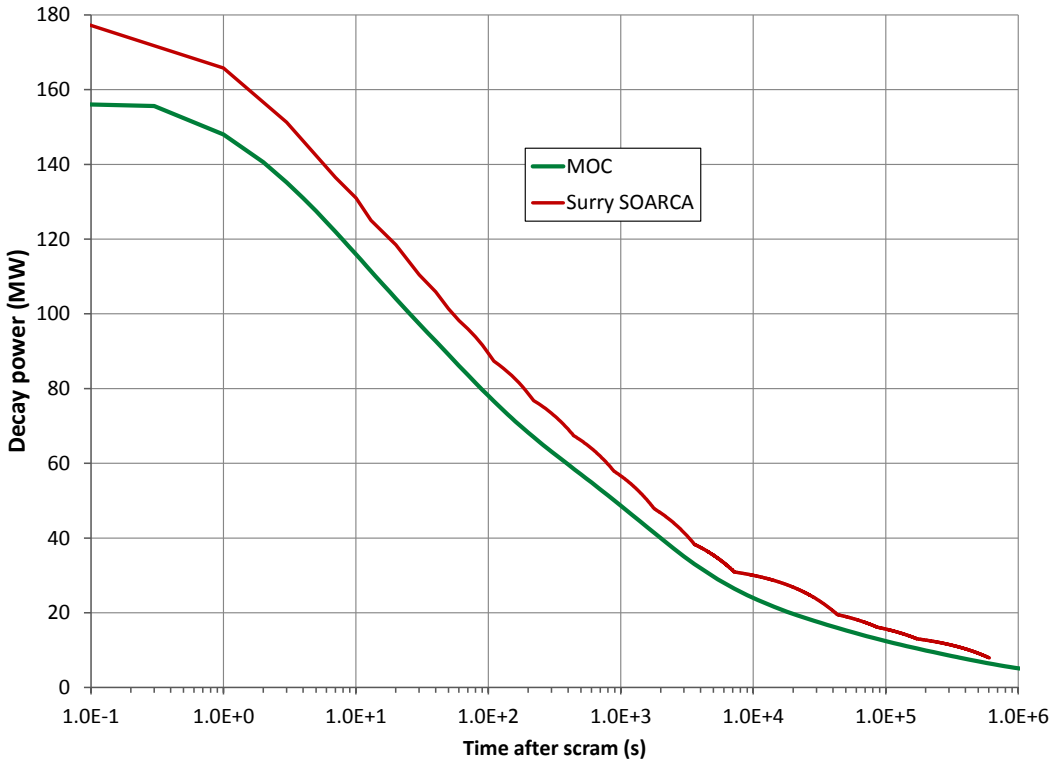

Figure 5.9. New base-case decay heat curve for MELCOR Surry model at MOC conditions.

5.2.3.2 MELCOR Decay Power and Inventory Inputs for the Surry MELCOR Model

The ORIGEN-S/ARP calculations and post-processing provides sets of consistent decay power and inventory information for MELCOR and MACCS to support uncertainty analyses with the Surry model. Three predetermined conditions are generated for BOC, MOC, and EOC to capture the inherent uncertainty of when the accident initiator occurs in the final cycle. It is observed in the scoping study that the decay power for 0-3 days of operation is very small compared to the EOC decay power, especially for hours after scram important for severe accident phenomena (i.e. after core uncovering and damage). Thus, a BOC operating time of 7 days is selected to permit investigation of significantly reduced decay power soon after shutdown (see Figure 5.8), but not such that it excessively reduces power to avoid gross core damage altogether. As discussed in the previous section, the MOC operating time of 200 days is chosen because it is relatively similar to the EOC decay power until about 18 hours after scram, and this facilitates examining the influence of varied decay power during later stages of severe accident progression. The EOC operating time is taken to be the actual operating duration of cycle 20 (about 505 days), which therefore considers the effects of a larger inventory and higher decay heat later into the accident for the UA, while still being a realistic burnup state of the reactor (i.e., it is not a hypothetical condition extrapolated to very high burnup). The BOC, MOC, and EOC decay power curves for Surry are depicted in Figure 5.10 on a severe accident time frame. The same information is portrayed by Figure 5.11, but normalized to the EOC decay power and on a logarithmic time scale. It better shows the quantitative details of the decay powers soon after shutdown and for longer cooling times up to 10^6 seconds, or about 278 hours.

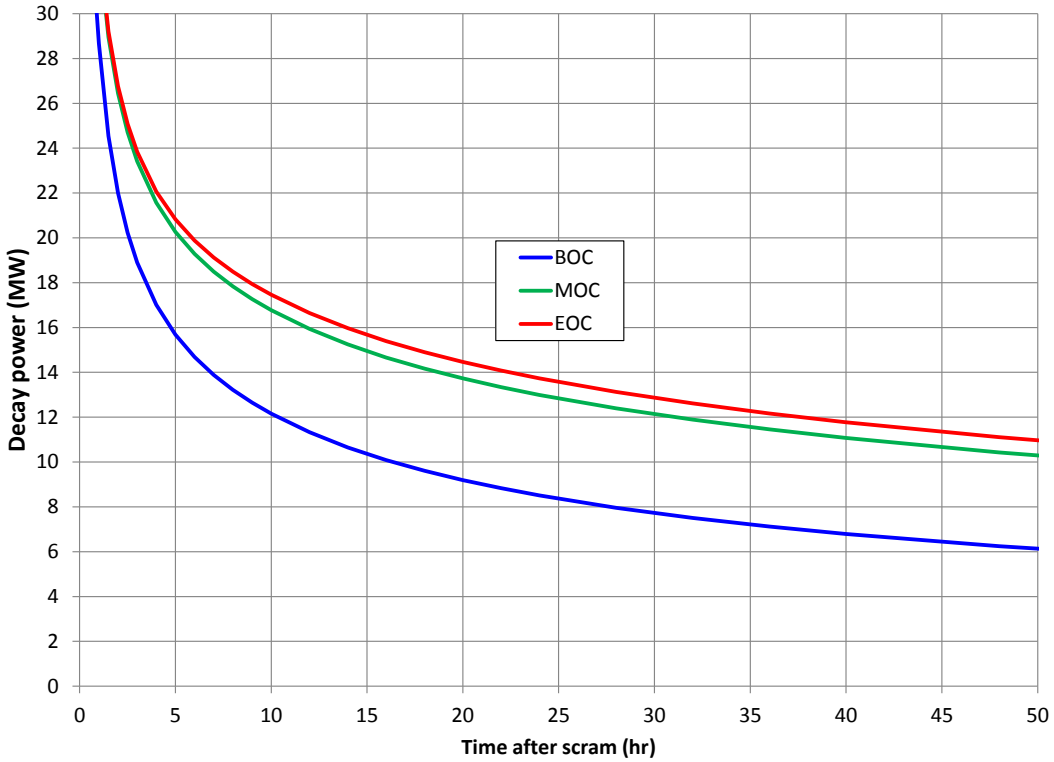

Figure 5.10. BOC, MOC, and EOC decay powers for Surry on severe accident time scale.

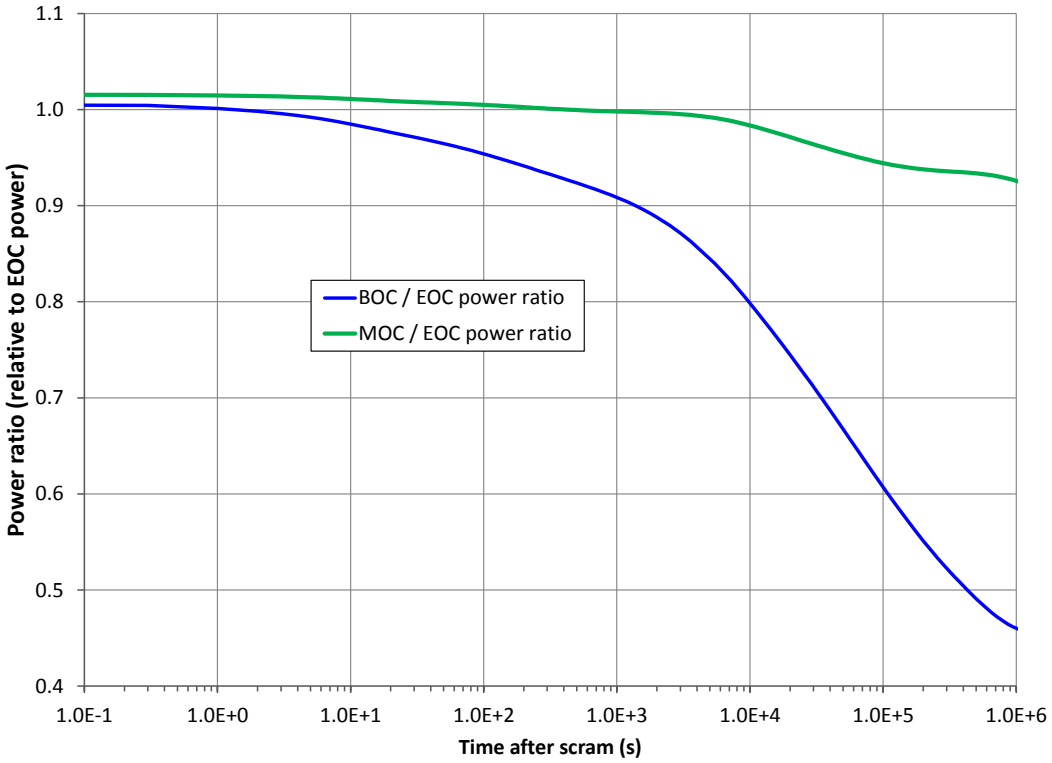

Figure 5.11. BOC and MOC decay power normalized to EOC power on a logarithmic scale.

The lumped MELCOR RN inventories calculated by ORIGEN-S/ARP for BOC, MOC, and EOC are listed in Table 5-4. The SOARCA inventory is also listed for comparison. MELCOR RN class masses are dominated by long-lived and stable nuclides (many fission products and decay daughters produced in the fuel are stable nuclides); thus RN class mass builds monotonically and nearly-linearly with burnup, excluding the uranium class mass, so therefore the scaled inventory used in SOARCA nearly matches the EOC inventory (however, larger differences can exist in the MACCS inventories for key nuclides). The inclusion of stable nuclides in RN mass is important for radionuclide transport calculations in MELCOR [1]. For example, overall aerosol masses affect the conglomeration and deposition of aerosols [1][31]. The selection of operating times from nearly-BOC (7 days) to the full 505 day cycle permits analyses that span the full range of potential MELCOR and MACCS inventories for a chosen cycle. The default speciation of cesium, iodine, and molybdenum classes for each point in the cycle is taken from SOARCA methodology [24][29], which is informed by experimental data from the Phebus and VERCORS programs [31]. The variations across the lumped MELCOR inventories (BOC vs. EOC) are summarized in Table 5-5.

Table 5-4. Lumped MELCOR RN inventories for Surry cycle 20.

#	Class (representative)	BOC (kg)	MOC (kg)	EOC (kg)	SOARCA (kg)
1	Noble Gases (Xe)	223.30	309.16	442.28	448.1
2	Alkali Metals (Cs)	5.99	8.20	11.54	11.7
3	Alkaline Earths (Ba)	94.43	132.12	184.86	187.6
4	Halogens (I)	all in CsI	all in CsI	all in CsI	all in CsI
5	Chalcogens (Te)	20.94	28.88	41.57	40.9
6	Platinoids (Ru)	148.45	205.11	308.71	309.5
7	Early Transition Elements (Mo)	125.48	170.04	243.26	243.3
8	Tetravalent (Ce)	676.80	934.36	1256.40	1225.9
9	Trivalents (La)	306.60	420.53	606.26	621.2
10	Uranium (U)	70800.93	70128.34	69137.32	66771.30
11	More Volatile Main Group (Cd)	4.23	5.62	8.74	7.263
12	Less Volatile Main Group (Sn)	4.75	6.55	10.08	9.19
16	Cesium Iodide (CsI)	17.53	24.31	35.15	34.82
17	Cesium Molybdate (Cs_2MoO_4)	154.76	212.15	298.46	302.47
	Total cesium class mass	128.67	176.53	248.83	251.76
	Total iodine class mass	8.56	11.87	17.17	17.01
	Total molybdenum class mass	166.53	226.30	322.41	323.52

Table 5-5. Variations in lumped MELCOR RN inventories for Surry.

#	Class (representative)	BOC to MOC % change	BOC to EOC % change	MOC to EOC % change	EOC vs. SOARCA
1	Noble Gases (Xe)	38.4	98.1	43.1	-1.3
2	Alkali Metals (Cs)	37.1	92.9	40.7	-1.4
3	Alkaline Earths (Ba)	39.9	95.8	39.9	-1.5
4	Halogens (I)	NA	NA	NA	NA
5	Chalcogens (Te)	37.9	98.5	43.9	1.6
6	Platinoids (Ru)	38.2	108.0	50.5	-0.3
7	Early Transition Elements (Mo)	35.5	93.9	43.1	0.0
8	Tetravalent (Ce)	38.1	85.6	34.5	2.4
9	Trivalents (La)	37.2	97.7	44.2	-2.5
10	Uranium (U)	-0.9	-2.3	-1.4	3.4
11	More Volatile Main Group (Cd)	32.9	106.5	55.4	16.9
12	Less Volatile Main Group (Sn)	37.9	112.3	54.0	8.8
16	Cesium iodide (CsI)	38.7	100.6	44.6	0.9
17	Cesium molybdate (Cs_2MoO_4)	37.1	92.9	40.7	-1.3
	Total cesium class mass	37.2	93.4	41.0	-1.2
	Total iodine class mass	38.7	100.6	44.6	0.9
	Total molybdenum class mass	35.9	93.6	42.5	-0.3

5.2.3.3 MACCS Inputs for Surry MELCOR Model

Isotopic masses and activities are automatically written to MELMACCS input format to allow for MACCS to properly decompose MELCOR source terms that have the new Surry inventory and decay heat. The SNL tool creates completely consistent information of the MELCOR and MACCS inputs for Surry. The isotopic and isomeric compositions of the MELCOR RN classes are calculated for BOC, MOC, and EOC conditions of cycle 20 at Surry.

Activities for key nuclides in cycle 20 at Surry are calculated by ORIGEN-S/ARP and compared in Table 5-6, Table 5-7, and Table 5-8. The SOARCA nuclide inventories are listed to highlight the important effects that different burnup levels and nuclear data (ENDF/B-VII.1) have on isotopic inventory predictions. Differences in isotope and isomer inventories are not nearly as simple and straight-forward as the lumped RN mass inventories. For example, the SOARCA inventory, which was extrapolated from high burnup Sequoyah data, over-predicts the quantities of several key nuclides by 2% to 20% relative to the newly calculated Surry EOC inventory. Conversely, the SOARCA inventory under-predicts the quantities of several actinides such as Pu-240, Pu-241, and Am-241. The wide spectrum of differences between the SOARCA and SNL-EOC nuclide inventories reflects the combined effects of different weighted cross sections, decay data, plant operating data, and overall core burnup used in the analyses. In general, nuclide activities are about 15% to 25% lower in the new Surry EOC inventory relative to the SOARCA inventories, likely owing to different gross core burnups and SOARCA's use of extrapolated data from the Sequoyah reactor.

Table 5-6. MACCS nuclide inventories (in Bq) for Xe, Cs, Ba, I, and Te classes.

Isotope	BOC	MOC	EOC	SOARCA	EOC % difference with SOARCA
Noble gases (Xe)					
Kr-85	1.57E+16	2.14E+16	2.90E+16	2.94E+16	-1.4
Kr-85m	8.48E+17	7.66E+17	6.66E+17	8.07E+17	-21.2
Kr-87	1.72E+18	1.53E+18	1.31E+18	1.60E+18	-21.7
Kr-88	2.30E+18	2.03E+18	1.73E+18	2.14E+18	-23.7
Xe-133	2.77E+18	5.31E+18	5.28E+18	6.07E+18	-15.1
Xe-135	1.57E+18	1.55E+18	1.44E+18	1.80E+18	-24.6
Xe-135m	1.05E+18	1.09E+18	1.13E+18	1.29E+18	-14.2
Alkali metals (Cs)					
Cs-134	1.96E+17	2.66E+17	4.44E+17	4.32E+17	2.7
Cs-136	2.04E+16	7.37E+16	1.12E+17	1.57E+17	-39.7
Cs-137	1.53E+17	2.11E+17	3.00E+17	3.05E+17	-1.6
Rb-86	1.07E+15	3.56E+15	5.86E+15	5.36E+15	8.6
Rb-88	2.32E+18	2.06E+18	1.76E+18	2.16E+18	-22.7
Alkaline earths (Ba)					
Ba-139	4.71E+18	4.77E+18	4.64E+18	5.54E+18	-19.5
Ba-140	1.72E+18	4.61E+18	4.46E+18	5.37E+18	-20.4
Sr-89	1.12E+18	2.72E+18	2.43E+18	2.98E+18	-22.6
Sr-90	1.17E+17	1.60E+17	2.19E+17	2.27E+17	-3.8
Sr-91	3.91E+18	3.50E+18	3.05E+18	3.75E+18	-23.1
Sr-92	4.08E+18	3.72E+18	3.29E+18	4.00E+18	-21.4
Ba-137m	1.46E+17	2.01E+17	2.86E+17	2.92E+17	-2.1
Halogens (I)					
I-131	1.09E+18	2.50E+18	2.56E+18	2.78E+18	-8.6
I-132	2.80E+18	3.75E+18	3.77E+18	4.08E+18	-8.2
I-133	5.31E+18	5.25E+18	5.22E+18	5.76E+18	-10.3
I-134	6.08E+18	5.99E+18	5.87E+18	6.48E+18	-10.4
I-135	5.03E+18	5.01E+18	5.00E+18	5.49E+18	-9.9
Chalcogens (Te)					
Te-127	1.14E+17	1.94E+17	2.29E+17	2.60E+17	-13.5
Te-127m	9.92E+15	1.70E+16	1.92E+16	4.22E+16	-120.0
Te-129	5.16E+17	6.16E+17	6.81E+17	7.79E+17	-14.4
Te-129m	3.57E+16	9.19E+16	1.01E+17	1.49E+17	-47.1
Te-131	2.14E+18	2.18E+18	2.20E+18	2.55E+18	-15.8
Te-131m	3.79E+17	4.41E+17	4.84E+17	5.71E+17	-18.1
Te-132	2.77E+18	3.60E+18	3.64E+18	4.29E+18	-17.9

Table 5-7. MACCS nuclide inventories (in Bq) for Ru, Mo, and Ce classes.

Isotope	BOC	MOC	EOC	SOARCA	EOC % difference with SOARCA
Platinoids (Ru)					
Rh-105	1.56E+18	1.97E+18	2.45E+18	2.90E+18	-18.3
Ru-103	1.40E+18	3.46E+18	3.97E+18	4.61E+18	-16.0
Ru-105	1.71E+18	2.23E+18	2.77E+18	3.14E+18	-13.3
Ru-106	6.39E+17	8.62E+17	1.29E+18	1.40E+18	-8.5
Rh-103m	1.39E+18	3.42E+18	3.93E+18	4.61E+18	-17.2
Rh-106	7.38E+17	9.97E+17	1.48E+18	1.56E+18	-5.5
Early transition metals (Mo)					
Nb-95	2.34E+18	3.96E+18	4.30E+18	5.18E+18	-20.4
Co-58	1.49E+13	2.86E+13	3.04E+13	4.79E+13	-57.6
Co-60	1.63E+15	2.25E+15	3.18E+15	2.65E+14	91.7
Mo-99	4.02E+18	4.81E+18	4.77E+18	5.68E+18	-19.2
Tc-99m	3.47E+18	4.24E+18	4.32E+18	5.03E+18	-16.3
Nb-97	4.58E+18	4.49E+18	4.35E+18	5.24E+18	-20.4
Nb-97m	4.36E+18	4.25E+18	4.11E+18	4.95E+18	-20.4
Tetravalents (Ce)					
Ce-141	1.57E+18	4.29E+18	4.19E+18	4.87E+18	-16.2
Ce-143	4.24E+18	4.15E+18	3.92E+18	4.55E+18	-16.0
Ce-144	1.80E+18	2.57E+18	3.13E+18	3.42E+18	-9.4
Np-239	3.82E+19	4.65E+19	5.12E+19	5.67E+19	-10.6
Pu-238	3.06E+15	4.42E+15	7.94E+15	8.31E+15	-4.6
Pu-239	5.88E+14	8.19E+14	9.77E+14	9.56E+14	2.1
Pu-240	6.63E+14	9.00E+14	1.32E+15	1.17E+15	11.5
Pu-241	1.77E+17	2.35E+17	3.57E+17	3.39E+17	5.1
Zr-95	1.98E+18	4.25E+18	4.28E+18	4.96E+18	-15.8
Zr-97	4.58E+18	4.47E+18	4.32E+18	5.00E+18	-15.7

Table 5-8. MACCS nuclide inventories (in Bq) for La class.

Isotope	BOC	MOC	EOC	SOARCA	EOC % difference with SOARCA
Trivalents (La)					
Am-241	1.98E+14	2.89E+14	4.65E+14	3.43E+14	26.2
Cm-242	3.82E+16	5.60E+16	1.06E+17	1.14E+17	-7.0
Cm-244	2.30E+15	3.59E+15	8.39E+15	1.13E+16	-34.6
La-140	1.34E+18	4.68E+18	4.58E+18	5.67E+18	-23.9
La-141	4.47E+18	4.36E+18	4.21E+18	5.10E+18	-21.0
La-142	4.38E+18	4.23E+18	4.05E+18	4.92E+18	-21.5
Nd-147	6.78E+17	1.69E+18	1.66E+18	2.04E+18	-23.0
Pr-143	1.23E+18	4.16E+18	3.92E+18	4.65E+18	-18.5
Y-90	1.19E+17	1.64E+17	2.25E+17	2.39E+17	-6.1
Y-91	1.47E+18	3.45E+18	3.15E+18	3.93E+18	-24.6
Y-92	4.13E+18	3.76E+18	3.33E+18	4.11E+18	-23.3
Y-93	4.46E+18	4.14E+18	3.77E+18	4.62E+18	-22.7
Y-91m	2.30E+18	2.07E+18	1.79E+18	2.20E+18	-22.7
Pr-144	1.80E+18	2.59E+18	3.15E+18	3.63E+18	-15.3
Pr-144m	2.12E+16	3.93E+16	4.53E+16	5.06E+16	-11.7

The isotopic inventories for BOC, MOC, and EOC calculated using ORIGEN-S are implemented into MELMACCS input for Surry consequence analyses. Consequently, three MELMACCS inventories can be utilized by MACCS uncertainty analyses of Surry source terms. A simple scheme can be used for easy identification of which MELMACCS inventory to use with the appropriate MELCOR plot file. For example, if 300 MELCOR realizations are to be analyzed, then realizations 1-100 are for BOC conditions, realizations 101-200 are for MOC conditions, and realizations 201-300 are for EOC conditions.

5.3 Scoping Studies for Peach Bottom

A preliminary analysis of the Peach Bottom reactor is conducted using ORIGEN-S/ARP and the automation tools. Detailed plant data for cycles 13 through 16 at Peach Bottom is available from the SOARCA project that is sufficient to perform an assembly-detailed analysis for these cycles, similar to the Fukushima and Surry analyses. Such an effort is planned for future work to further validate the new SNL tools. The scoping study of Peach Bottom, however, performs a simple whole-core (i.e. single input model) analysis with ORIGEN-S/ARP that is then post-processed using the SNL scripts to create MELCOR and MACCS inputs. These new MELCOR and MACCS inputs are compared to the SOARCA inputs used in Peach Bottom. Lumped RN inventories are presented in Section 5.3.1. Total core decay powers are discussed in Section 5.3.2. Inventories for nuclides are discussed in Section 5.3.3.

5.3.1 Lumped RN Inventories

The calculated RN inventories for Peach Bottom are compared to the SOARCA information for EOC of cycle 16 in Table 5-9. The RN masses in Table 5-9 reflect the inventories before partitioning over the CsI and Cs_2MoO_4 combination classes. The predicted inventories are very similar to the SOARCA inventories for all classes except the trivalent (La) and the more volatile main group (Cd) classes. Trivalent mass is under-predicted by about 11%, but this class mass can be very sensitive to the assumed gadolinium mass in the core. BWR cores can contain significant gadolinium from Gd-based burnable poisons. Volatile main group mass is over-predicted by about 21% compared to the SOARCA information; this class can also be sensitive to the assumed concentrations of impurity elements in the fuel such as cadmium and zinc.

The ORIGEN-S/ARP calculations use the SCALE6 library for GE 10x10 fuel (i.e., ge10x10-8) at a void fraction of 0.4. The whole-core is irradiated to the core-average burnup for EOC of cycle 16, which is about 33 GWd/t. The assumed density used for whole-core and axially-integrated burnup analyses of BWRs can strongly influence the predictions of actinide masses, mainly affecting the tetravalent (Ce) class due to plutonium buildup.

Table 5-9. Peach Bottom RN inventories (kg).

#	Class (representative)	EOC Peach Bottom SOARCA	SNL α=0.4 ρ=0.46g/cc	Percent difference
1	Noble Gases (Xe)	749.22	758.61	1.25
2	Alkali Metals (Cs)	444.73	447.19	0.55
3	Alkaline Earths (Ba)	324.13	326.10	0.61
4	Halogens (I)	28.36	28.65	1.01
5	Chalcogens (Te)	69.24	69.64	0.58
6	Platinoids (Ru)	510.63	502.46	-1.60
7	Early Transition Elements (Mo)	558.21	573.68	2.77
8	Tetravalent (Ce)	2005.45	2073.40	3.39
9	Trivalents (La)	2108.50	1870.90	-11.27
10	Uranium (U)	131239.78	131200.00	-0.03
11	More Volatile Main Group (Cd)	11.31	13.66	20.73
12	Less Volatile Main Group (Sn)	14.94	14.87	-0.46
13	Boron (B)	8.52×10^{-5}	8.67×10^{-5}	1.76

5.3.2 Whole-core Decay Powers

Whole-core decay power for EOC of cycle 16 at Peach Bottom is extracted from ORIGEN-S/ARP and OPUS outputs. These predictions agree well with the EOC SOARCA information for Peach Bottom. However, the time-mesh of the SOARCA decay heat curve is rather coarse, particularly between 2 and 12 hours, which is an important time period for typical severe accident scenarios similar to unit 1 and those from SOARCA; i.e. this is when core degradation and oxidation are occurring. This introduces error in the decay heat curve for the severe accident

simulation since MELCOR linearly interpolates the tabular function linked to DCH_DPW. Figure 5.12 compares the SOARCA decay power to the newly calculated decay power for Peach Bottom using ORIGEN-S/ARP and the SNL post-processing tools. The class decay powers are also quickly inspected and found to very comparable, as shown by Figure 5.13 for a few classes.

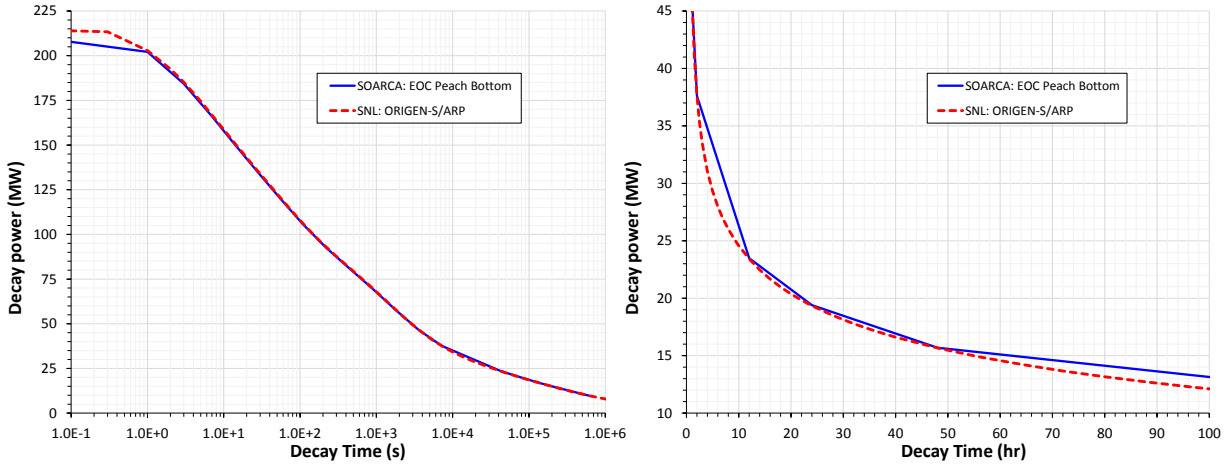

Figure 5.12. Peach Bottom decay power on log (left) and linear (right) time scales.

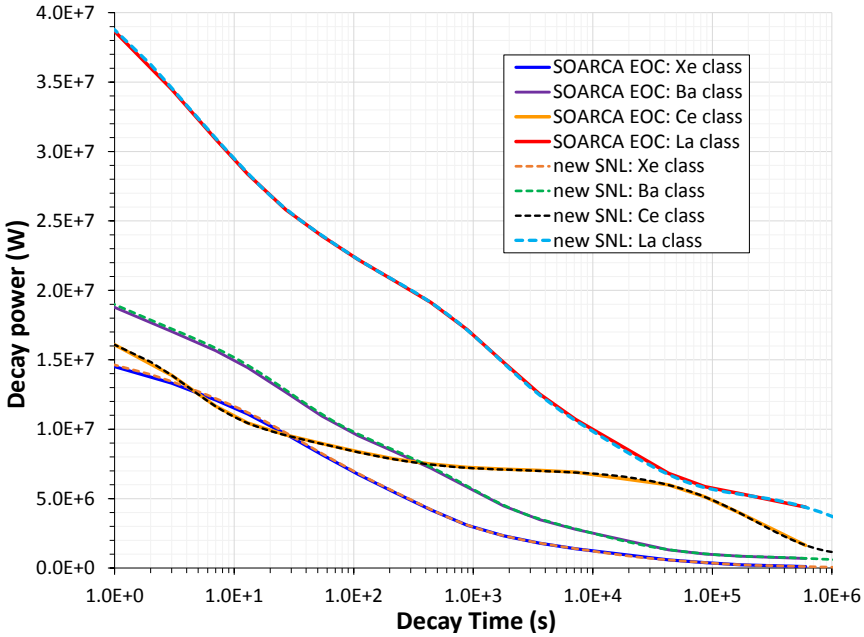

Figure 5.13. Class decay powers for Peach Bottom.

5.3.3 Nuclide Inventories for MACCS

A detailed review of the nuclide quantities predicted by the Peach Bottom scoping study is not performed here. SOARCA information for EOC nuclide inventories is not readily available since SOARCA analyzed Peach Bottom at MOC conditions. Future work will re-evaluate the Peach Bottom MOC conditions using ORIGEN-S/ARP with the SNL tool in a similar fashion as the Fukushima burnup analyses. These results will then be compared to the MOC nuclide inventories from SOARCA.

6 REVIEW OF APPROXIMATIONS FOR RADIONUCLIDE CLASSES

MELCOR has been in continual development for about thirty years. Overly simple and parametric models in the code have been gradually expanded into more mechanistic treatments to support best-estimate severe accident analyses and detailed decision support (e.g. severe accident management). Nonetheless, many of the original fundamental assumptions remain deeply ingrained in the code; simplifying assumptions were necessary in part due to 1980s computing capabilities, and partly due to limited phenomenological understanding.

One of the primary uses of MELCOR is to calculate radionuclide source terms to the containment and environment. Hence, the code must simulate mechanisms for radionuclide decay heating, releases, transport, chemistry, and deposition. Given phenomenological uncertainties and computing limitations of the time, MELCOR developers adopted the concept of radionuclide classes to allow the code to model the behavior of radionuclides during a severe accident. RN classes abstract the complicated behavior of over 1000 fission products, actinides, activation products, and decay daughters into a handful of classes based on chemical and physical characteristics. Moreover, the class assumption avoids the need to consider hundreds to thousands of distinct radionuclide species (i.e., compounds and molecules) for the transport calculations in MELCOR, the existence and behaviors of which are not fully understood for severe accident conditions. A completely honest accounting of all known species and reactions was prohibitive with 1980s computing hardware for the millions of time steps required for a 2-7 day source term simulation; such calculations are likely still exorbitant for serial computing, and may only be practical using highly parallelized supercomputing.

This section discusses and analyzes three major MELCOR approximations for RN classes: spatial distribution of RN mass and power over COR cells (Section 6.1), formation of RN class masses (Section 6.2), and the partitioning of decay power over RN classes (Section 6.3). A few additional approximations related to RN speciation are briefly discussed in Section 6.4.

6.1 Spatial Allocation of MELCOR RN Mass and Decay Power

MELCOR input allows for unique specification of 2D mass distributions for each RN class. The user can also specify unique specific power curves (in W/kg) for each class as a function of time after shutdown. By default, this limits the spatial distributions of decay power and RN class mass to be the same. In reality, decay power and lumped RN mass are not synonymous, since RN mass is mostly comprised of long-live and stable nuclides, while decay power is driven mainly by many short-lived nuclides soon after shutdown (which have relatively small masses). Modern fuel shuffling schemes that allocate high burnup assemblies around the periphery of the core can amplify this divergence. Many long-lived (e.g. Cs-137) and stable nuclides build nearly-linearly with increasing burnup; thus RN inventories of first-order importance for consequence effects can have radial distributions opposite that of the decay power distribution, which intrinsically follows the operating power distribution for any significant operation time.

6.1.1 Examination of the Effects of Modern Fuel Shuffling

Figure 6.1 (Surry MOC) and Figure 6.2 (Fukushima unit 1) show that the radial distributions of decay power and burnup, as calculated by the ORIGEN-S/ARP process, are very different. Also depicted on the figures are the radial distributions of Cs-137 mass predicted by ORIGEN-S/ARP. The mass distribution of Cs-137 nearly matches the burnup distribution when normalized to account for the different sizes of each ring, as expected. The absolute distribution of any long-lived or stable radionuclide is a strong function of both the number of fuel assemblies in the ring and the average ring burnup. The shuffling of high burnup assemblies to the periphery of the core results in concentrating Cs-137 mass in the outer COR rings. Allocating the mass of the alkali metal class to match either the power densities or absolute powers of the rings would over-concentrate Cs-137 in the inner COR rings, which is opposite of the true distribution.

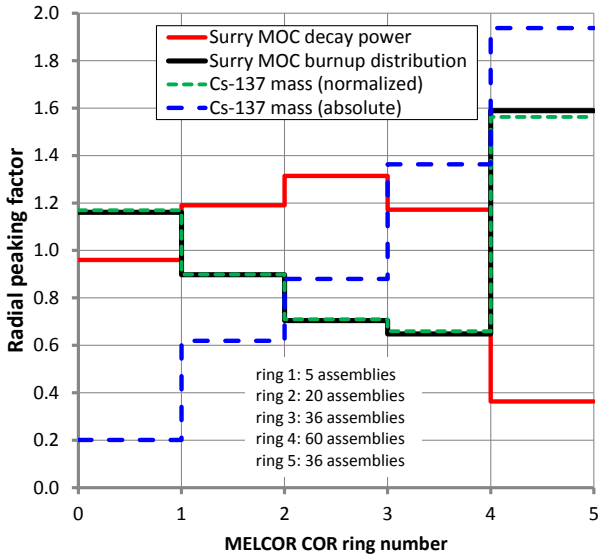

Figure 6.1. Surry distributions of decay power, burnup, and Cs-137 over COR rings.

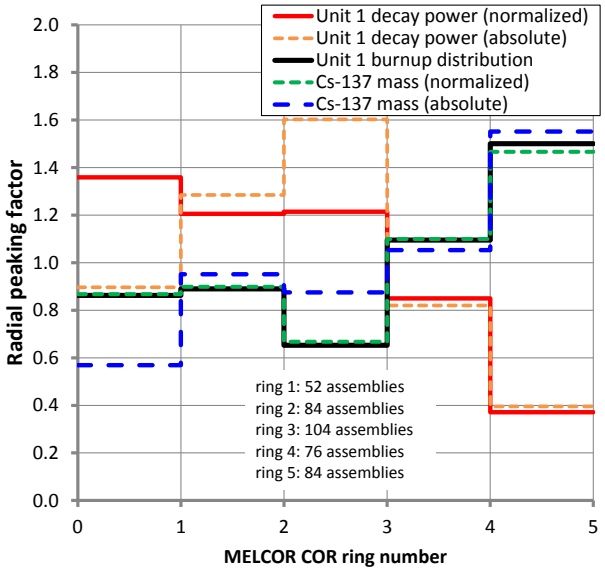

Figure 6.2. Unit 1 distributions of decay power, burnup, and Cs-137 over COR rings.

6.1.2 Spatial Allocation Approximations for SOARCA Models

The default MELCOR approach is to apportion all RN mass according to the desired decay power distribution. This approach was used in both Peach Bottom and Surry SOARCA models; this method may therefore over-predict radionuclide releases from the fuel for certain classes, since it usually requires concentrating RN masses in the central regions of the core (see Figure 6.1). Over-predictions of RN releases from fuel would be limited to accident scenarios with partial core overheating and damage/relocation, perhaps similar to the Fukushima accidents. Thus for the SOARCA unmitigated SBO scenarios, which almost always exhibit near-total core damage, the over-prediction error is likely very minor (or near zero) by the end of the severe accident simulation, which is many hours after total core destruction. The new calculations for Surry (Section 5.2) simply allocate RN masses over COR rings according to the decay power distribution. Axially, the burnup and power distributions are relatively similar due to core symmetry and the lack of axial fuel shuffling, so the axial allocation of RN mass/power is a much simpler task. A reevaluation of the radial distribution of RN masses in the Peach Bottom model is planned for future work to support accident scenarios that exhibit partial core damage, due to lower decay heat long after shutdown and/or assumed mitigative actions.

6.1.3 Spatial Allocation Approximations for Fukushima Models

In contrast to SOARCA accident scenarios, the Fukushima accidents exhibited wide variations in event timing. For example, units 2 and 3 likely did not reach core uncovering and damage until approximately 70 hours and 35 hours after shutdown, respectively [1][2][3][4][5]; significantly lower decay power during the in-vessel accident progression inhibits total core damage and relocation [5]. Furthermore, operators performed mitigative actions that likely resulted in partial success–i.e. core damage was reduced but not totally prevented. Indeed, several MELCOR simulations of the Fukushima units have resulted in intact outer core rings that never reach very high temperatures for complete RN release of volatile species [1].

It is a worthwhile effort to capture the effects of the true RN inventory distributions in the core for the Fukushima models and accident scenarios. Therefore, the SNL post-processing tools allow for a few different options for allocating RN masses for key classes (see Section 3.3). However, as discussed in Section 3.3, these options are really just compromises that workaround MELCOR's input limitations. The Fukushima inventories presented in Section 4.3 implemented the option to allocate all RN mass radially according to the calculated decay power distribution, excluding the alkali metal (Cs), tetravalent (Ce, Pu), and uranium classes, which are distributed radially according to the ORIGEN-S/ARP predictions. Axially, RN masses for the Fukushima models are apportioned according to an average power and burnup distribution, but the uranium class is distributed uniformly over all axial COR nodes in the MELCOR models.

6.1.4 Future Investigations

A truly faithful accounting of RN mass, composition, and power likely requires unique RN classes to be defined for each COR node or ring, or perhaps an inner-core vs. outer-core treatment. For example, the cesium class would require decomposition into cesium in ring 1,

cesium in ring 2, and so on. Each 'sub-class' would thus require unique total inventory, spatial distribution, and specific decay power inputs; the sub-classes would also require distinct isotopic breakdowns in MELMACCS input. This would of course significantly increase CPU times and would complicate post-processing in MELCOR and MACCS. Substantial source code revisions are probably required to thoroughly support such an effort.

A simpler workaround may allow for some improved accounting of the initial RN mass and decay power distributions, but it would not permit a consistent MACCS treatment of RN compositions in each COR ring. The user can specify just one RN class for each species, as done in SOARCA, but define each to be comprised of several fictitious 'elements' that represent the unique specific decay powers of the class in each ring. This is demonstrated for the cesium class by the following MELCOR input records (Figure 6.3):

```
! DCH input for user-defined cesium class
DCH_CL 'CS'  USER  5  ! user-defined class named 'CS' with 5 total member elements
               1  'C1' ! cesium class fictitious element name for COR ring 1
               2  'C2' ! cesium class fictitious element name for COR ring 2
               3  'C3' ! cesium class fictitious element name for COR ring 3
               4  'C4' ! cesium class fictitious element name for COR ring 4
               5  'C5' ! cesium class fictitious element name for COR ring 5

! specific decay heat records for element fictitious 'elements' in the cesium class
DCH_EL 'C1' ELMMAS-Cs-ring1 NMPAIR  ! ELMMAS-Cs-ring1 = Cs mass in ring 1
       1 TIME(0) DCHEAT_Cs-ring1(0) ! NMPAIR = number of entries for time vs. W/kg
       2 TIME(1) DCHEAT_Cs-ring1(1)
                 …
  NMPAIR TIME(n) DCHEAT_Cs-ring1(n) ! specific decay power table for cesium in ring 1

DCH_EL 'C2' ELMMAS-Cs-ring2 NMPAIR  ! ELMMAS-Cs-ring2 = Cs mass in ring 2
       1 TIME(0) DCHEAT_Cs-ring2(0) ! NMPAIR = number of entries for time vs. W/kg
       2 TIME(1) DCHEAT_Cs-ring2(1)
                 …
  NMPAIR TIME(n) DCHEAT_Cs-ring2(n) ! specific decay power table for cesium in ring 2
```

Figure 6.3. Potential MELCOR input workaround for RN mass and decay power.

These records could be continued for all of the core rings. When used properly in conjunction with RN1_FPN input, which specifies the spatial distribution of the 'CS' class over all core nodes, this approach may permit a better accounting of initial RN mass and power distributions– at a minimum, it may simplify the post-processing of ORIGEN outputs for several regions of the core into MELCOR input records. Currently, the user must choose between matching a desired decay power distribution and honoring the actual RN mass distribution, as discussed in Section 3.3. The simpler workaround that uses fictitious class elements would not increase CPU burden like the more laborious multi-class approach, but it would also not allow for consistent MACCS accounting of unique RN compositions in the COR cells.

6.2 Summation of Radionuclide Class Masses

The Perl post-processing script generates lumped class inventories using the default element members of each MELCOR class, which are listed in Table 6-1 [10]. ORIGEN-S calculates quantities of isotopes and isomers separated by light elements, actinides, and fission products (these are called ORIGEN 'libraries'). The creation of the lumped class masses is a simple matter of summation over the isotopes and isomers from each library and from each fuel assembly; the

radial locations of the assemblies are tracked in this process for radial allocation over MELCOR rings (see Section 6.1). Isotope and isomer masses are lumped into element masses, which are then lumped into class masses. The OPUS auxiliary tool in SCALE is also used to double-check the summation calculations directly from ORIGEN-S output files. The formation of the RN class masses and powers using the SNL tools is largely consistent with historical treatments for MELCOR classes [10][32][33].

Table 6-1. MELCOR RN class compositions

Class Name	Representative	Member Elements
1. Noble Gases	Xe	He, Ne, Ar, Kr, Xe, Rn, H, N
2. Alkali Metals	Cs	Li, Na, K, Rb, Cs, Fr, Cu
3. Alkaline Earths	Ba	Be, Mg, Ca, Sr, Ba, Ra, Es, Fm
4. Halogens	I	F, Cl, Br, I, At
5. Chalcogens	Te	O*, S, Se, Te, Po
6. Platinoids	Ru	Ru, Rh, Pd, Re, Os, Ir, Pt, Au, Ni
7. Early Transition Elements	Mo	V, Cr, Fe, Co, Mn, Nb, Mo, Tc, Ta, W
8. Tetravalent	Ce	Ti, Zr*, Hf, Ce, Th, Pa, Np, Pu, C
9. Trivalents	La	Al, Sc, Y, La, Ac, Pr, Nd, Pm, Sm, Eu, Gd, Tb, Dy, Ho, Er, Tm, Yb, Lu, Am, Cm, Bk, Cf
10. Uranium	U	U
11. More Volatile Main Group	Cd	Cd, Hg, Zn, As, Sb, Pb, Tl, Bi
12. Less Volatile Main Group	Sn	Ga, Ge, In, Sn, Ag

*Stable oxygen in UO_2 is excluded from the Chalcogen class mass. This oxygen mass is modeled automatically via the molecular weight of the uranium class via sensitivity coefficient 7120(2). Likewise, large structural masses such as Zr are not included in MELCOR class masses, but Zr fission products created in the fuel are included.

6.2.1 Mass Compositions of RN classes

Because MELCOR does not allow for time-dependent class masses with respect to radioactive decay, the user-specified inventories are notionally a snap-shot at a particular time, which is usually taken to be the moment of reactor shutdown. As mentioned before, short-lived nuclides inherently contribute little mass relative to the lumped class inventories [1], i.e. short half-life precludes significant mass accumulation as the reactor operates [33]. The class masses are predominately comprised of stable and long-lived nuclides, as demonstrated by ORIGEN-S/ARP in Figure 6.4 for a typical LWR that shutdown near MOC at a core-averaged burnup near 20 GWd/t. The cesium class is mostly long-lived Cs-137 ($t_{1/2}$ ~ 30.2 years) and stable Cs-133, while the iodine class is mostly long-lived I-129 ($t_{1/2}$ ~ 1.6×10^7 years) and stable I-127.

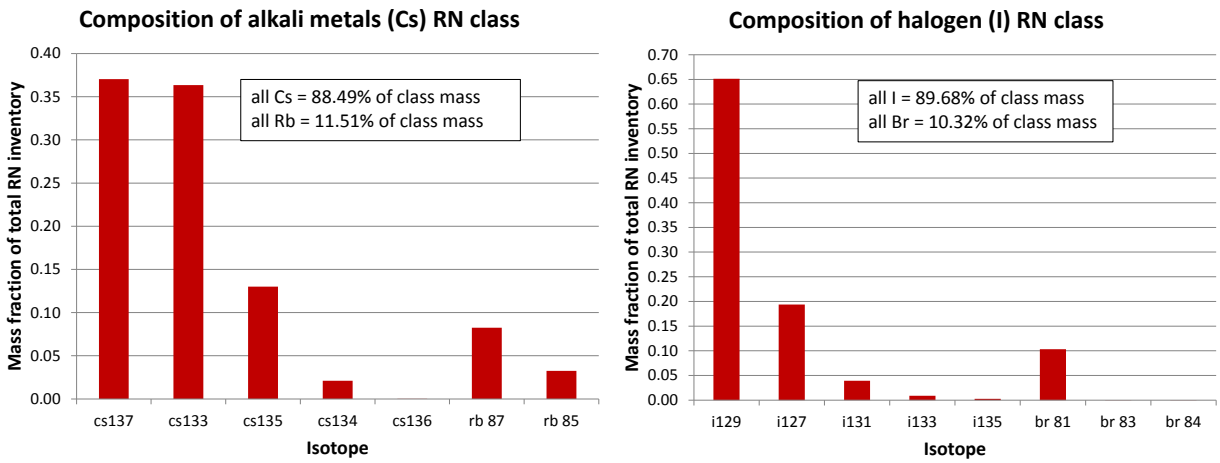

Figure 6.4. Typical compositions of cesium and iodine classes for 20 GWd/t LWR.

The mass compositions for other notable RN classes are depicted in Figure 6.5 (noble gases and alkaline earths), Figure 6.6 (chalcogens and platinoids), Figure 6.7 (transition metals and tetravalents), and Figure 6.8 (trivalents). A cursory inspection of each class with the chart of nuclides [35] confirms that the top isotopes by mass are all stable or long-lived relative to severe accident time frames:

- Noble gases: comprised by mass mostly of Xe-136, Xe-134, Xe-132 and Kr-86, which are all stable or essentially stable[2];
- Alkaline earths: mostly Ba-138 (stable), Sr-90 ($t_{1/2}$~28.9 years) and Sr-88 (stable);
- Chalcogens: mostly Te-130 and Se-82, which are both essentially stable;
- Platinoids: mostly Ru-101, Ru-102, Ru-104, Rh-103, and Pd-105, which are all stable or essentially stable;
- Transition metals: mostly Mo-100, Mo-97, Mo-98, Mo-95 (all stable or essentially stable), and Tc-99 (long-lived with $t_{1/2} \sim 2.1 \times 10^5$ years);
- Tetravalents: mostly Pu-239, Pu-240, Ce-140, Ce-142, Zr-96, Zr-94, and Np-237. Pu-239 and Pu-240 are long-lived actinides with half-lives of 2.41×10^4 years and 6.56×10^3 years, respectively. Ce-140, Ce-142, Zr-96 and Zr-94 are all stable or essentially stable. Np-237 is long-lived with a half-life of 2.14×10^6 years.

[2] The term "essentially stable" refers to isotopes with extremely long half-lives and very rare decay modes such as double beta decay. Such nuclides have half-lives over 10^{18} years, which is essentially stable for severe accidents.

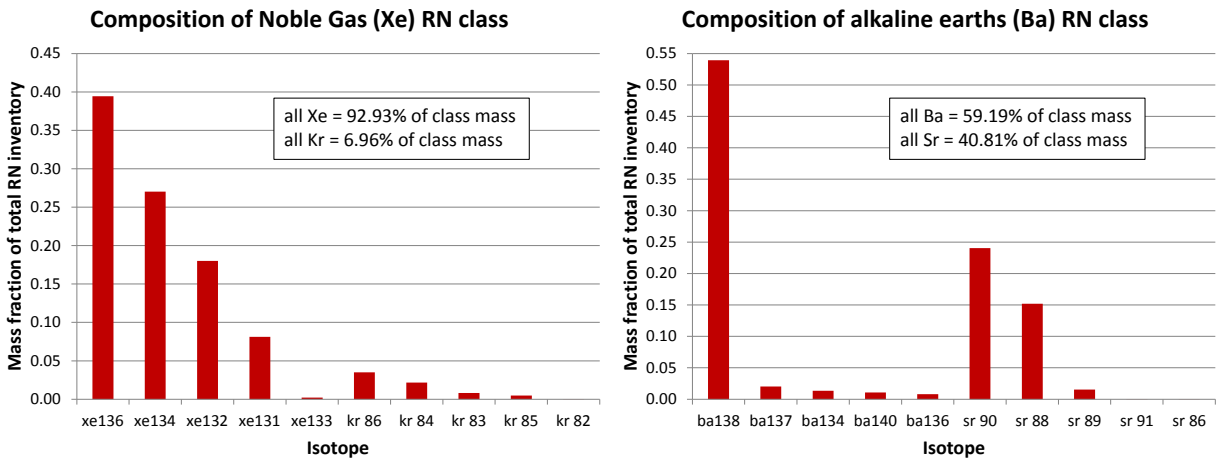

Figure 6.5. Typical compositions of Xe and Ba classes for 20 GWd/t LWR.

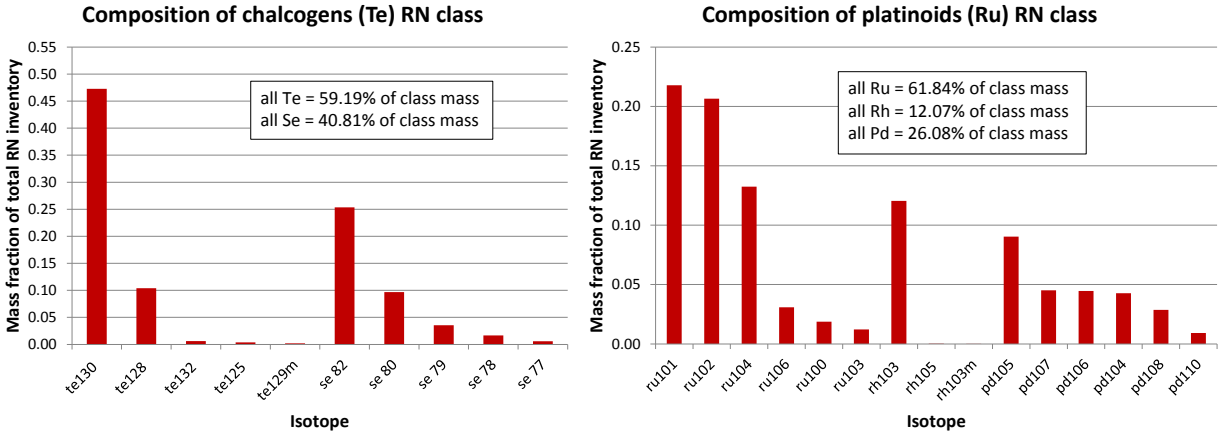

Figure 6.6. Typical compositions of Te and Ru classes for 20 GWd/t LWR.

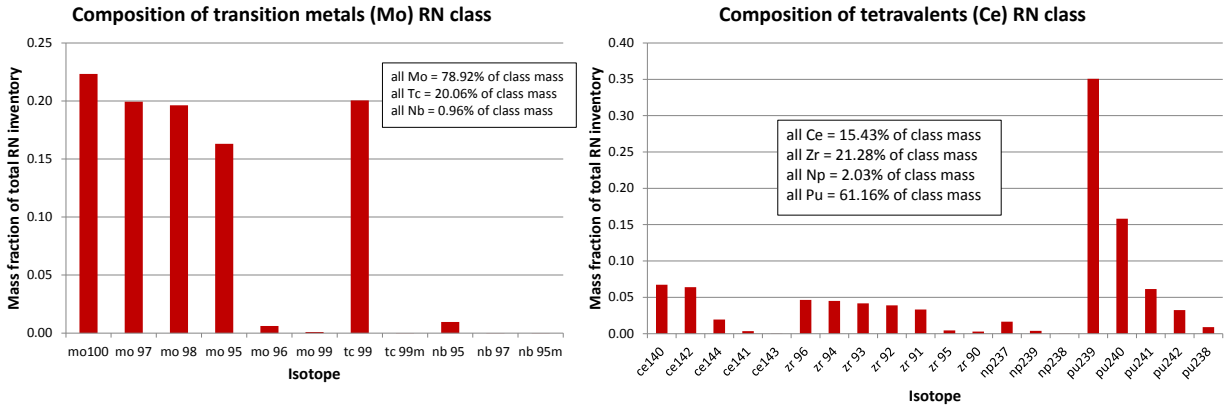

Figure 6.7. Typical compositions of Mo and Ce classes for 20 GWd/t LWR.

The mass composition of the trivalent class is complex due to the large number of member elements, as shown in Figure 6.8. Although usually unimportant for consequences, the trivalent class dominates total core decay power due to its plethora of nuclides that have wide ranges of half-lives. The trivalent class mass can be particularly sensitive to Gd-based burnable poisons in

the fuel (typically Gd_2O_3). Since this 'impurity' is located in the fuel, it would logically be released with its appropriate class, the trivalents, upon sufficient fuel overheating. The mass breakdown depicted by Figure 6.8 is for a BWR (unit 3) that contains a considerable mass of gadolinium in the core. PWRs generally do not use Gd-based burnable poisons, and instead use dissolved boron in the coolant (which is controlled by the operators) in conjunction with boron-based burnable poisons that are fixed in the fuel assemblies (e.g., IFBA, WABA, and flux suppression inserts). Thus, the trivalent class for PWRs contain considerably less mass from Gd-158, Gd-156, and Gd-160, which are all stable isotopes. Like the other RN classes, the trivalent class mass is mostly stable nuclides.

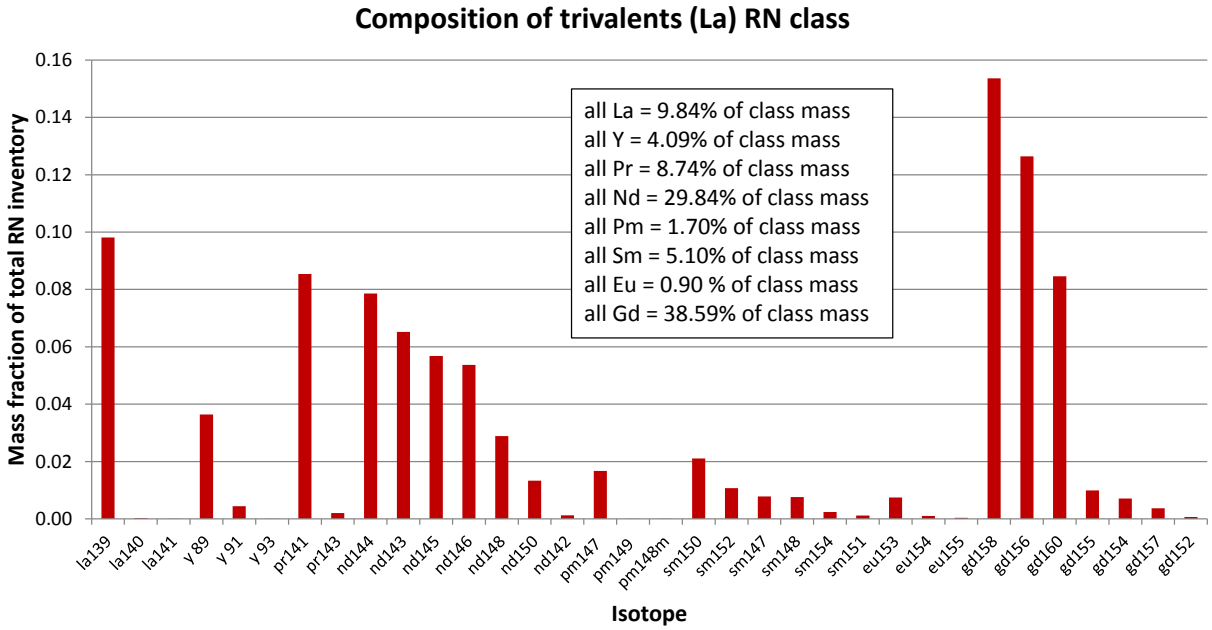

Figure 6.8. Typical composition of trivalent class for 20 GWd/t LWR with Gd-based burnable poison.

6.2.2 RN Class Mass and Decay Time

Similar RN mass information is portrayed in Figure 6.9 and Figure 6.10 as a function of time after shutdown. Excluding the halogen (I) class, MELCOR RN masses are nearly constant soon after shutdown. Iodine class mass only decreases by 1-2% for severe accident time scales due to decay of I-131, I-133, and I-129. For much longer shutdown times (Figure 6.10), trivalent (La) and alkaline earth (Ba) mass grows due to the large number of member elements and cesium decay (Cs-137 and Cs-134 to Ba-137 and Ba-134), respectively. Alkali metal (Cs) mass decreases congruently long after shutdown. Therefore, the compulsory assumption of constant class mass in MELCOR with respect to radioactive decay is acceptable for severe accident time frames (0 to 7 days). For LWR inventories and source terms, the transfer of short-lived nuclide mass from the class of origin to the destination class (parent to daughter), given a-priori knowledge of when core damage and releases occur, is a laborious effort with little utility or impact on the RN masses used for the transport calculation. This conclusion is consistent with NUREG/CR-4481 [32] and NUREG/CR-4169 [33]. Decay effects on inventory are much more important and relevant for the MACCS calculations, and radioactive decay is modeled in MACCS to account for time-varying quantities of key isotopes and isomers.

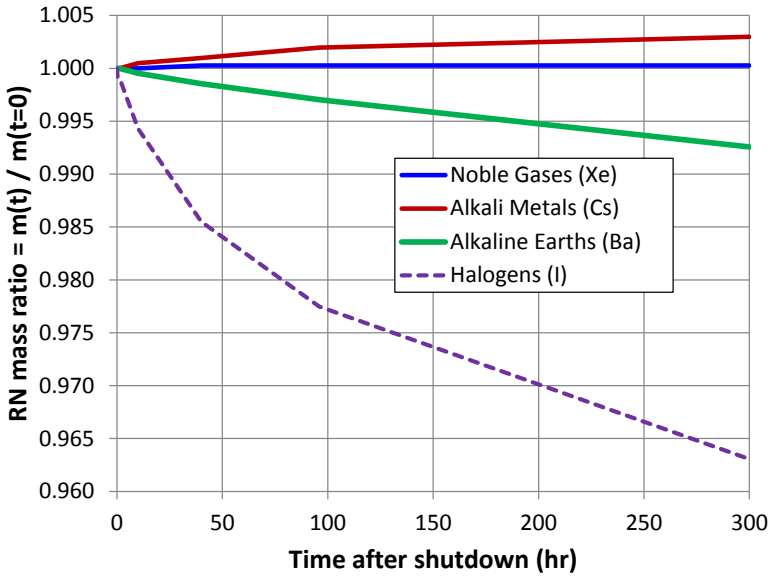

Figure 6.9. Typical MELCOR RN mass variation with time since shutdown, 0-300 hours.

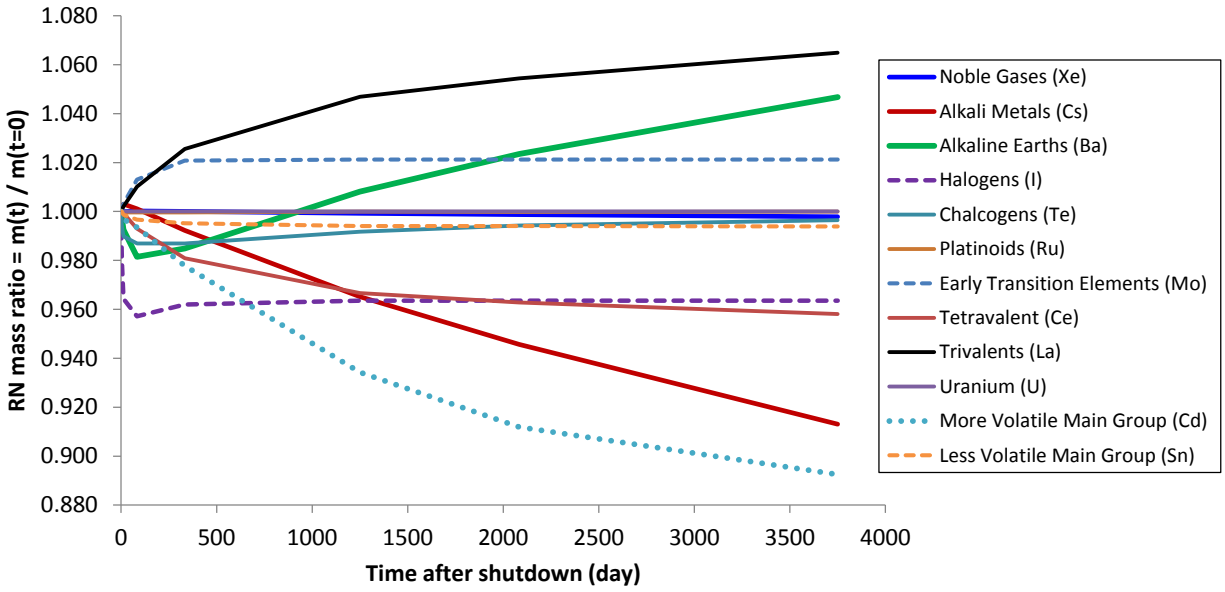

Figure 6.10. Typical MELCOR RN mass variation with time since shutdown, 0-3700 days.

6.3 Summation of Radionuclide Class Decay Powers

The process to generate RN class decay powers has an analogous complication to the RN masses. As an isotope decays, the rate of energy generated is a function of the emitted particle energy and decay rate, which is tallied for its corresponding RN class–this is the parent decay power. Subsequently, the daughter may exist in a different class and undergo its own decay scheme–this is the daughter decay power. In the static situation where radionuclide classes are not released and transported uniquely, it makes more sense to separate the daughter decay power

from the parent decay power (i.e. allocate the powers between their respective classes). During severe accidents the radionuclide classes can relocate independently according to unique release rates and transport characteristics, and thus classes can be separated by physical distances and/or compartments. Thus, it may not be ideal to separate the parent and daughter decay powers for severe accidents. Analyses is this section provide insights into the methods and approximations for decay heat partitioning over RN classes.

6.3.1 Background

The historical MELCOR work-around (i.e. the internal SANDIA-ORIGEN data) for the problem of decay heat partitioning over RN classes is to assume the daughter decay power remains in the parent class [10][33]. Ideally, however, only daughter decay power generated after shutdown due to parent in-growth should be retained in the parent class, since daughter power from the inventory at shutdown should justly remain in the daughter class. Furthermore, daughter decay power due to in-growth should only remain in the parent class if the daughter class is not present in the same region of the model (in order to avoid 'teleporting' power to a different location). Although such efforts may improve the realism of the model, for most fission products the daughter decay power is only a few percent of the parent decay power [33], and overall decay power for the time frames of severe accidents is intrinsically driven by the decay powers of parents in each RN class, as well as the significant amounts of daughter products that are already present at shutdown (since decay is occurring all the time during operation).

The SCALE analyses for SOARCA [29] actually separated the parent and daughter decay powers, since this is the default behavior of ORIGEN and OPUS outputs. It is actually more difficult, and probably requiring of manual post-processing, to calculate daughter decay powers as remaining in the parent RN classes using SCALE. This may not be the optimum approach to decay power partitioning over the classes, but the introduced error is likely quite minor for LWR severe accidents based on past work [10][29][32][33] and the analyses presented in Sections 6.3.2 and 6.3.3. Since the SNL tools also separate the parent and daughter decay powers via OPUS outputs, the distributions of decay powers over RN classes for the Fukushima units are compared to the SOARCA class powers to confirm the consistency of this approach. The class decay powers are very similar for all classes, as demonstrated in Figure 6.11 for select classes. The left plot in Figure 6.11 shows class decay powers that are normalized to the total decay power for the respective reactors, Peach Bottom and Fukushima unit 3; the right plot depicts the class powers from Peach Bottom down-scaled by the thermal power ratio with unit 3 (i.e., 2381 MW / 3511 MW), and juxtaposed with the class powers from unit 3. The class powers for Surry SOARCA were also found to exhibit analogous trends. These plots verify that the class powers generated by the SNL scripts are consistent with class powers derived for the SOARCA models.

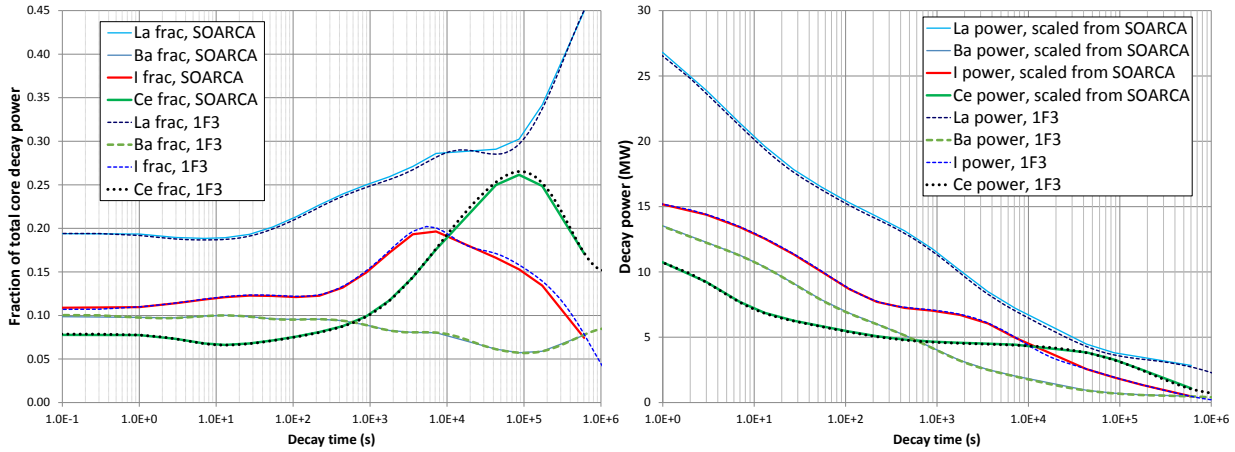

Figure 6.11. Comparison of SOARCA and Fukushima class decay powers.

The decay powers of daughters generated soon after shutdown due to parent in-growth are usually quite small compared to the decay powers of nuclides present at shutdown. This is generally true for nuclides that are important for decay heating, particularly the decay chains where daughter half-life is greater than the parent half-life, which is the trend for many isobaric fission product decay chains [16][33] excluding most of the intermediate nuclear excited states that follow the beta decay of the parent (however some key metastable isomers such as Te-127m ($t_{1/2} \approx 109$ days) have rather long half-lives). For these decay chains, the parent nuclide exists in smaller quantities at shutdown due to shorter half-life, while the daughter nuclide naturally accumulates to higher equilibrium concentrations due to longer half-life. Since decay power is proportional to both number density and decay rate, this inevitably causes the daughter decay power to be driven predominately by its inventory present at shutdown, and not the due to decay in-growth from the parent nuclide. Of course, neutron transmutation, decay energy differences between parent and daughter, and in-growth from multiple parents (especially for actinides) can still be important for particular decay chains. In fact, there are indeed some parent-daughter nuclides that exist in two different classes and are important for decay power. These nuclides are identified and analyzed in Section 6.3.3.

6.3.2 Examination of RN Class Powers

The SCALE analyses for the Fukushima and Surry models take a similar approach to SOARCA in allocating decay power over RN classes. This maintains model consistency and simplifies the post-processing of SCALE outputs for generation of MELCOR inputs. Decay powers for MELCOR RN classes are examined here to ascertain the behavior of parent and daughter decay powers in relation to lumped class powers.

As shown in Figure 6.12, the relative contribution of class decay power to overall decay power varies substantially with time, which is mainly due to the wide spectrum of half-lives in each class that are present at shutdown. For example, the increase in relative contribution of halogen class power after 1000 seconds can be traced back to I-134 ($t_{1/2} \approx 52.5$ min), I-132 ($t_{1/2} \approx 2.3$ hr), I-135 ($t_{1/2} \approx 6.7$ hr), I-133 ($t_{1/2} \approx 20.8$ hr), and I-131 ($t_{1/2} \approx 8$ days). All of these nuclides are present in significant quantities at shutdown, but some I-132 power is indeed due to in-growth from Te-132, as discussed in Section 6.3.3.

The increase in tetravalent (Ce) power after 10^4 seconds is attributable to initial Np-239 inventory at shutdown, which contributes significantly for all times less than 10^6 seconds and is insensitive to in-growth from U-239 (this is also discussed more in Section 6.3.3), as well as Ce-143, Ce-141, Zr-95, and Zr-97. The decay of Zr-95 and Zr-97 to Nb-95 and Nb-97m drive a small increase in the decay power of the transition metal class. Decay in-growth from Y-95 and Y-97 (of the trivalent class) do not significantly affect the decay powers of Zr-95 and Zr-97 in the tetravalent class. The Zr-95 and Zr-97 decay chains are discussed some more in Section 6.3.3.

Due to the large size of the trivalent (La) class, it is most responsible for decay power for all times. Its near-monotonic increase in contribution is mostly due to its plethora of isotopes and isomers present at shutdown that have a wide range of half-lives (e.g., La-140, La-142, La-144, Pm-148, Pm-149, Pm-149m, Pm-151, Pr-142, Pr-143, Pr-144, Pr-145, Y-91, Y-92, Y-94, Y-95, Y-98, Y-100, Nd-147). The parents and daughters that drive decay power most significantly are already present in the trivalent class at the time of shutdown. However, as discussed in Section 6.3.3, Ba-140/La-140 and Te-132/I-132 are noteworthy in their ability to create considerable daughter decay heat due to parent in-growth, relative to the respective RN class powers.

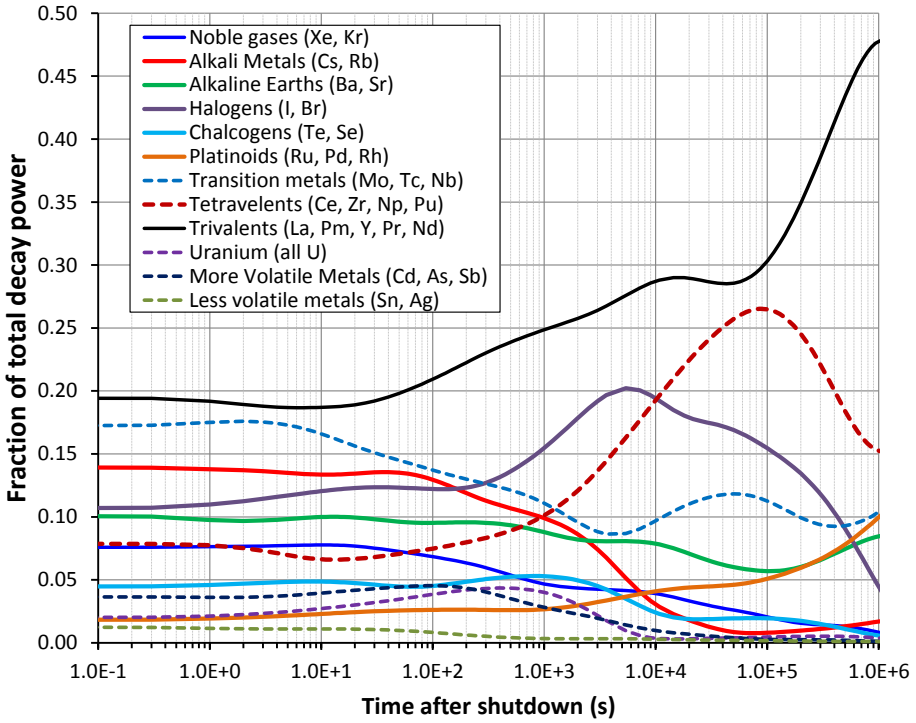

Figure 6.12. Typical distribution of decay power for LWRs over default MELCOR classes.

To further confirm that the class decay powers are driven by the nuclides initially present at shutdown, it is meaningful to plot the absolute class decay powers as a function of decay time – if the individual class power curves are nearly exponential in shape, then that is evidence that the decay heat of daughters produced after shutdown (due to in-growth) are not of first-order importance for overall power distribution over the RN classes. Otherwise, some or all of the individual powers curves would display large peaks and valleys that deviate substantially from the exponential curve. Figure 6.13 and Figure 6.14 the absolute RN class powers on logarithmic

and severe accident time scales, respectively. All of the RN class powers are nearly exponential and monotonically decreasing with respect to decay time. The rapid decay of key short-lived nuclides that drive early decay power is evident in Figure 6.14 for the uranium, tetravalent, transition metal, and platinoid classes. The decay powers for these classes decrease rapidly as their short-lived nuclides decay, and flatten as decay power transitions to the longer lived nuclides. Classes with a larger and more continuous range of nuclide half-lives, namely the trivalent, halogen, and alkaline earth classes, exhibit decay powers curves with smaller effective decay constants (i.e., the exponential curves decrease more gradually). Perhaps most important for releases and consequences, the cesium class power is almost perfectly exponential.

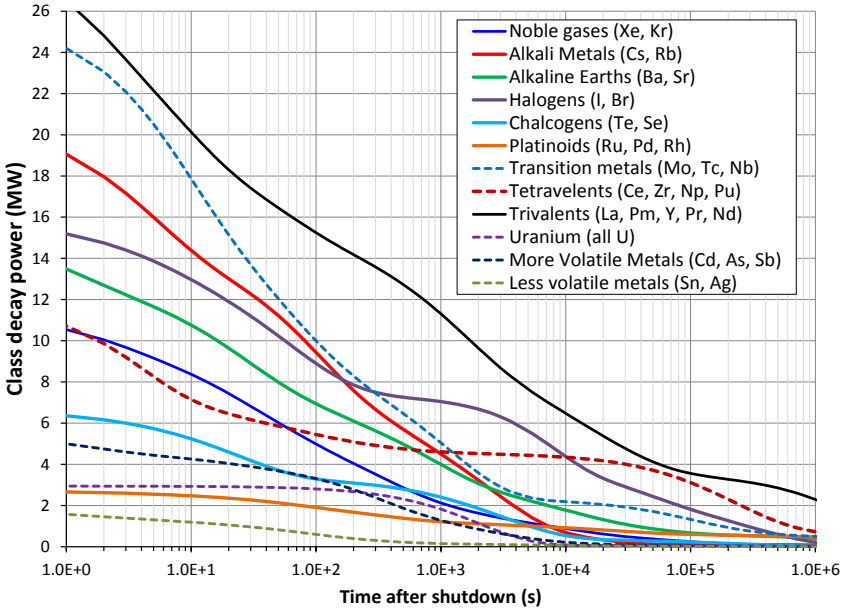

Figure 6.13. Absolute decay powers of MELCOR RN classes on logarithmic scale.

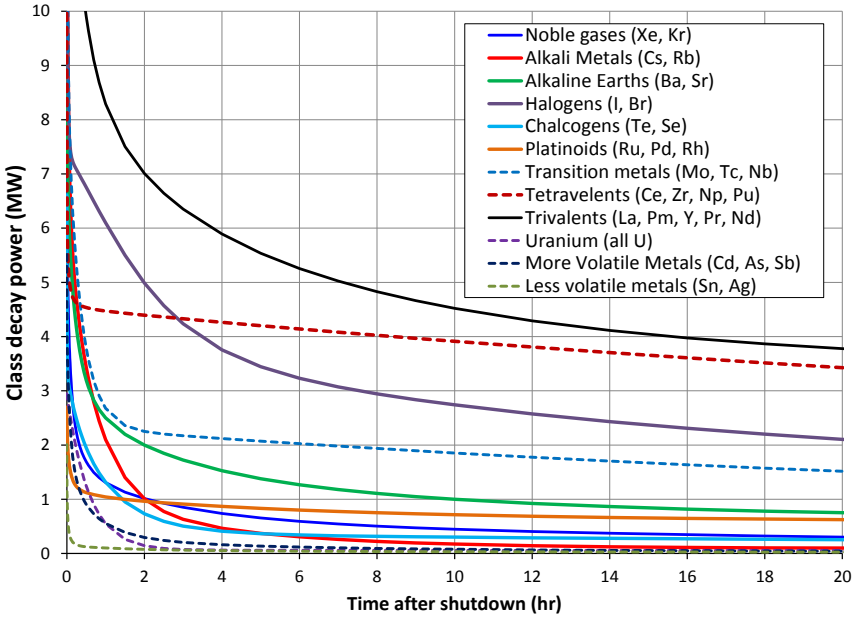

Figure 6.14. Absolute decay powers of MELCOR RN classes on severe accident time scale.

6.3.3 Key Parent-daughter Decay Powers

Arguably two of the more important parent/daughter isotopes to consider for decay heat are the actinide U-239 (created via U-238 neutron absorption) and its decay daughter Np-239, which is in the tetravalent (Ce) class. Both of these isotopes generate considerable decay power, being the top two nuclides driving decay power from 0 to ~100 seconds after shutdown; U-239 decays quickly ($t_{1/2}$ ~ 23 min) and is insignificant for heating a few hours after scram. Np-239 ($t_{1/2}$ ~ 2.4 days) has a strong impact on decay power for all times for severe accident time scales. Figure 6.15 depicts the results of a simple study to ascertain the quantitative effects of parent-daughter decay powers for U-239 and Np-239. It shows ORIGEN-S calculations of decay power starting with 100 g of U-239 (left figure) and with unit 3 inventories for both U-239 and Np-239 (right figure), which amounts to 31.7 g of U-239 and 4.55 kg of Np-239. The calculation with 100 g of U-239 demonstrates that the decay power of Np-239 daughters produced after shutdown are several orders of magnitude less than the parent U-239 decay power and are therefore rather insignificant. The decay calculation with the unit 3 inventories demonstrates that the decay power for Np-239 is indeed significant, but is due to the Np-239 already present at the time of shutdown (which is naturally the product of continual and prolonged U-239 decay during reactor operation). Despite being two of the top individual creators of decay heat, the effect of lumped class powers in the other classes – particularly the large trivalent (La) class – inevitably makes partitioning of U-239 and Np-239 decay heat rather inconsequential in the uranium and tetravalent classes.

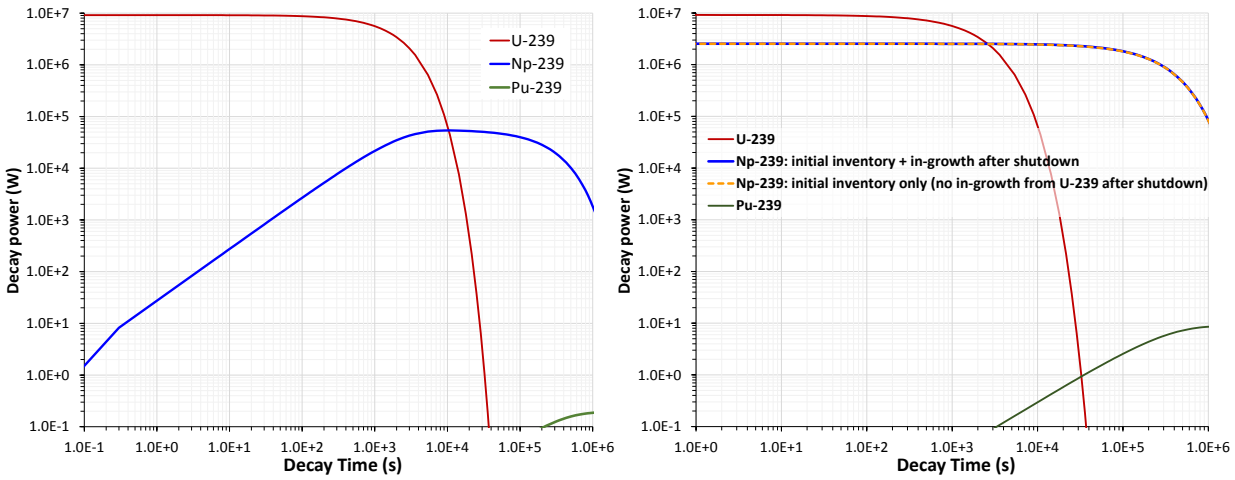

Figure 6.15. Decay powers due to 100 g of U-239 (left) and with unit 3 inventories of U-239 and Np-239 (right).

As discussed in Section 6.3.1, U-239 and Np-239 can be considered 'well-behaved' for decay heat partitioning in MELCOR. The differences in half-life, decay energies, and inventory at shutdown between these two nuclides are such that the decay power of the daughter (Np-239) is insensitive to in-growth from the parent (U-239) after shutdown. There are, conversely, parent-daughter nuclides that do not behave as conveniently for MELCOR. These decay chains tend to have daughter half-life that is shorter or comparable to the parent half-life. Similarly, daughter inventory at shutdown is usually less than or comparable to the parent inventory. In all likelihood

there are many such decay chains, but only those that contain key nuclides for decay heating are considered here.

Several parent-daughter pairs that are important for overall decay heat are identified that exhibit significantly increased daughter power due to decay in-growth from the parent. These nuclides are identified by having ORIGEN-S and OPUS report the top 100 nuclides that drive decay power at several timesteps after scram; the demonstrative reactor model for this analysis is Fukushima unit 3. Parent and daughter pairs are selected to be analyzed based on the lists of top nuclide decay powers. Although further analysis of such nuclides is probably warranted, a preliminary set of key parent-daughter pairs are shown in Table 6-2. The table lists the half-life and unit 3 inventory of the parent and daughter, as well as the potential percent change in the daughter class power if the daughter power due to in-growth were to be reassigned to the parent class. This percent difference is an estimated average value over later time periods for severe accidents, which is defined to be 10 hours to 100 hours for Table 6-2. The potential change in class decay powers due to in-growth increases with decay time. Many other decay chains were analyzed and found to be 'well-behaved' for class decay powers in MELCOR; like U-239 and Np-239, the additional daughter power due to in-growth after shutdown can be neglected for most nuclides that are important for decay power. The lists of dominant nuclides for decay power are shown in Table 6-3. As decay time increases, the powers from many short-lived nuclides diminishes, and decay heat generation becomes concentrated over fewer nuclides, namely Np-239, La-140, I-132, and Pr-144.

Table 6-2. Parent-daughter pairs with complicated decay powers for RN classes.

Parent, daughter	Parent half-life	Daughter half-life (metastable / ground state)	Parent inventory 1F3 (g)	Daughter inventory 1F3 (g) (metastable / ground state)	Potential % difference in RN powers(1)
Ba-140, La-140	12.8 days	1.67 days	1595	213.6	La class: 25%
Ce-144, Pr-144	284.9 days	7.2 min(2) / 17.3 min	2.11×10^4	0.0052 / 0.90	La class: 10%
Ru-106, Rh-106	372 days	131 min(3) / 30 s	7062	0.081 / 0.0072	None (same class)
Te-132, I-132(4)	3.20 days	2.30 hours	300	9.11	I class: 35%
Te-134, I-134(4)	41.8 minutes	52.5 minutes	3.68	5.67	I class: 3%
I-135, Xe-135(4)	6.57 hours	9.14 hours	35.9	17.1	Xe class: 4%
Zr-95, Nb-95(4)	64.0 days	34.99 days	4863	2447	Mo class: 1%

(1) The calculated powers include the decay energies of metastable beta and gamma decay, if applicable.
(2) Ce-144 can beta decay first to Pr-144m, which then undergoes isomeric transition to Pr-144.
(3) Ru-106 can beta decay first to Rh-106m, which then undergoes isomeric transition to Rh-106.
(4) These nuclides also have metastable isomers that are present in much smaller quantities at shutdown compared to the ground energy states; thus the metastable quantities are not listed.

Table 6-3. Dominant nuclide decay powers after shutdown by fraction of total decay power.

t = 0		t = 2.5 hr		t = 12 hr		t = 28 hr		t = 72 hr	
u239	0.0226	**np239**	0.1209	**np239**	0.1616	**np239**	0.1680	**la140**	0.1960
np239	0.0198	**la140**	0.0831	**la140**	0.1239	**la140**	0.1543	**np239**	0.1327
i134	0.0190	**i132**	0.0649	**i132**	0.0888	**i132**	0.0972	**i132**	0.0886
cs138	0.0178	**i135**	0.0470	**pr144**	0.0404	**pr144**	0.0510	**pr144**	0.0688
nb100	0.0151	**i133**	0.0319	**zr95**	0.0345	**zr95**	0.0433	**zr95**	0.0576
la144	0.0148	**y92**	0.0318	**i133**	0.0350	**nb95**	0.0420	**nb95**	0.0569
cs140	0.0146	**nb97**	0.0296	**nb95**	0.0332	**ru103**	0.0268	**rh106**	0.0358
tc104	0.0142	**pr144**	0.0269	**nb97**	0.0304	**rh106**	0.0265	**ru103**	0.0351
la140	0.0133	**i134**	0.0368	**i135**	0.0259	**ba140**	0.0253	**ba140**	0.0311
la142	0.0126	**y93**	0.0257	**mo99**	0.0218	**y91**	0.0229	**y91**	0.0304
rb92	0.0130	**zr95**	0.0231	**ru103**	0.0214	**mo99**	0.0233	**sr89**	0.0221
sr95	0.0119	**la142**	0.0285	**zr97**	0.0217	**i133**	0.0260	**mo99**	0.0199
rb91	0.0117	**nb95**	0.0221	**rh106**	0.0210	**sr89**	0.0167	**i131**	0.0192
sr93	0.0110	**zr97**	0.0214	**ba140**	0.0208	**ce143**	0.0188	**pr143**	0.0188
y95	0.0109	**sr91**	0.0217	**ce143**	0.0208	**i131**	0.0164	**ce141**	0.0160
i132	0.0106	**nb97m**	0.0175	**y93**	0.0202	**nb97**	0.0199	**eu156**	0.0140
nb102	0.0109	**la141**	0.0185	**y91**	0.0182	**pr143**	0.0147	**xe133**	0.0126
y94	0.0104	**ce143**	0.0169	**nb97m**	0.0177	**ce141**	0.0123	**cs134**	0.0121
nb98	0.0101	**mo99**	0.0161	**sr91**	0.0164	**te132**	0.0118	**te132**	0.0107
rb90	0.0099	**rb88**	0.0181	**i131**	0.0136	**eu156**	0.0112	**cm242**	0.0105
i135	0.0098	**sr92**	0.0169	**sr89**	0.0133	**zr97**	0.0141	**ce143**	0.0101
cs141	0.0098	**ru103**	0.0144	**y92**	0.0136	**xe133**	0.0111	**nd147**	0.0093
zr99	0.0107	**ba140**	0.0141	**pr143**	0.0118	**nb97m**	0.0116	**i133**	0.0081
nb101	0.0097	**rh106**	0.0140	**xe135**	0.0113	**cs134**	0.0090	**pm148**	0.0079
xe139	0.0094	**ru105**	0.0144	**te132**	0.0107	**cm242**	0.0078	**u237**	0.0078
tc106	0.0094	**kr88**	0.0138	**ce141**	0.0098	**nd147**	0.0077	**ce144**	0.0061
cs139	0.0091	**y91**	0.0122	**eu156**	0.0091	**pm148**	0.0074	**tc99m**	0.0050
xe137	0.0090	**i131**	0.0093	**xe133**	0.0091	**u237**	0.0070	**np238**	0.0047
rb93	0.0093	**sr89**	0.0089	**cs134**	0.0071	**np238**	0.0064	**nb97**	0.0044
mo101	0.0089	**pr145**	0.0089	**pm148**	0.0064	**y93**	0.0086	**y90**	0.0036
total	**0.3695**	**total**	**0.8293**	**total**	**0.8897**	**total**	**0.9192**	**total**	**0.9560**

Judging by the results described in Table 6-2 and Table 6-3, the Ba-140/La-140 and Te-132/I-132 chains appear to be the most significant drivers of decay power that also pose a challenge to the user in specifying MELCOR inputs for class powers. Over severe accident time frames, the classes powers for the trivalent (La) and halogen (I) classes are still mostly dictated by the nuclides (both parents and daughters) present at shutdown. Nonetheless, the decay power of La-140 due to in-growth alone from Ba-140 is about 25% of the total trivalent class power for later times after shutdown, as shown in Table 6-2, Table 6-3, and Figure 6.16. Figure 6.16 depicts the

decay power of La-140 in Fukushima unit 3 with and without in-growth from Ba-140. If this decay power due to in-growth was reallocated to the parent class (i.e. the alkaline earth (Ba) class), then trivalent decay power could decrease by as much as 25% during later time frames. And because the decay power of the alkaline earths is quite small hours after scram, the additional La-140 power following Ba-140 decay could greatly increase the parent class power– the increase in the Ba-class power could be nearly a factor of two after long decay time (50-100 hours).

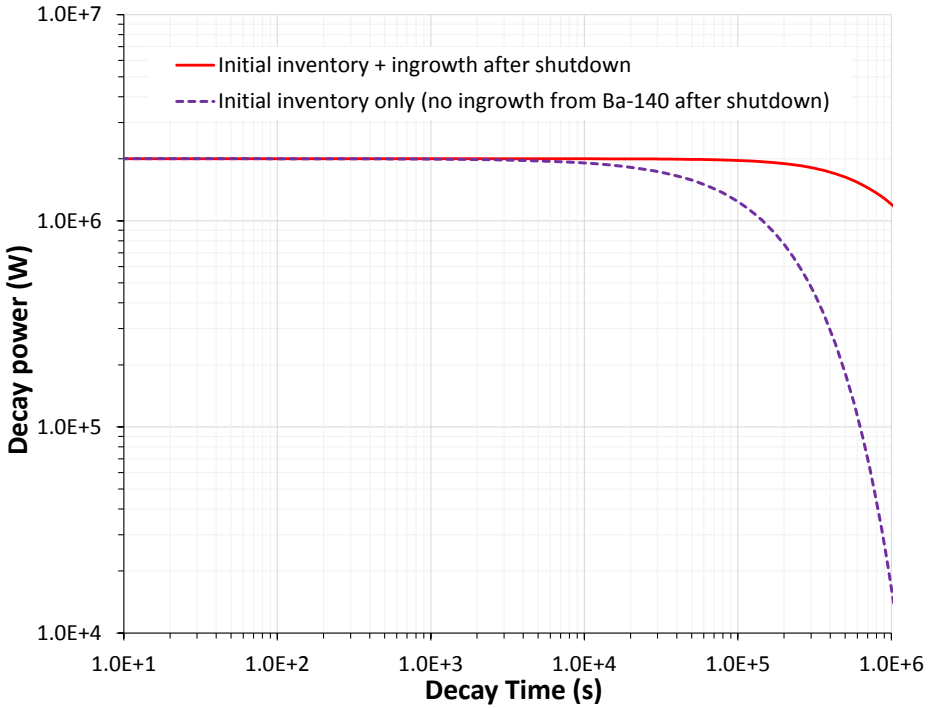

Figure 6.16. Decay power of La-140 in unit 3 with and without in-growth from Ba-140.

Fortunately, the Ba class is not very volatile and remains mostly in the fuel or in the corium following RPV lower head failure. Typical release fractions from fuel of the Ba class are depicted in Figure 6.17 for the Fukushima units 1 and 3 models and for the Surry SOARCA STSBO. Total in-vessel and ex-vessel releases range from 1% to 6%. The trivalent and alkaline earth classes basically remain together throughout the severe accident. Thus, the decision of which class to assign the decay power of La-140 due to in-growth from Ba-140 – in either the trivalent class or the alkaline earth class – is largely unimportant for MELCOR simulations of LWR severe accidents. However, accident scenarios with enhanced barium release from fuel should reconsider this conclusion.

The decay powers associated with Ce-144 and Pr-144 exhibit similar behavior since neither class (tetravalents and trivalents) is particularly volatile; further, the total powers for these classes are much greater than the individual nuclide powers of Ce-144 and Pr-144, making the choice of allocating the in-growth power less important for MELCOR. Ru-106 and Rh-106 have the potential to create large daughter decay power due to in-growth based on half-lives and shutdown inventories, but these nuclides are conveniently in the same class (i.e. platinoids).

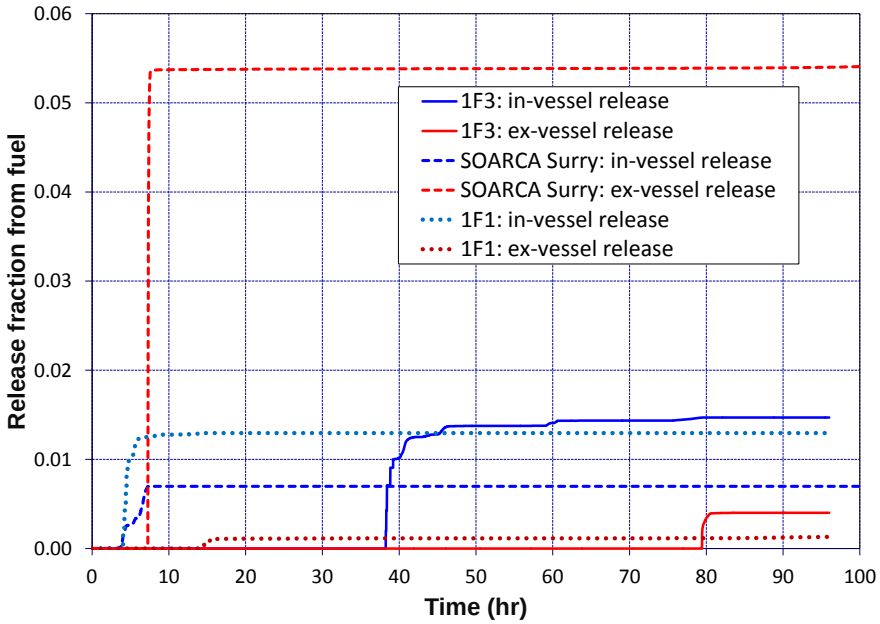

Figure 6.17. Typical release fractions of the barium class.

The decay power generated by I-132 is also significantly influenced by in-growth from its parent, Te-132, after shutdown. The additional power due to in-growth amounts to about 35% of the total halogen class power for decay time over 10 hours–that is, the decay power of the halogen class is still mostly determined by the nuclides present at shutdown. After 100 hours, however, the I-132 power due to in-growth generates over 50% of the halogen class power. The decay power of I-132 with and without in-growth from Te-132 is shown by Figure 6.18. Similar to the alkaline earth class, the chalcogen (Te) does not generate considerable decay power hours after shutdown. The reapportioning of I-132 decay power to the parent class could increase the chalcogen decay power by a factor of 2-5 for longer decay times. Hence, further analyses with SCALE6, MELCOR, and MACCS are necessary to ascertain the effects that Te-132 and I-132 have on source terms. The tools developed in this report could generate two sets of halogen and chalcogen decay powers for MELCOR, one where all I-132 power remains in the halogen class, and one where I-132 power from in-growth is moved to the chalcogen class. Subsequent MELCOR and MACCS calculations could assess the impact that parent and daughter decay powers have on radionuclide releases. Separating parent and daughter decay power, which was done in SOARCA and in the new SNL tools, may in fact be conservative since it increases decay power of the halogen class. Te-134 and I-134 exhibit the same trend as Te-132 and I-132, but with a greatly lower quantitative impact on the respective class powers (only about 3% of the halogen class power), as shown in Table 6-2 and Figure 6.19. Figure 6.19 shows the decay power of I-134 with and without in-growth from Te-134 after shutdown.

Decay power curves for Xe-135 and Nb-95 are presented in Figure 6.20 and Figure 6.21, respectively. Decay power with and without in-growth from the parent nuclides (I-135 and Zr-95) is compared. The decay powers for these nuclides are not appreciably influenced by in-growth, as summarized in Table 6-2. It is also worth noting that the inventory of Xe-135 at shutdown is determined greatly by its enormous thermal absorption cross section. Several additional decay chains, such as Zr-97 and Nb-97m/Nb-97, were analyzed and the nuclide decay

powers were found to have nearly no dependence on in-growth after shutdown for severe accident time frames. Most fission product decay chains behave in such a manner due to inherent differences in half-life and shutdown inventory between parents and daughters [16][33].

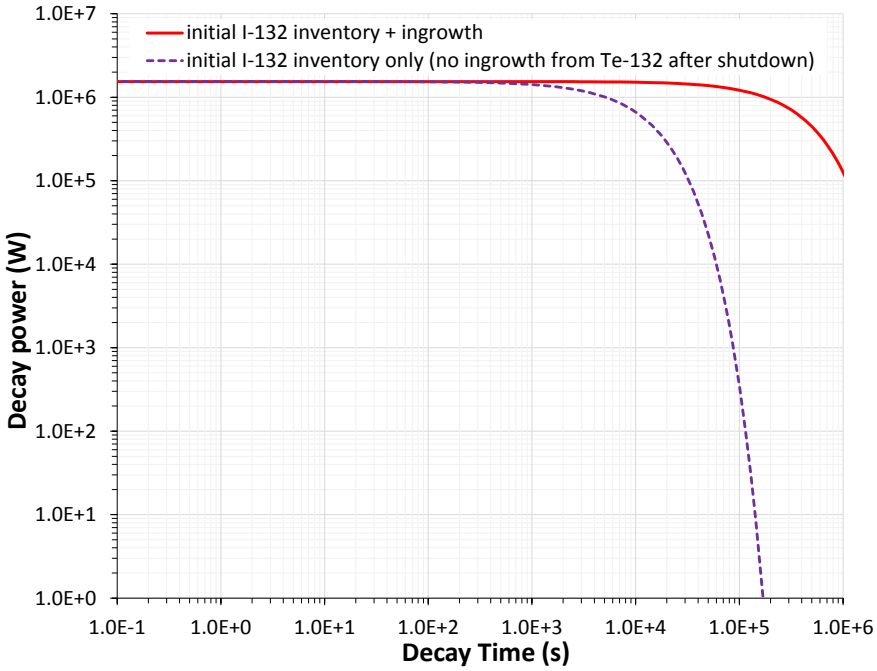

Figure 6.18. Decay power of I-132 in unit 3 with and without in-growth from Te-132 after shutdown.

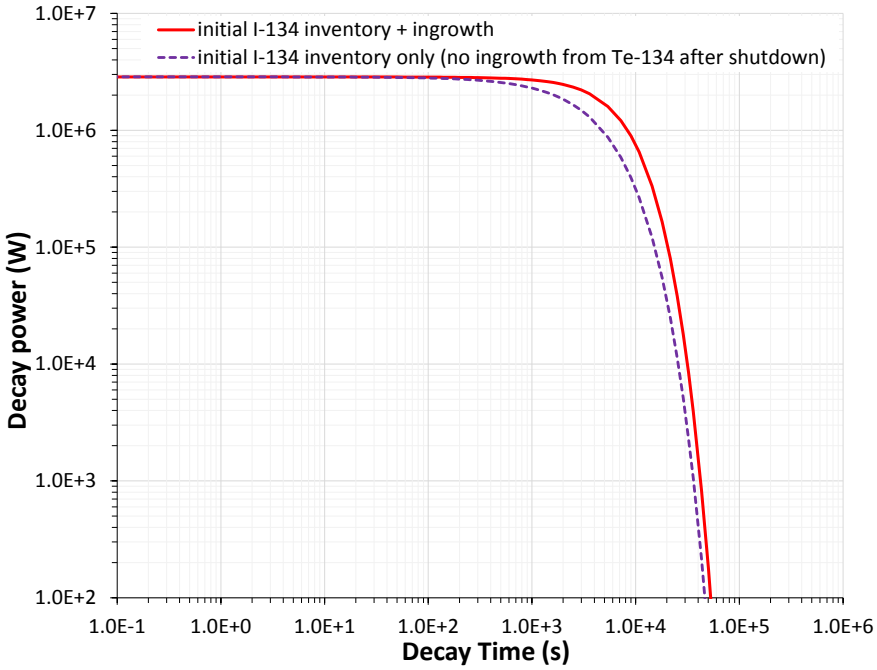

Figure 6.19. Decay power of I-134 in unit 3 with and without in-growth from Te-134 after shutdown.

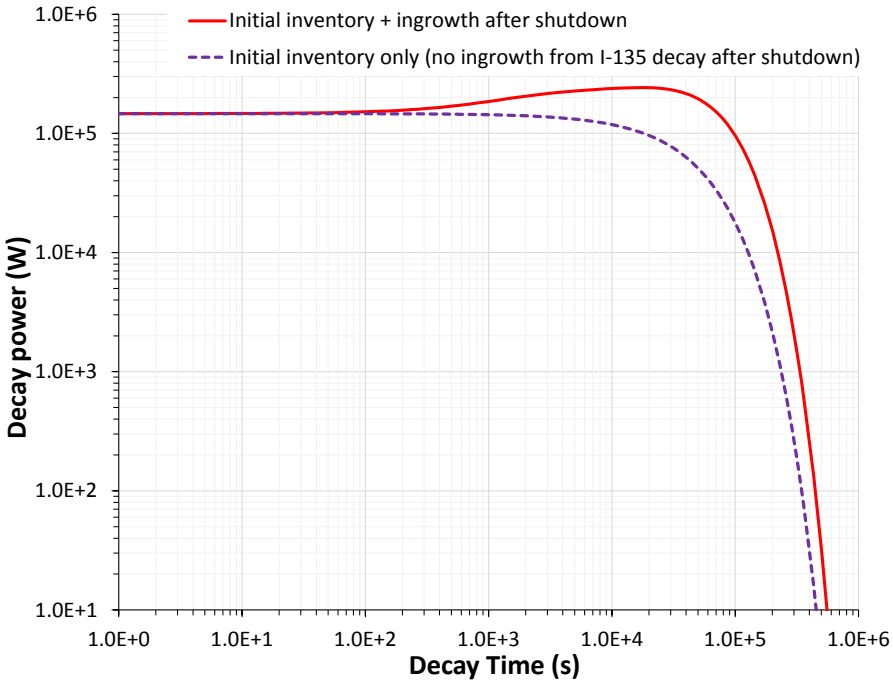

Figure 6.20. Decay power of Xe-135 in unit 3 with and without in-growth from I-135 after shutdown.

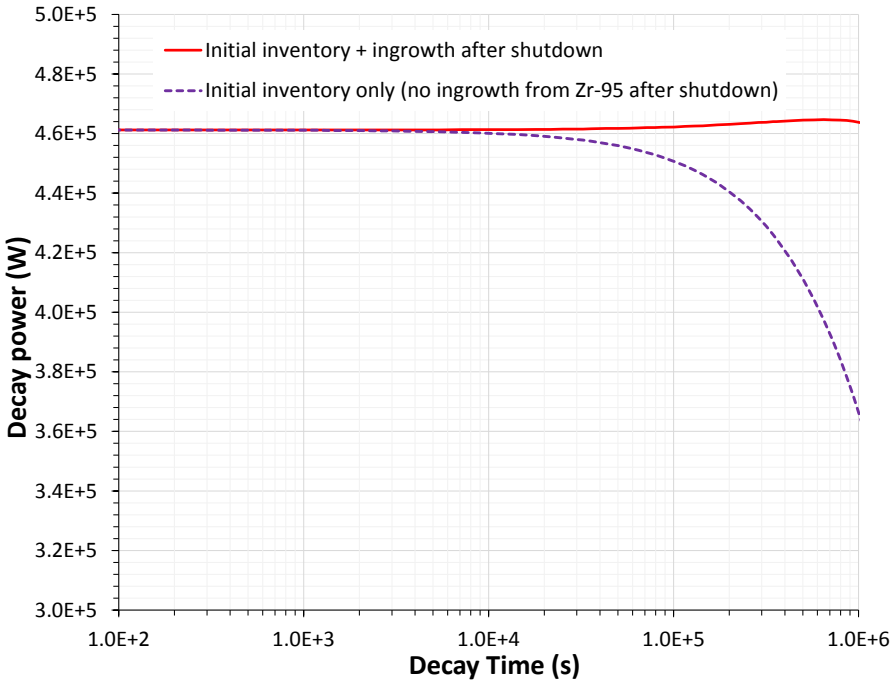

Figure 6.21. Decay power of Nb-95 in unit 3 with and without in-growth from Zr-95 after shutdown.

Separating vs. retaining daughter heat and parent heat is probably a trivial choice for most LWR severe accident simulations with MELCOR. Some important exceptions, namely Te-132 and I-132, have been identified that warrant more rigorous analyses. The relatively short time scale of severe accident simulations, usually 4-7 days, is short enough to preclude large changes in RN class quantities due to class-to-class decay. Other severe accident uncertainties, including boundary conditions and core relocation, are known to dwarf the uncertainty associated with radionuclide mass/heat partitioning over the classes–the largest introduced uncertainty in this process is likely the choice to limit the code to a handful of RN classes in the first place. Like the issues involved with creating RN class masses, the 'fix' to address decay behavior principally requires an isotopic summation code like ORIGEN to be internal or coupled to MELCOR.

6.4 Approximations for RN Speciation in MELCOR

This section briefly discusses approximations for RN speciation that are required by severe accident codes. Detailed scrutiny of these issues requires more advanced analyses that are outside the scope of this report. The true processes behind these approximations are likely very complicated and coupled phenomena for radionuclide transport, chemistry, radiation effects, and material behavior for the fuel. Some of these issues are present research activities funded by the NRC, particularly the behavior of radio-iodine chemistry in containment.

The tools and analyses documented in this report do not have the capability to determine speciation of radionuclides. SCALE6 calculates the fundamental inventories and heating of fission products, actinides, and decay products that comprise the elements and compounds of RN species. The SNL scripts then make a number of assumptions concerning RN class formation and the creation of key combination species (CsI and Cs_2MoO_4) to directly generate MELCOR and MACCS inputs. Two principal approximations for RN speciation in MELCOR are briefly discussed here: radioactivity effects on RN species and the pre-formation of RN combination classes. Revisions to these approximations, perhaps due to knowledge advancement, should be incorporated into the post-processing scripts that create input records for MELCOR and MACCS.

6.4.1 Radioactive Decay Effects on RN Species

Radioactive decay likely has a real impact on MELCOR source terms due its effects on radionuclide speciation and subsequent transport properties, but these effects are generally not simulated directly in codes like MELCOR. For example, I-131 beta decays to stable Xe-131 via several nuclear excited states, including a metastable isomer with an 11.8 day half-life. Hence after decay, the nuclide actually no longer exhibits the physio-chemical behavior of iodine and thereafter behaves as a noble gas. The particle energy for gamma emissions (i.e. isomeric transition) following beta decays of certain fission products can also be sufficient to break chemical bonds, potentially altering the physio-chemical speciation of the radionuclide. Although MELCOR can account for some of these effects for the iodine class via the iodine pool model [10], it is currently not a best practice to enable the model due to code stability and runtime issues.

No attempt is made here to analyze or substantiate the neglect of decay effects on RN speciation. Such efforts are outside the scope and capabilities of this work. These issues are only highlighted because of the potential impacts on the SNL tools for radionuclide inventory quantification. For example, if the capability to model these effects is incorporated into MELCOR if in the future, then it will likely be necessary to provide MELCOR with additional inputs (e.g., nuclide activities, decay data, dose rates) that will require modifications to the ORIGEN-S models and post-processing tools developed in this work.

6.4.2 Pre-formation of MELCOR RN Combination Classes

As alluded to in Section 2.1.1 and Section 3.3.2.3, the CsI and Cs_2MoO_4 combination classes are pre-combined for the fuel and gap inventories even before core overheating and radionuclide release; this is not technically correct. Furthermore, the release coefficients for these combination classes are set equal to coefficients for the pure alkali metal (Cs) class. In actuality, these species probably do not exist in substantial quantities until high fuel temperatures and radionuclide release from the fuel. MELCOR does have limited capability to form the user-specified combinations from pure RN classes in a dynamic fashion. This is accomplished through use of the RN1_CLS record. One of the principal features of this approach is that the code automatically calculates stoichiometric constraints on the amount of the combination class formed, which therefore allows each of the pure classes to retain their true release rates. For the CsI class, for instance, the alkali metal and halogen classes are released at their distinctive release rates and combined automatically by MELCOR–excess of any member class relative to stoichiometric limitations at any given time step would be remain in the pure class form.

Unfortunately, the class combination feature in MELCOR is not amenable to two combination classes, i.e. CsI and Cs_2MoO_4, where the user needs to specify unique gap fractions for the pure alkali metal class (treated as CsOH in the gap) and CsI. The desired gap fraction can only be attained by pre-separating the classes based on a number of assumptions, e.g. most cesium mass exists as Cs_2MoO_4, (see Section 3.3.2.3). These assumptions are characterized as MELCOR ‘best practices’ for RN speciation, and are therefore incorporated into the SNL post-processing tools that generate MELCOR input records.

Again, no attempt is made here to analyze or substantiate what impacts the pre-formation of RN combination classes have on source term. Such efforts are outside the scope of this work, and would require uncertainty and sensitivity studies using MELCOR. A full investigation may also require code revisions to permit more flexible class combination modeling by MELCOR. Still, any changes in the MELCOR best practices for pre-formation of RN classes will accordingly require modifications and enhancements to the ORIGEN-S models and post-processing tools developed in this work.

7 SUMMARY

SNL has developed accurate and automated methods using SCALE6 in conjunction with automation scripts to directly generate MELCOR and MACCS input records for decay heating and inventories. Further validation of the new SNL tools is required depending on the application. For the creation of inventories and decay power for severe accident consequences, the tools are well-suited and should provide reasonably accurate information. These tools were applied to units 1-3 of Fukushima Daiichi, the Surry reactor, and the Peach Bottom reactor; the results of these analyses appear very reasonable compared to other analyses and past research. However, the tools should be used cautiously for inventory and decay heat quantification of other MELCOR applications, such as spent fuel pools. The algorithms to easily formulate RN class quantities require certain assumptions with respect to decay time that are not directly applicable for other modelling applications such as SFPs. Simple script modifications and additions would probably be sufficient grant the tools enhanced flexibility to consider applications beyond LWR source terms.

7.1 Tool and Method Documentation

This report has provided reasonable documentation on the use of SCALE6, TRITON, ORIGEN-S/ARP, and supporting scripts to generate MELCOR and MACCS input records. The methodologies and user-requirements for these processes are documented in Section 3. The relevant MELCOR and MACCS input records themselves were discussed briefly in Section 2. This report has documented the steps necessary to conduct depletion and decay analyses of a reactor using the developed models and tools; these steps were:

- Pre-processing of plant data to provide input to the automation scripts (Section 3.1);
- Automated creation of ORIGEN-S/ARP input files by the SNL scripts and the pre-processed plant data (Section 3.2);
- Post-processing to generate consistent MELCOR and MACCS input records (Section 3.3).

The tools are quite flexible by means of several user variables that control input creation and post-processing, as described in Section 3.2.1 and Section 3.3.1. A number of assumptions that are necessary in these steps have been documented and, in some cases, analyzed and substantiated with in-depth calculations (Section 6). The tools make use of assumptions and approximations that are informed by years of severe accident research, but the user should still be aware of the potential limitations inherent to class abstractions for radionuclide modeling used in MELCOR and MACCS.

7.2 Future Work

Several potential avenues of future work have been identified. The tools for automated creation and post-processing of ORIGEN-S/ARP models can be expanded to include additional user-options for allocating lumped RN quantities over MELCOR COR cells. This may include further control over the radial allocation of each RN class, unique RN classes for each COR ring, and more advanced options for axial modeling of RN masses (e.g., if several axial nodes are

considered by ORIGEN-S). Additional axial modeling features would of course require axial burnup calculations by ORIGEN-S/ARP and sufficient ARP libraries.

The depletion and decay analyses of the Fukushima units have significant room for improvement. Most importantly, the use of surrogate ENDF/B-V ARP libraries, which are pre-shipped with SCALE6, for the Fukushima fuel assemblies will no longer be necessary after generation of new Fukushima ARP libraries using the TRITON sequence in SCALE6. The detailed fuel assembly information in Fukushima units 1-3 is given in Section 4.2.3. Future analyses can take a quasi-3D approach comprised of many ORIGEN-S/ARP simulations for each fuel assembly at several axial nodes. The 3D TEPCO core data supports such an approach. The SNL automation tools can be easily extended to consider axial variations in power, burnup, fuel assembly geometry and materials (e.g. partial fuel rods and control blades), and void fraction. Standalone use of ORIGEN-S/ARP naturally still requires adequate ARP libraries generated by TRITON–i.e. several TRITON calculations would need to be performed for a range of void fractions.

The SNL tools developed in this work can be applied to new MELCOR and MACCS analyses of historical SNL models; this includes Surry, Sequoyah, Monticello, and Peach Bottom. SCALE analyses of Sequoyah and Monticello will facilitate modernizing the inventory and decay heat inputs for these models, while simultaneously providing a consistent set of MACCS inputs. A detailed analysis of Surry has already been completed using plant data from cycles 18 through 20. A preliminary analysis of the Peach Bottom plant has also been completed using plant information from cycles 13 through 16. The Peach Bottom analysis can be expanded by undertaking a more detailed approach similar to the Fukushima and Surry analyses that consider the distinct characteristics (e.g. burnup, power, location, enrichment) of each assembly for several cycles. A detailed analysis of MOC conditions for Peach Bottom would facilitate comparison to the SOARCA inventory and decay heat information, which was generated by highly detailed TRITON calculations performed by ORNL.

Finally, further analysis is warranted of decay chains that create significant daughter decay power via in-growth after shutdown, as discussed in Section 6.3.3. In particular, the effects of Te-132 and I-132 should be quantified by a combined analysis using SCALE, MELCOR, and MACCS. It was found that the additional power generated by I-132 from in-growth of Te-132 is about 35% of the halogen class power after 10 hours of decay time, and over 50% of the halogen class power after 100 hours. The SNL tools, as done in SOARCA, automatically apportion all decay power generated by iodine to the halogen class, while it may be more realistic to move I-132 power from in-growth to the chalcogen (Te) class (i.e., assume daughter heat stays in the parent class). Ideally, the decay power generated by the initial inventory of I-132 at shutdown should correctly stay in the halogen class. The tools developed in this report could generate two sets of halogen and chalcogen decay powers for MELCOR, one where all I-132 power remains in the halogen class, and one where I-132 power from in-growth is moved to the chalcogen class. Subsequent MELCOR and MACCS calculations could assess the impact that parent and daughter decay powers have on radionuclide releases.

REFERENCES

[1] J.N. Cardoni and D.A. Kalinich, "Fukushima Daiichi Unit 1 Uncertainty Analysis -- Preliminary Selection of Uncertain Parameters and Analysis Methodology," SAND2014-1170, Sandia National Laboratories: Albuquerque, NM (2014).

[2] R.O. Gauntt, D.A. Kalinich, et al., "Fukushima Daiichi Accident Study," SAND2012-6173, Sandia National Laboratories: Albuquerque, NM (2012).

[3] R.O. Gauntt, D.A. Kalinich, et al., "MELCOR Simulations of the Severe Accident at the Fukushima 1F1 Reactor," *Proceedings of 2012 ANS Winter Meeting & Nuclear Technology Expo*, San Diego, CA, November 11-15 (2012).

[4] J. Phillips, J.N. Cardoni, et al., "MELCOR Simulations of the Severe Accident at the Fukushima 1F2 Reactor," *Proceedings of 2012 ANS Winter Meeting & Nuclear Technology Expo*, San Diego, CA, November 11-15 (2012).

[5] J.N. Cardoni, R.O. Gauntt, et al., "MELCOR Simulations of the Severe Accident at the Fukushima 1F3 Reactor," *Proceedings of 2012 ANS Winter Meeting & Nuclear Technology Expo*, San Diego, CA, November 11-15 (2012).

[6] K.M. Groth, M.R. Denman, et al., "Proof of Principle Framework for Developing Risk-Informed Severe Accident Management Guidelines," SAND2013-8324, Sandia National Laboratories, Albuquerque, NM (2013).

[7] M.R. Denman, J.N. Cardoni, et al., "Discrete Dynamic Event Tree Capability Study for Advanced Small Modular Reactors," SAND2013-2514, Sandia National Laboratories, Albuquerque, NM (2013).

[8] K. Robb, et al., "Fukushima Daiichi Unit 3 MELCOR Investigation," *Proceedings of 2012 ANS Winter Meeting & Nuclear Technology Expo*, San Diego, CA, November 11-15 (2012).

[9] G.M. Martinez, et al., "Independent Review of SCDAP/RELAP5 Natural Circulation Calculations," SAND91-2089, Sandia National Laboratories, Albuquerque, NM (1994).

[10] R.O. Gauntt, et al., NUREG/CR-6119, "MELCOR Computer Code Manuals, Vol. 2: Reference Manuals, Version 1.8.6 (Vol. 2, Rev. 3)," Sandia National Laboratories, Albuquerque, NM (2005).

[11] D.I. Chanin and M.L. Young, NUREG/CR-6613, "Code Manual for MACCS2: Volume 1, User's Guide," U.S. Nuclear Regulatory Commission, Washington, DC (1997).

[12] Oak Ridge National Laboratory, "Scale: A Comprehensive Modeling and Simulation Suite for Nuclear Safety Analysis and Design," ORNL/TM-2005/39, Version 6.1,

June 2011. Available from Radiation Safety Information Computational Center at Oak Ridge National Laboratory as CCC-785.

[13] W. B. Wilson, et al., "A Manual for CINDER'90 Version 07.4 Codes and Data," LA-UR-07-8412, Los Alamos National Laboratory (2008).

[14] T. Downar, "Nuclear Fuel Cycle: Nuclear Source Characterization," Purdue University, March 2005.

[15] J.J. Duderstadt and L.J. Hamilton, *Nuclear Reactor Analysis*, John Wiley & Sons, Inc. New York, NY (1976).

[16] A. Tobias, "Decay Heat," *Progress in Nuclear Energy*, Vol. 5, pp. 1-93 (1980).

[17] M.L. Fensin, M.R. James, et al., "The New MCNP6 Depletion Capability," LA-UR11-07032, *Proceedings of ICAPP 2012*, Chicago, IL, June 24-28 (2012).

[18] K. Okumura, et al., "SRAC2006: A Comprehensive Neutronics Calculation Code System," JAEA-Data/Code 2007-004, Japan Atomic Energy Agency, 4-49 Muramatsu, Tokai-mura, Naka-gun, Ibaraki 319-1184, Japan (2007).

[19] Soffer, L., et al., "Accident Source Terms for Light Water Nuclear Power Plants," NUREG 1465, U.S. Nuclear Regulatory Commission, 1995.

[20] R.O. Gauntt, "Synthesis of VERCORS and Phebus data in Severe Accident Codes and Applications," SAND2010-1633, Sandia National Laboratories, April 2010.

[21] TEPCO Plant Data, http://www.tepco.co.jp/nu/fukushima-np/plant-data/f1_3_Keihou3.pdf, accessed April 6 (2014).

[22] N.E. Todreas and M.S. Kazimi, *Nuclear Systems I: Thermal Hydraulic Fundamentals*, CRC Press Taylor and Francis Group, Boca Raton, FL (2012).

[23] American National Standard for Decay Heat Power in Light Water Reactors, ANSI/ANS-5.1-2005, American Nuclear Society (2005).

[24] Sandia National Laboratories, NUREG/CR-7110, "State-of-the-Art Reactor Consequence Analyses Project Volume 2: Surry Integrated Analysis," U.S. Nuclear Regulatory Commission, Washington, DC (2012).

[25] S.G. Ashbaugh, et al., "Accident Source Terms for Pressurized Water Reactors with High-Burnup Cores Calculated Using MELCOR 1.8.5," SAND2008-6664, Sandia National Laboratories, Albuquerque, NM (2008).

[26] D. Brown, "Release of the ENDF/B-VII.1 Evaluated Nuclear Data File," Proceedings of 2012 ANS Winter Meeting & Nuclear Technology Expo, San Diego, CA, November 11-15 (2012).

[27] I. Gauld, "Validation of ORIGEN-S Decay Heat Predictions for LOCA Analysis," Proceedings of PHYSOR-2006, ANS Topical Meeting on Reactor Physics, Vancouver, BC, Canada. September 10-14 (2006).

[28] I.C. Gauld and B. D. Murphy, "Updates to the ORIGEN-S Data Libraries Using ENDF/B-VI, FENDL-2.0, and EAF-99 Data," ORNL/TM-2003/118, Oak Ridge National Laboratories, Oak Ridge, TN (2004).

[29] U.S. NRC, "State-of-the-Art Reactor Consequence Analysis (SOARCA) Report," NUREG/CR-7110, U.S. Nuclear Regulatory Commission: Washington D.C. 2012.

[30] B. J. Ade, NUREG/CR-7041, "SCALE/TRITON Primer: A Primer for Light Water Reactor Lattice Physics Calculations," ORNL/TM-2011/21, Oak Ridge National Laboratory, Oak Ridge, TN (2012).

[31] R.O. Gauntt, "Synthesis of VERCORS and Phebus data in Severe Accident Codes and Applications," SAND2010-1633, Sandia National Laboratories (2010).

[32] D.A. Powers, NUREG/CR-4481, "Fission Product Behavior during Severe LWR Accidents: Modeling Recommendations for MELCOR Code System," Volume 1: Fission Product Release from Fuel, SAND85-2743, Sandia National Laboratories, Albuquerque, NM (1988).

[33] R.M. Ostmeyer, NUREG/CR-4169, "An Approach to Treating Radionuclide Decay Heating for Use in the MELCOR Code System," SAND84-1404, Sandia National Laboratories, Albuquerque, NM (1985).

[34] J.T. Goorley, et al., "MCNP6 User's Manual Version 1.0," LA-CP-13-00634, Los Alamos National Laboratory (2013).

[35] E.M. Baum, H.D. Knox, T.R. Miller, *Nuclides and Isotopes, Chart of the Nuclides: 16th Edition*, Knolls Atomic Power Laboratory (2002).

APPENDIX A. FUKUSHIMA ORIGEN-S/ARP TEMPLATE INPUT FILES

This information is available in the Official Use Only (OUO) version of this report (SAND2014-3966).

SAND2014-17667

DISTRIBUTION

Internal Distribution (electronic copy)

1	MS0748	Jeff Cardoni	6232
1	MS0748	Doug Osborn	6232
1	MS0748	Don Kalinich	6232
1	MS0748	Jesse Phillips	6232
1	MS0748	Matt Denman	6231
1	MS0899	Technical Library	9536


Sandia National Laboratories